

Review

Eco-Friendly Physical Activation Methods for Suzuki–Miyaura Reactions

Katia Martina, Maela Manzoli, Emanuela Calcio Gaudino and Giancarlo Cravotto *

Dipartimento di Scienza e Tecnologia del Farmaco and NIS—Centre for Nanostructured Interfaces and Surfaces, University of Turin, Via P. Giuria 9, Turin 10125, Italy; katia.martina@unito.it (K.M.); maela.manzoli@unito.it (M.M.); emanuela.calcio@unito.it (E.C.G.)

* Correspondence: giancarlo.cravotto@unito.it; Tel.: +39-011-670-7684

Academic Editor: Ioannis D. Kostas

Received: 31 December 2016; Accepted: 16 March 2017; Published: 23 March 2017

Abstract: Eco-compatible activation methods in Suzuki–Miyaura cross-coupling reactions offer challenging opportunities for the design of clean and efficient synthetic processes. The main enabling technologies described in the literature are microwaves, ultrasound, grinding (mechanochemistry) and light. These methods can be performed in water or other green solvents with phase-transfer catalysis or even in solventless conditions. In this review, the authors will summarize the progress in this field mainly from 2010 up to the present day.

Keywords: Suzuki–Miyaura cross-coupling reaction; Pd catalysts; microwaves; ultrasound; ball milling; light

1. Introduction

The present review deals with the use of non-conventional methods for Suzuki–Miyaura reactions (SMC) [1]. In particular, the results obtained with different unconventional techniques were described by following a Green Chemistry approach, and focusing on recent methodologies based on microwave (MW) and ultrasound (US) irradiations, grinding and photo-activated processes. We aimed at describing several original works published in the field after 2010; however, we also took on board previous papers which can be considered seminal works on the topic and which therefore cannot be ignored. Here, the main advantages and drawbacks of the abovementioned methodologies will be comprehensively covered, serving as a guide for further research on innovative SMC transformations under unconventional activation. Moreover, due to length limits, these topics have been briefly explored, and readers are encouraged to refer to the cited reviews for in depth dissertation.

In particular, MW-assisted chemistry relies on the ability of the reaction mixture to efficiently absorb MW energy, producing rapid internal heating (in-core volumetric heating) by the direct interaction of electromagnetic irradiation with the molecules in the reaction mixture. Although MW irradiation are currently applied as non conventional method to promote fast chemical transformations, there has been considerable speculation on their own effect. Indeed, the debate is still open and focused on discerning between thermal effects due to the rapid heating and high bulk reaction temperatures reached under MW dielectric heating, and other specific or nonthermal microwave effects. These effects, which are not linked to a macroscopic change in reaction temperature, have been hypothesized to originate from a direct interaction of the electromagnetic field with specific molecules, intermediates, or even transition states in the reaction medium [2].

Mechanochemistry is a branch of solid-state chemistry where intramolecular bonds are broken by mechanical action followed by further chemical reactions. At the same time, mechanochemistry can also generate radicals via the breaking of weak bonds and under extreme surface plasma conditions generated by mechanical impact. However, mechanochemistry is not usually be applied to liquid or

to solid–liquid reactions but in this frame, sonication could represent a viable alternative by virtue of the mechanical and chemical events occurring in liquid medium via the unique phenomenon of acoustic cavitation: the rapid nucleation, growth and collapse of micrometer-scale bubbles generate in the sonicated liquid.

Cavitation, that is a non linear phenomenon that generally depend on external parameters such as frequency, intensity and nature of sonicated solvents, could act by means of two classes of different effects: radical and mechanical ones. The former arises from the sonolysis of molecules which can occur mainly at the bubble interface as well as in the interior cavity. While the latter effect, that follow cavity collapse, originates from shear forces, microjets and shock waves that occur outside the bubble, resulting in profound physical changes when solids or metals are present. Both effects are responsible for speeding up organic transformations thanks to the so-called “mass transfer effect” induced by reaction mixture sonication [3].

Among the above mentioned innovative technologies, sunlight is an abundant and easily accessible energy supply and therefore it can display great potential to activate environmentally benign organic transformations. The use of light would favour chemical synthesis at room temperature, as well as it would avoid thermally induced side reactions. However, this approach suffers from two main drawbacks: the high energy ultraviolet (UV) component is often required to drive the reactions, and usually photochemical reactions give low selectivity to the desired products. Photocatalytic reactions, which can be performed under mild conditions to obtain high product selectivity can easily overcome these disadvantages [4].

This review encompasses four main sections specifically dedicated to the different activation methodology type: MW, US, grinding and light. Each section guides the readers through a series of reactions—from the most common reaction to the more complex one—while examining reaction conditions and peculiar features. The discussion is directed to the importance of combining the homogeneous or heterogeneous catalyst (mainly Pd-based catalyst) with the unconventional techniques in order to overcome the current limitations of organochemistry.

Due to the variety of nanostructured materials and substrates, it has been very difficult to rationalize the order chosen to describe the reported examples. After a brief paragraph on the SMC reaction without any activation procedure, the discussion is focused on the MW-assisted reaction carried out in the presence of an homogeneous and then an heterogeneous catalyst, with the aim to give an overall description on the effects observed on the reactivity (in terms of yields, reaction time and temperature and so on) under MW irradiation. A very short paragraph has been dedicated to Ni catalyzed couplings. Moreover, some information on the effect of MW on the heterogeneous catalysts have been also reported. A special section has been dedicated to the preparation of heterogeneous catalysts for SMC reaction by using MW. Then the discussion moves to the US-assisted SMC and to the use of US to synthesise heterogeneous catalysts for SMC reaction and for MW-assisted SMC reaction. At this point, mechanochemical activation is described and the overview finishes with the use of light to promote the SMC reaction in the presence of opportunely designed photocatalytic systems. The conclusion section gives a description of the main open questions and of the opportunities given by the innovative methodologies in the future scenario.

A Table of contents, that summarises how the review is organized, is here provided for the sake of clarity:

1. Introduction

Some Insights into the Suzuki–Miyaura reaction

2. Microwave-Assisted SMC Reactions

2.1. MW Irradiation in Homogeneous Catalyzed SMC

2.1.1. SMC from Arene to Heterocycle Decoration

2.1.2. Organotrifluoroborates in MW-Assisted SMC

2.1.3. MW-Assisted One-Pot Protocols

- 2.1.4. Ligands in MW-Assisted SMC
- 2.1.5. MW Promoted Ni Catalyzed SMC
- 2.2. Moving from Homogeneous to Heterogeneous Catalysis in MW Promoted SMC
- 2.3. Solid Supported Pd Catalyzed MW Promoted SMC
- Use of MWs for the Synthesis of the Catalysts for the SMC Reaction
- 3. Ultrasound-Assisted SMC Reactions
 - 3.1. Ultrasound-Assisted SMC Reactions
 - 3.2. Ultrasound Assisted Heterogeneous Preparation of Catalysts Suitable for SMC Reactions
 - 3.3. Ultrasound Assisted Heterogeneous Catalyst Preparation for MW Promoted SMC Reactions
- 4. Mechanochemical Activation of SMC
- 5. When the SMC Reaction is Driven by Light
- 6. Conclusions and Future Perspectives

Some Insights into the Suzuki–Miyaura Reaction

The Suzuki–Miyaura cross-coupling reaction (SMC hereafter) was first reported in 1979 and was rapidly adopted by most synthetic labs as the method of choice for the formation of aliphatic and aromatic C–C bonds [5–8]. The coupling of organoboron reagents with organic halides or pseudohalides in the presence of a palladium (or nickel) catalyst and a base is now a classic procedure, even at the industrial level, for the synthesis of fine chemicals, natural products, pharmaceuticals and polymers [9,10]. The literature bears witness to the enormous impact that this reaction has had, as documented by the 700 reviews published. Furthermore, every year of the last decade has seen around 50–60 surveys highlight the versatility and the peculiar advantages of SMC. Of these advantages, low toxicity, easy access to organoboron reagents, their chemoselectivity and mild reaction conditions are perhaps most significant [11]. Greener protocols have been widely described, several of which are carried out in aqueous solvents thanks to the stability of boronic acids in water [12–14], however, the poor solubility of substrates and the low stability of metal catalysts in water mean that phase-transfer catalysts and water-soluble phosphine ligands have been used [15]. Transition metal nanoparticles (e.g., Pd, Fe) can be deposited onto the surface of the mesoporous nanocomposites through a mechanochemical protocol recently SMC have been performed in the solid-state under mechanochemical activation and a green approach to protocol optimization evaluates the catalyst recycling [16]. In this review, the most important eco-compatible activation methods in SMC, including microwaves (MW), ultrasound, grinding (mechanochemistry), light, and the main advances made over last few years will be described. The use of non-conventional energy sources is a challenging topic that has paved the way for new opportunities in the design of clean and efficient synthetic processes.

2. Microwave-Assisted SMC Reactions

2.1. MW Irradiation in Homogeneous Catalyzed SMC

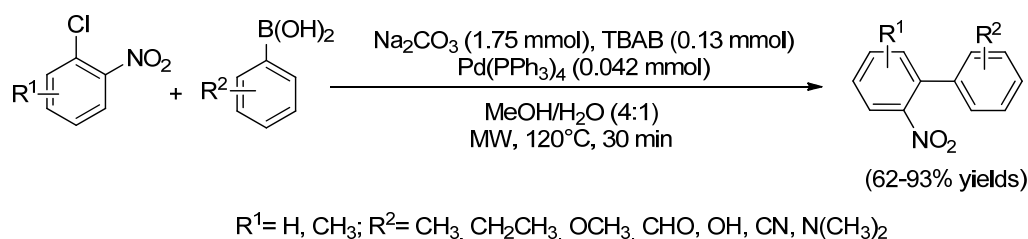
2.1.1. SMC from Arenes to Heterocycles

MW-assisted organic syntheses have recently been receiving ever increasing attention as they are seen as a viable alternative to conventional heating. It enables the rapid optimization of procedures to be carried out without the need for direct contact between chemical reactants and the energy source. The main advantage of MW irradiation is fast volumetric heating. Differences in solvent and reactant dielectric constants mean that selective dielectric heating can furnish notable enhancement in the directly transfer of energy to the reactants, which induces an instantaneous internal temperature increase [17]. Recent years have seen the use of MW-induced heating become one of the most efficient procedures for carrying out organic syntheses and, in the last 20 years, the scientific community has focused on the search for MW assisted procedures to carry out environmentally friendly SMC [18,19]. Moreover, the high versatility of SMC is becoming more prominent thanks to

the number of commercially available reagents and several SMC procedures have been already reported in the *Journal of Chemical Education* [20–22]. A valuable example describes MW-assisted methods for the preparation of 5-phenyl-2-hydroxyacetophenone derivatives in water with K_2CO_3 , tetrabutylammonium bromide (TBAB) and $Pd(OAc)_2$ (15 min irradiation at 400 W, 150 °C) [23].

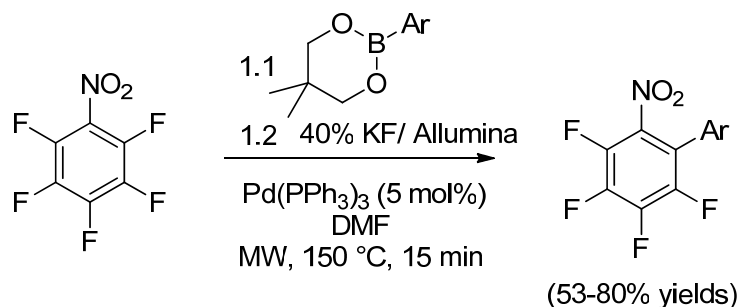
The haloaromatic electrophilic species used in metal-catalyzed processes are commonly aryl iodides or bromides as the catalyst can undergo oxidative addition into fairly weak carbon-iodine or carbon-bromine bonds quite easily, while aryl chlorides are employed more rarely as the electrophilic coupling partner is much less reactive due to the higher carbon-chlorine bond strength. SMC can also be performed with aryl pseudohalides such as sulfonates (such as triflates, mesitates and tosilates) affording to biaryl under mild condition.

The low reactivity of chloro-arenes as reaction partners in cross-coupling reactions means that advances in these protocols have only been obtained in presence of various palladium complexes and using ingenious and dedicated ligands. The efficacy of MW irradiation in this protocol has been demonstrated by Bjørsvik et al. who developed a MW-promoted C–C coupling between highly substituted and congested 1-chloro-2-nitrobenzene and phenylboronic acid (Scheme 1) [24]. The reactions were performed in MeOH and water (4:1), using $Pd(PPh_3)_4$ as the catalyst, Na_2CO_3 and TBAB for 30 min under MW irradiation at 120 °C.



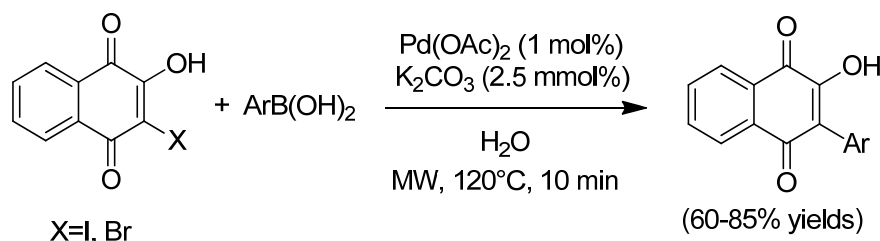
Scheme 1. Microwave (MW)-promoted C–C coupling between highly substituted and congested 1-chloro-2-nitrobenzene and phenylboronic acid.

For the same reasons to those that have already been discussed, analogous reactions involving metal-catalyzed C–F activation are rarer still due to the very strong carbon-fluorine bond. Nevertheless, different nickel catalyzed SMC [25] and some successful reactions involving cobalt [26], platinum [27] and titanium [28] species have been reported. There remain only a few other examples of analogous Pd-catalyzed syntheses [29]. In fact, Cargill et al. have reported [30] the first example of a Pd-catalyzed SMC reaction of perfluoroaromatic systems under MW irradiation. They described how highly fluorinated nitrobenzene derivatives undergo regioselective SMC reactions via the $Pd(0)$ catalyst's insertion into a C–F bond located *ortho* to the nitro group. The arylation of pentafluoronitrobenzene is the synthetic strategy used to obtain the previously unreported 2,3,4,5-tetrafluoro-6-nitrobiphenyl derivatives. Tetrafluoronitrobenzene and trifluoronitrobenzene systems are less reactive than pentafluoronitrobenzene, by virtue of the corresponding decrease in the aromatic ring electrophilicity. The MW irradiation for this SMC process was applied across a rapid and reproducible heating profile. C–F activation was ensured by a catalytic cycle in which the nitro group directs the nucleophilic Pd center to the contiguous C–F bond which also explains the *ortho* regiospecific arylation. Of the various catalytic systems tested, $Pd(0)$ catalysts were noted to be far more efficient than $Pd(II)$ analogues, especially in polar solvents. Pentafluoronitrobenzene was effectively coupled to different boronic acids and esters bearing both electron-withdrawing and -donating groups and giving yields of 53%–80% under MW irradiation (15 min) in the presence of $Pd(PPh_3)_4$ (5 mol %) (Scheme 2).



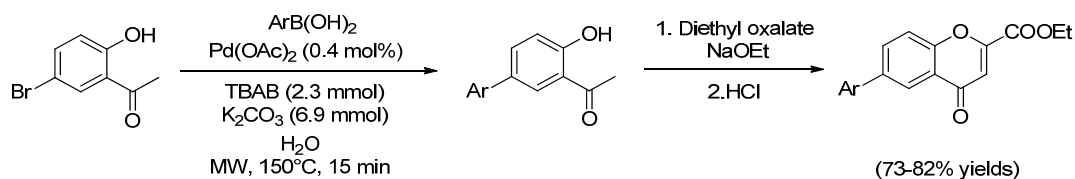
Scheme 2. Pd catalyzed MW promoted SMC of pentafluoronitrobenzene.

Arylation is an approach that affords structural modifications to quinones and naphthoquinones as well as being able to synthesize new substances with biological activity. Besides a few reports related to the arylation of unprotected 2-hydroxy-1,4-naphthoquinones, an interesting green approach has been published by Louvis et al. [31]. A set of 3-aryl-2-hydroxy-1,4-naphthoquinone analogues of atovaquone were synthesized from 3-iodo-2-hydroxy-1,4-naphthoquinone under aqueous conditions either using conventional heating or MW irradiation and phosphine-free sources of Pd (Scheme 3). MW irradiation improved the reaction rate (10 min versus 6 h) and good results were obtained using a lower loading of palladium (1% with irradiation versus 5% with conventional, $P = 300$ W, $T = 120$ °C, 10 min). In fact, intensive deiodination to obtain the Lawsone derivative occurred when 5% Pd(OAc)₂ was used, but side product production was surprisingly limited when using MW heating and a lower amount of catalyst. Furthermore, the authors also obtained the greatest conversion from 3-bromo-2-hydroxy-1,4-naphthoquinone with 5% of the Pd(OAc)₂ after 25 min at 120 °C under MW irradiation; 40% yield was obtained using phenylboronic acid.



Scheme 3. Synthesis of 3-aryl-2-hydroxy-1,4-naphthoquinone analogues.

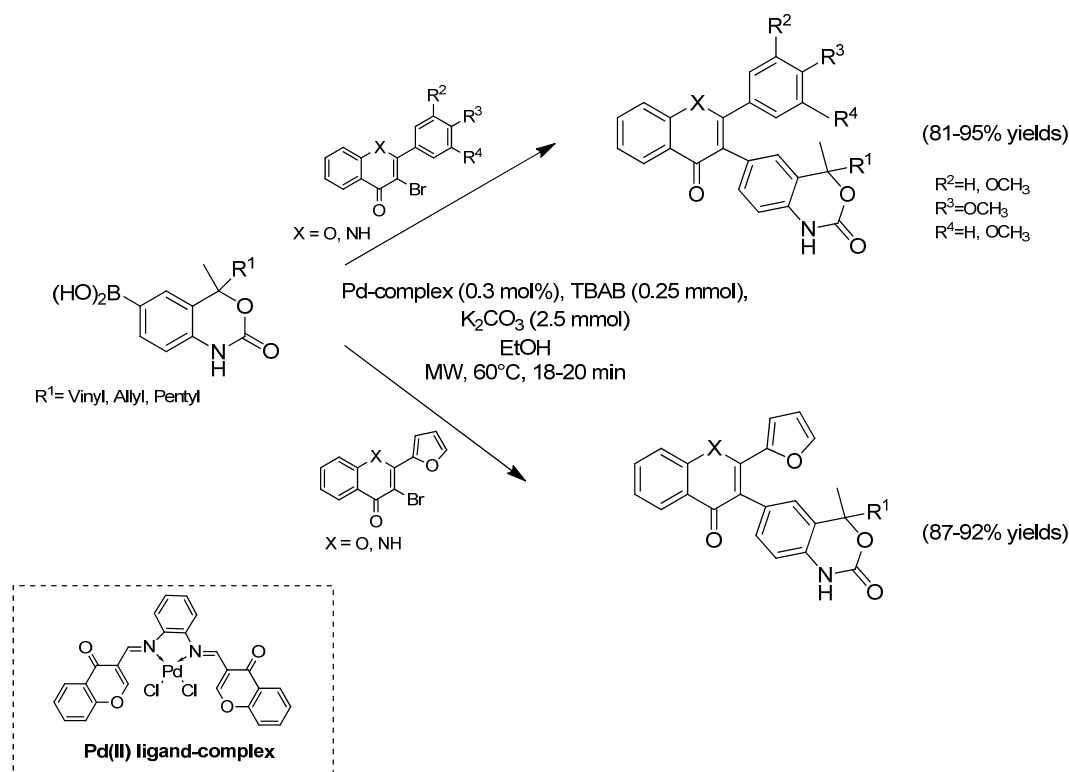
Biaryl chromone can be obtained in two steps route by performing a MW promoted SMC from 5-bromo-2-hydroxyacetophenone followed by condensation reaction with ethyl oxalate and intramolecular cyclization in HCl in acetic acid (Scheme 4). The Suzuki reaction gave high yields (73%–82%) when performed with a series of boronic acids in water with TBAB, K₂CO₃ and Pd(OAc)₂ at 150 °C for 15 min [32].



Scheme 4. Synthetic strategy used for the obtention of ethyl-6-phenyl-4-oxo-4H-chromene-2-carboxylate.

3-bromo-4H-chromen-4-one derivatives were also successfully arylated under MW irradiation at 60 °C in ethanol using K₂CO₃ and TBAB with 0.3 mol % of the Pd-complex derived from the

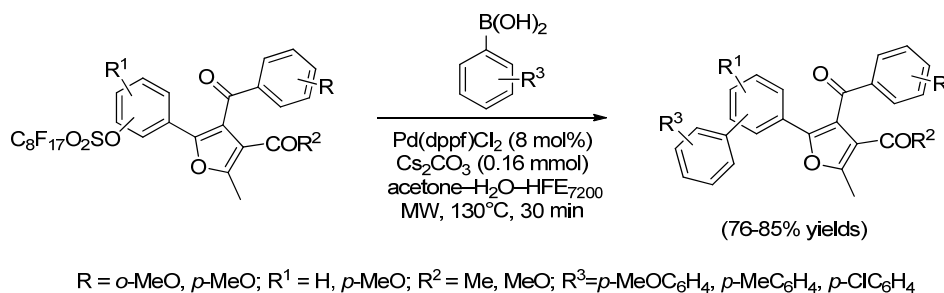
chromen-4-one and naphthalene-1,2-diamine, (Scheme 5). The ligand was synthesized by the authors and a series of 24 different chromen-4-ones were obtained via SMC with excellent yields (81%–95%) [33].



Scheme 5. Synthesis of 3-aryl-4H-chromen-4-one derivatives.

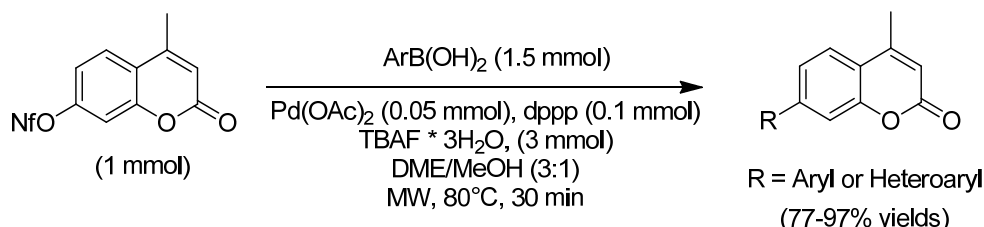
Pseudo halide such as sulfonate can be efficiently employed in the MW promoted SMC and recently 6-aryl salicilates were obtained from the triflates with 1% of $Pd(PPh_3)_4$ and 2 equiv. of $NaHCO_3$ in dimethyl ether (DME) at 110 °C in 4–10 min. The reaction tolerated significant structural modification of the aryl boronic acid and both electron rich, electron poor aryl as well as alkenyl boronic acid afforded good yields [34].

Furans are a key class of compounds that exist in many natural and pharmaceutical products. In fact, Kadam et al. [35] envisioned that MW irradiation may be used for the fast preparation of tetrasubstituted furanes. They described a fast three-step synthesis for tetrasubstituted furanes which included the condensation of a fluoros benzaldehyde with acetophenone followed by a Michael-type [3 + 2] cycloaddition with an 1,3-diketone and a Pd-catalyzed coupling reaction for fluoros linker cleavage. A fluoros sulfonate linker facilitated furane intermediate purification via fluoros solid-phase extraction and proved to be an effective triflate alternative for Pd-catalyzed SMC. Tetra-substituted furan products were produced from MW assisted SMC reactions between arylboronic acids and fluoros furan intermediates. Good yields (76%–85%) were described in 30 min at 130 °C when using $Pd(dppf)Cl_2$ (8 mol %) as a catalyst and Cs_2CO_3 as a base in acetone– H_2O –HFE7200 (hydrofluoroether 7200) (Scheme 6).



Scheme 6. Synthesis of tetra-substituted furans by SMC.

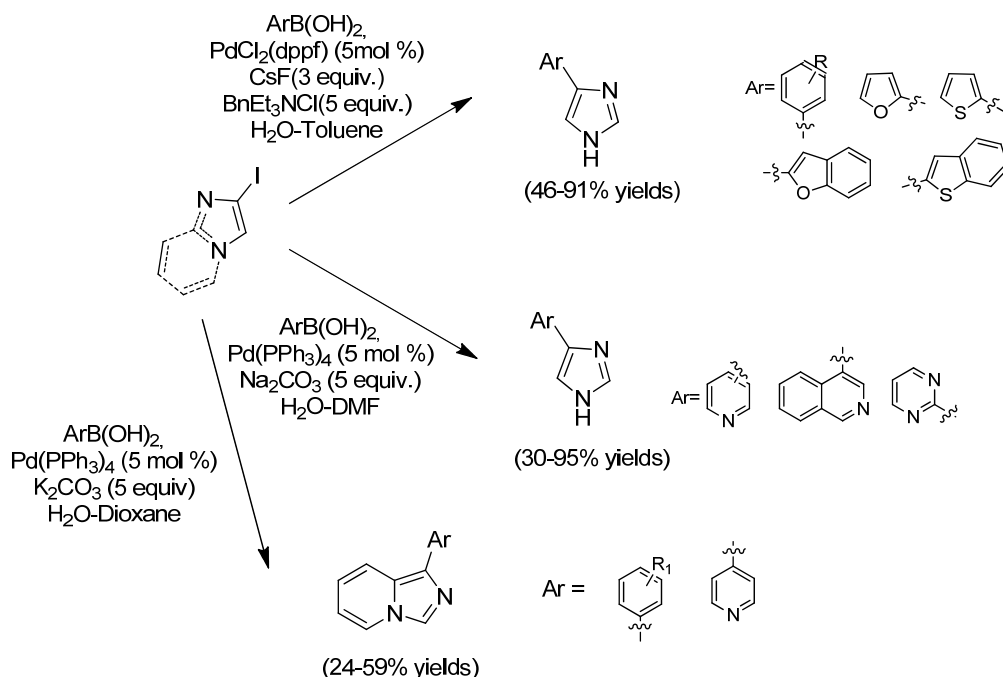
The considerable pharmacological activity of 7-substituted coumarins has made them the focus of great interest as the scientific community searches for new synthetic protocols for the preparation of biologically active molecules. SMC under MW irradiation has been studied by Joy et al. to modify coumarine 7-nonaflate, which shows higher stability and reactivity over the corresponding triflate [36]. In the optimization of the reaction conditions, the authors thought that the nature of the ligand would have a critical influence on achieving the desired product. 1,3-bis(diphenylphosphino) propane (dppp) gave the best results, as ligands with a moderate bite angle can form a divalent square planar complex which, in turn, enhances reductive elimination despite the presence of competitive side reactions, such as β -hydride elimination and substitution reactions. As depicted in Scheme 7, the reaction afforded the preparation of a large series of compounds in moderate to excellent yields using $\text{Pd}(\text{OAc})_2$, dppp and tetrabutylammonium fluoride (TBAF) in DME-MeOH at 80 °C for 30 min. Electron poor boronic acid was the most critical substrate and provided lower yields even when reaction time was increased to 1 h. In an attempt to explain the mechanism, the authors suggested that TBAF was able to influence the stabilization of the oxidative adduct, which facilitates the transmetalation.



Scheme 7. SMC applied to 7-substituted coumarins preparation.

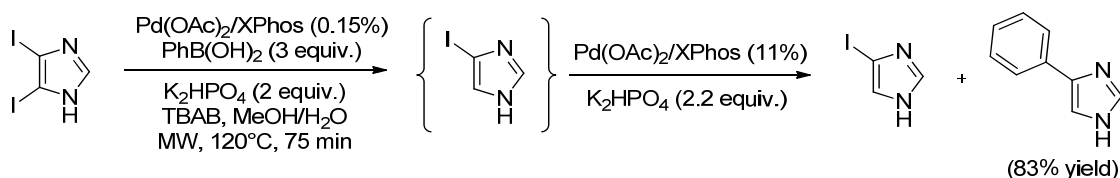
As part of the search for new procedures for the production of original small-molecules, a MW promoted SMC for the preparation of a wide range of 4(5)-arylated imidazoles has been introduced by Pochet et al. (Scheme 8) [37]. The C-4 arylation of (NH)-imidazole generally requires long reaction times (up to 48 h) and is limited to stable arylboronic acid. 4-iodo and 4-bromo-1*H*-imidazole were reacted with 2-naphthylboronic acid in the presence of 2 equiv. of CsF, 5 mol % of $\text{PdCl}_2(\text{dppf})$ and 5 mol % of BnEt_3NCl in a 1/1 mixture of toluene/water under MW irradiation at 110 °C. After 2 h, the bromide derivative was totally converted and the expected compound was isolated in a 90% yield (92% of yield after 72 h under classical thermal conditions); total conversion of the iodine was obtained in 2 h. Furthermore, other boronic acids, bearing nitrogen (pyridinyl, isoquinoline and pyrimidinylboronic acids) and sensitive functional groups (aldehyde), were reacted with the 4-iodo-1*H*-imidazole with $\text{Pd}(\text{PPh}_3)_4$ as the catalyst and Na_2CO_3 in a mixture of dimethylformamide (DMF)/ H_2O at 110 °C under MW irradiation, furnishing the desired products in moderate to excellent yields (35%–95%). Analogously, the imidazo[1,5-*d*]pyridine ring was used as a core structure and was decorated by SMC, in position 1, in the presence of $\text{Pd}(\text{PPh}_3)_4$ and K_2CO_3 in 1,4-dioxane at reflux temperature for 24 h. MW-irradiation (110 °C) was found to accelerate the reaction. In a separate

work, a starting aryl iodide was fully converted to afford the desired products in a comparable yield in 1 h [38].



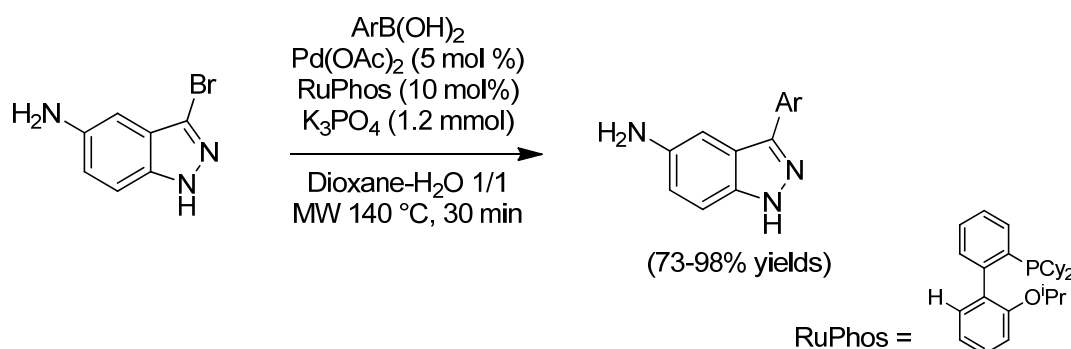
Scheme 8. Synthesis of arylated imidazoles and arylated imidazo[1,5-*a*]pyridine.

Sandtorv and Bjørsvik [39] have reported the first three-way switchable Pd-catalyzed protocol for the selective arylation and hydrodehalogenation of imidazole backbones. Using these MW promoted strategies, they prepared a wide range of 4,5-diaryl- and 4(5)-iodo-1*H*-imidazoles via the selective arylation and the hydrodehalogenation of the imidazole backbone, respectively. When the two strategies were combined in a sequential tandem reaction, they were able to successfully produce 4(5)-aryl-1*H*-imidazoles in excellent yields. Pd(OAc)₂/Xphos was used as the catalytic system in the presence of K₂HPO₄ for the SMC reaction, but two different products were achieved; a cross-coupling product and the unexpected hydrodehalogenation ones (Scheme 9). A series of control experiments was performed in order to shed light on this issue. The tuning of reaction conditions highlighted the fact that only a base was essential in the reaction mixture for hydrodehalogenation. However, they observed that it was possible to perform dehalogenation in the absence of PhB(OH)₂ and base by increasing the reaction temperature and time slightly. The author realized that hydrodehalogenation and cross-coupling processes could be coupled into a “dose-promoted” MW assisted tandem reaction in which the “trigger” for the subsequent catalytic cycle was a rise in the base and catalyst loadings to achieve a mono-arylated imidazole in excellent yields (83%).



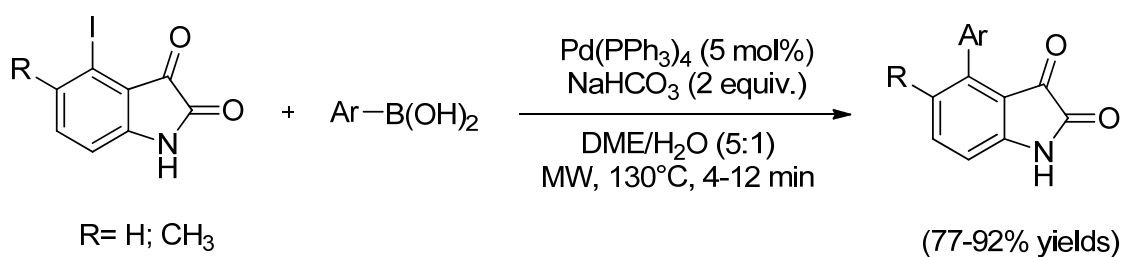
Scheme 9. “Dose promoted” assisted tandem reaction involving a hydrodehalogenation and a SMC to perform synthetic transformations on the imidazole.

Furthermore, (NH) free 3-bromo-indazol-5-amine can react with arylboronic acid in the presence of 5 mol % of Pd(OAc)₂, 10 mol % of RuPhos and K₃PO₄ in dioxane/H₂O = 1/1 at 140 °C under MW-assisted conditions for 30 min. In fact, a series of 19 azaindole derivatives have been synthesized, by Wu et al., with excellent yields (Scheme 10) using this method [40]. Following the same procedure the authors reacted heteroaryl boronic acid and moderate to good yields were obtained. Only thiophen-2-ylboronic acid and pyridin-3-ylboronic acid requested more excess and only pyridin-4-ylboronic acid provided a poor yield in this system even though the loading of the boronic acid was increased and the reaction time was prolonged.



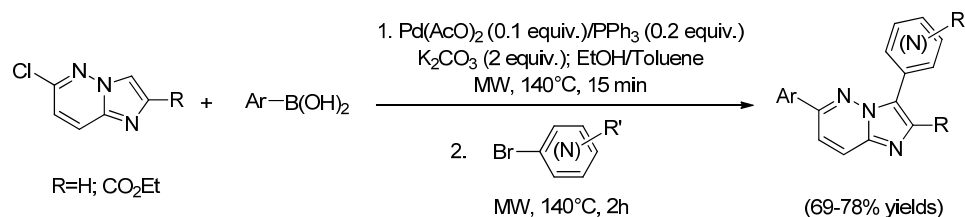
Scheme 10. SMC applied to derivatization of (NH) free 3-bromo-indazol-5-amine.

Another important class of bioactive heterocycle is isatin derivatives (indoline-2,3-diones). A limited number of reports have dealt with the the synthesis of 4-substituted-arylisatins. MW irradiation has been used in the synthesis of bulky 4-substituted-arylisatins via SMC, by Liu et al., using a wide range of substrates [41] (Scheme 11). All of the Pd catalyzed reactions were carried out using 5 mol % of Pd(PPh₃)₄ in the presence of 2 equiv. of NaHCO₃ and afforded very good yields (77%–92%) in DME/H₂O (5:1). This result indicates that electronic effects and steric modification have little influence on the reaction.



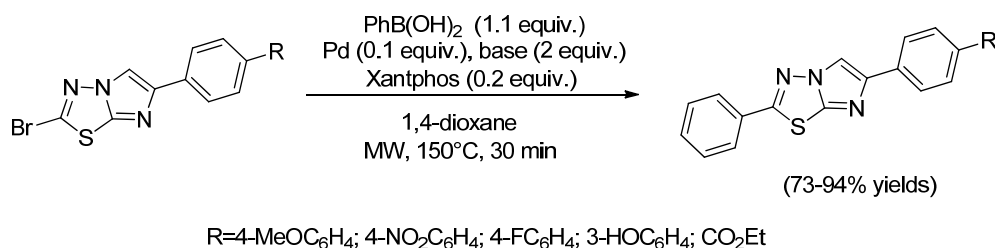
Scheme 11. MW-assisted reaction of various boronic acids and 4-iodo isatin.

El Akkaoui et al. (2010) [42] have demonstrated the flexibility of a MW-assisted, one-pot, two-step SMC/Pd-catalysed arylation process for the fast preparation of a library of different polysubstituted imidazo[1,2-*b*]pyridazine products in good yields (69%–78%) (Scheme 12). The first arylation step was performed in toluene/EtOH from 6-chloroimidazo[1,2-*b*]pyridazine in the presence of Pd acetate (0.1 equiv.), triphenylphosphine (0.2 equiv.), K₂CO₃ (2 equiv.) and various boronic acids (1.1 equiv.). The reaction was irradiated first for 15 min at 140 °C (SMC) and subsequently for 2 h at the same temperature for the final arylation, after aryl bromide was added (1.5 equiv.).



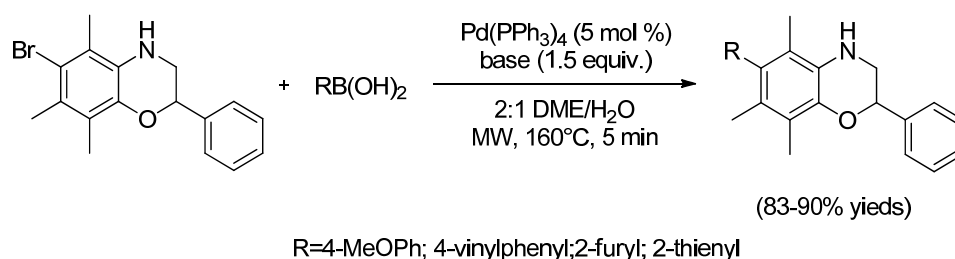
Scheme 12. Pd-catalysed one pot arylation of imidazo[1,2-*b*]pyridazines under MW irradiation.

Imidazo[2,1-*b*][1,3,4]thiadiazole scaffolds are another useful building block in pharmaceutical chemistry. Hence, there has been massive interest in establishing efficient synthetic methodologies for the regioselective preparation of polysubstituted imidazo[2,1-*b*][1,3,4]thiadiazoles. Copin et al. (2012) [43] has carried out some extensive research into developing preparative methods for these molecules, starting from a number of 2-bromo-imidazo[2,1-*b*][1,3,4]thiadiazole derivatives and using a MW assisted SMC strategy (Scheme 13). The Pd catalyzed coupling reaction was optimized under MW conditions using Pd(AcO)₂ (0.1 equiv.) as the catalyst in the presence of Xantphos (0.2 equiv.) and K₂CO₃ (2 equiv.) in 1,4-dioxane at 150 °C. The final compounds, which contain the rare imidazo[2,1-*b*][1,3,4]thiadiazole central skeleton, were obtained after 30 min MW irradiation in noticeable yields (73%–94%) in the presence of acid-sensitive- and both electron-withdrawing and electron-donating groups.



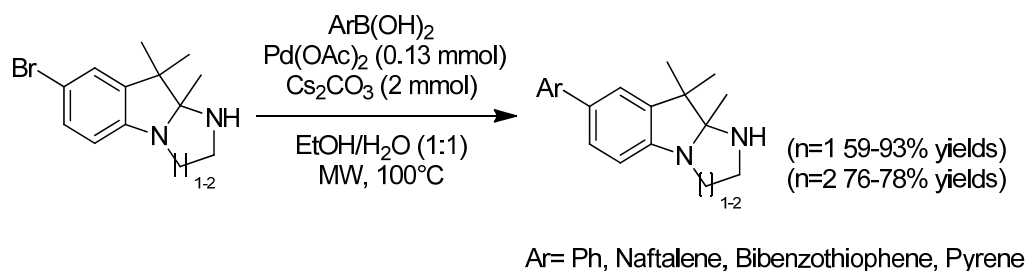
Scheme 13. Decoration of imidazo[2,1-*b*][1,3,4]thiadiazole derivatives through MW promoted SMC reaction.

The 3,4-dihydro-2*H*-1,4-benzoxazine and the 2*H*-1,4-benzoxazine-3-(4*H*)-one structures are widely applied in the synthesis of a plethora of biologically active molecules. No reports on the MW-assisted synthesis of 6-aryl-1,4-benzoxazines/ones, with the most sterically hindered 5,7,8-trimethyl-1,4-benzoxazine/one core, had, until quite recently, appeared in the literature. It is in this context that Koini et al. (2012) [44] reported on an effective MW-assisted SMC strategy for the preparation of 6-substituted-5,7,8-trimethyl-1,4-benzoxazines(ones), using Pd(PPh₃)₄ as the catalyst (Scheme 14). This approach enabled the rapid incorporation of alkyl, aryl, and heteroaryl functionalities into benzoxazine moieties. Under MW heating, the SMC provided good yields at 160 °C in only 5 min using 5 mol % Pd catalyst, Na₂CO₃ and nearly equimolar boronic acid stoichiometry.



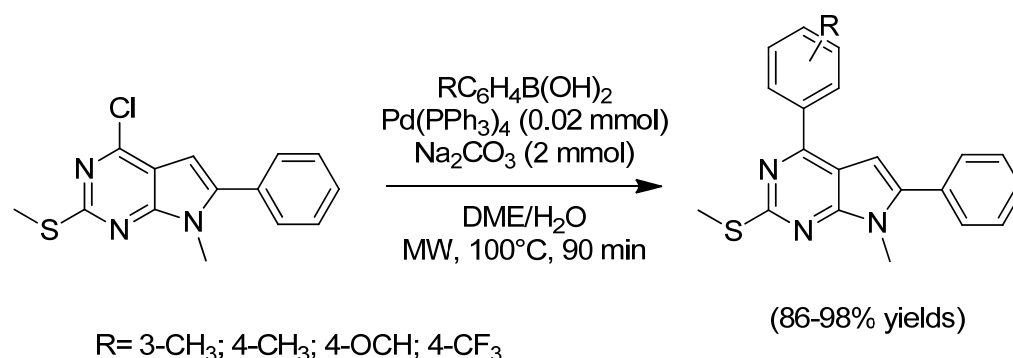
Scheme 14. MW-promoted SMC of 2-phenyl-6-bromo-5,7,8-trimethyl-1,4-benzoxazine with various boronic acids.

Building blocks that bear a benzo[*e*]-annelated indoline moiety exhibit strong fluorescence and can be used as fluorescence emitting dyes. The synthesis of arylated imidazo- and pyrimido-[1,2-*a*]indolone compounds has been approached by Zukauskaitė et al. SMC was performed in the presence of a series of boronic acids that possess a π -conjugated biaryl-based structural unit as a fluorophore (phenylboronic, naphthalen-2-ylboronic, pyren-1-ylboronic and dibenzo[*b,d*]thiophen-4-ylboronic acids). The synthetic protocol was performed in water with ligand-free Pd(OAc)₂ and MW irradiation (50 W) was chosen as the power source (Scheme 15) [45].



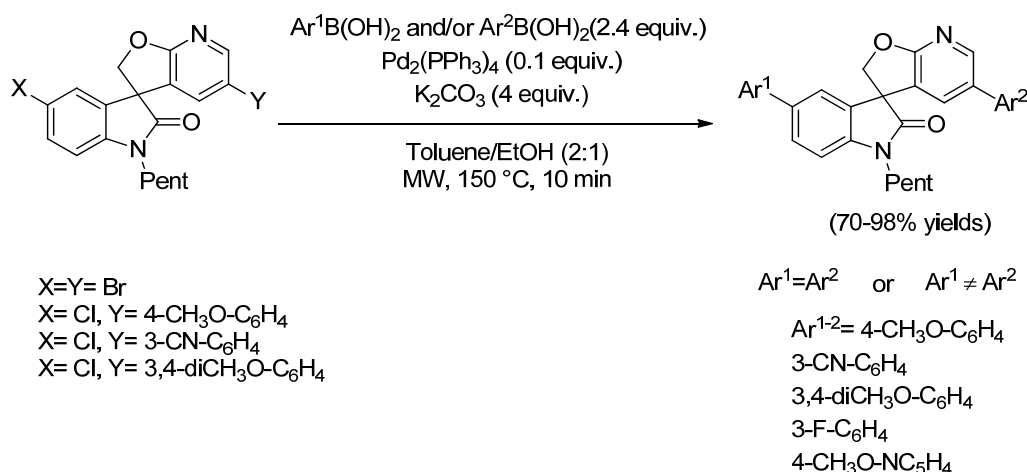
Scheme 15. Synthesis of arylated imidazo- and pyrimido-[1,2-*a*]indolone derivatives.

Arylation of purines and pyrrolopyrimidine at the C-4 and C-2 positions is an interesting task. Conventional condition approaches are known, however, SMC of 4-chloropyrrolopyrimidine derivatives has been performed by Prieur et al. under MW irradiation (Scheme 16) [46]. The synthesis of a series of compounds proved the versatility of the protocol and neither the position nor the nature of the aryl substituent on the boronic acid affected the reaction outcome (yield from 86% to 98%).



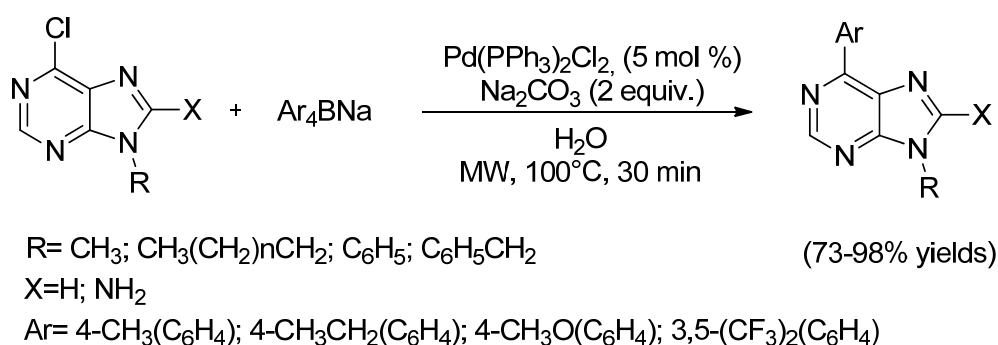
Scheme 16. Derivatization of 4-chloropyrrolopyrimidines derivatives by MW promoted SMC.

The synthesis of highly substituted spirooxindoles remains a great challenge for organic chemists due to their broad biological activities mainly related to voltage-gated ion channels (Na⁺, K⁺, Ca²⁺) regulation related to nociception. Guillaumet et al. (2015) [47] have recently developed a new original method for the preparation of multi-substituted spirooxindoles via SMC strategy (Scheme 17). Through a fast MW assisted palladium catalyzed protocol, the authors prepared a plethora of new C-5'- or C-5-monosubstituted and C-5,C-5'-disubstituted 1'-pentyl-2*H*-spiro[furo[2,3-*b*]pyridine-3,3'-indolin]-2'-one derivatives in only 10 min under MW irradiation at 150 °C by using Pd₂(PPh₃)₄ (0.1 equiv.) in presence of K₂CO₃. This SMC protocol was focused on the functionalization of the phenyl part of the oxindole core or the pyridine nucleus of the starting regioselective brominated or chlorinated spirooxindole moieties to give mono- or disubstituted- derivatives in good to excellent yields (70%–98%).



Scheme 17. MW-promoted C–C coupling leading to disubstituted 5,5'-di(het)aryl-1'-pentyl-2H-spiro[furo[2,3-*b*]pyridine-3,3'-indolin]-2'-ones.

Qu et al. [48] have described a fast and sustainable process for the synthesis of 6-arylpurines from 6-chloropurines and sodium tetraarylborates via a MW assisted SMC reaction in water at 100 °C (Scheme 18). Furthermore, most of the reactions involved are efficient when using Pd(PPh₃)₂Cl₂, 5 mol % catalyst in the presence of Na₂CO₃ (2 equiv.) and furnish the desired products in high yields (73%–98%) in short reaction times (30 min). This eco-friendly MW-assisted method is a promising, green strategy for the preparation of these main nucleoside compounds.

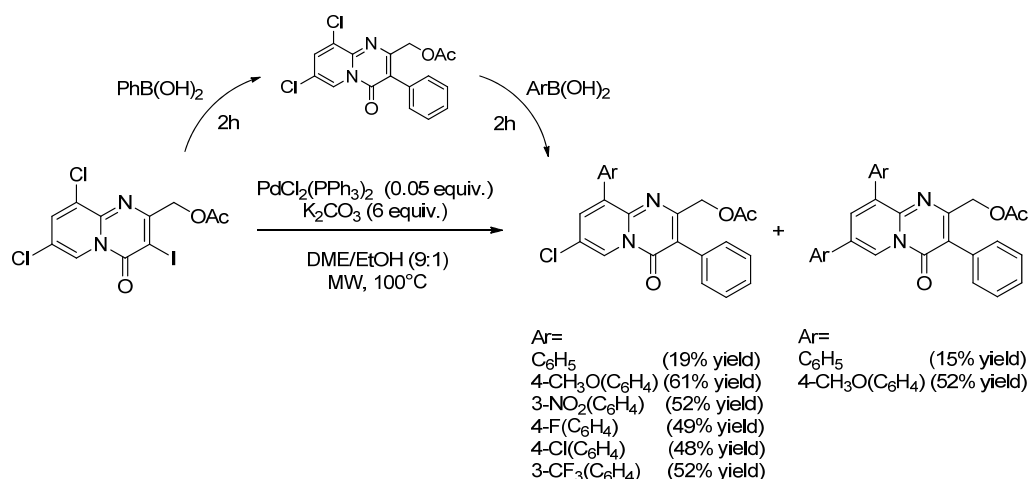


Scheme 18. MW-assisted SMC of Ph₄BNa with various 6-chloropurines.

The 4*H*-pyrido[1,2-*a*]pyrimidin-4-one core has shown itself to be a useful scaffold for the disclosure of new bioactive compounds. In this context, Kabri et al. [49] have reported the first example of a MW assisted Pd catalyzed SMC reaction for the synthesis of a series of 3-aryl, 3-heteroaryl and 3-styryl-4*H*-pyrido[1,2-*a*]pyrimidin-4-ones. The coupling process was proven to be extremely tolerant to electron-poor, electron-rich and bulky boronic acid derivatives, giving the target products in good yields (70%–90%) in 2 h MW irradiation at 100 °C. The best conditions for the MW-assisted, Pd-mediated coupling reactions of aryl, heteroaryl and styrylboronic acid compounds with 7-chloro-3-iodo-4-oxo-4*H*-pyrido[1,2-*a*]pyrimidin-2-yl)methyl acetate were described in DME–EtOH (9:1), using PdCl₂(PPh₃)₂ (0.05 equiv.) as the catalyst in the presence of the base, K₂CO₃ (3 equiv.).

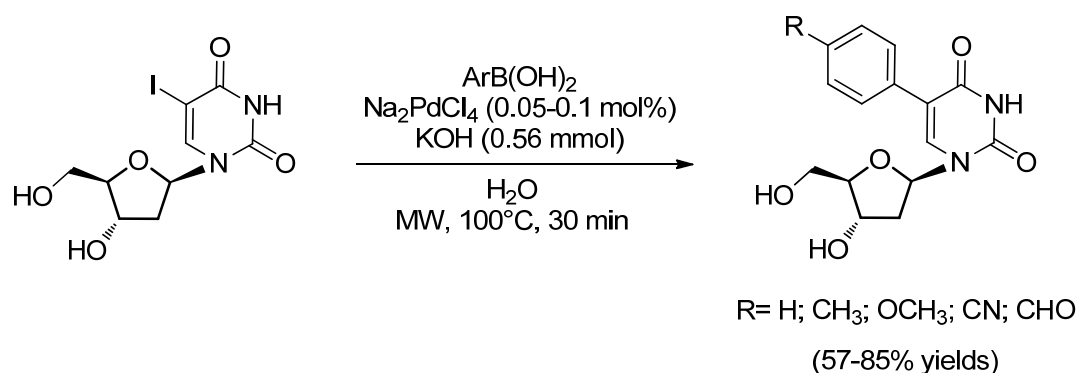
Another study [50] adopted the same efficient Pd-catalyzed procedure to design new and unique asymmetrical 3,9-bis-[(hetero)aryl]-4*H*-pyrido[1,2-*a*]pyrimidin-4-one compounds. They developed a MW one-pot chemoselective bis-SMC protocol that almost gave good 4*H*-pyrido[1,2-*a*]pyrimidin-4-ones yields (Scheme 19). Stepwise substitution at the 3- and then at the 7- and/or 9-position of 7,9-dichloro-

3-iodo-4-oxo-4*H*-pyrido[1,2-*a*]pyrimidin-2-yl)methyl acetate, using a range of boronic acids in a one-pot process, enabled the efficient and fast synthesis of chemical libraries of bioactive derivatives to be carried out. The same approach was more recently pursued by the same authors to obtain 2,6,8-trisubstituted 4-aminoquinazolines through MW-assisted consecutive one-pot chemoselective tris-SMC or *S*_NAr/bis-SMC reactions in water [51].



Scheme 19. One-Pot chemoselective bis-SMC gives simple access to 3,9-biaryl and 3,7,9-triaryl-4*H*-pyrido[1,2-*a*]pyrimidin-4-ones.

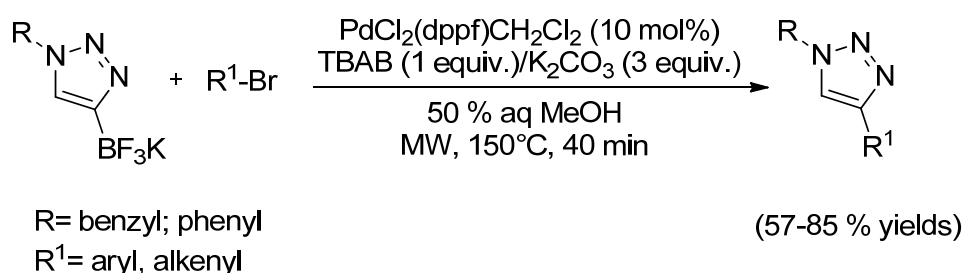
Several nucleoside analogues have recently attracted considerable attention due to their potential biological properties. Analogues that bear a C-aryl group on the glycone or aglycone section have been more intensively studied. In fact, an easy and efficient procedure for the direct synthesis of 5-aryl-2'-deoxyuridines has been reported, by Gallagher-Duval et al. [52], via a ligand-free SMC strategy which starts with totally deprotected 5-iodo-2'-deoxyuridine and different boronic acids and is carried out in pure water. The desired 5-arylated uridine derivatives were synthesized in satisfactory (57%–85%) yields in short reaction times (5–30 min) in the presence of very low Na₂PdCl₄ Pd catalyst loading amounts (0.05–0.1 mol %) and KOH (0.56 mmol) as the base. One protocol was carried out under classical thermal heating, another was performed under MW irradiation at 100 °C (Scheme 20). All reported results show that the desired cross-coupling products were obtained up to three times faster under MW irradiation than classic heating, even in the presence of electron-withdrawing groups in the boronic acid *para* position. Sterically demanding boronic acids proved to be most troublesome substrates for this process.



Scheme 20. Ligandless MW-promoted SMC starting from 5-iodo-2'-deoxyuridine.

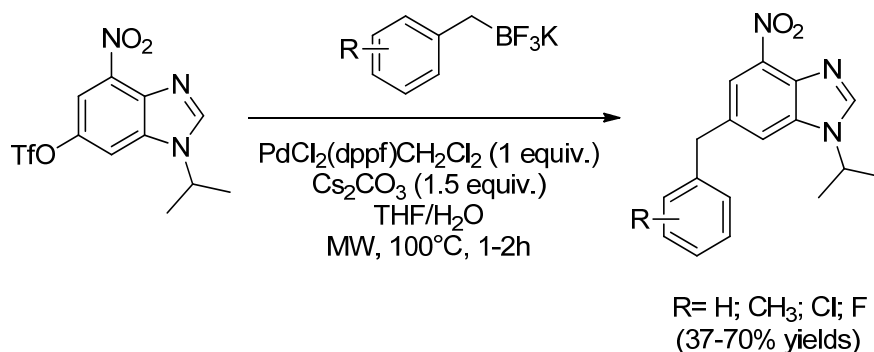
2.1.2. Organotrifluoroborates in MW-Assisted SMC

Potassium organotrifluoroborates have recently become powerful synthetic building blocks for the formation of new carbon–carbon bonds via SMC, as these compounds show greater nucleophilicity than their corresponding organoboranes or boronic acid derivatives and are simple to synthesize and purify. Moreover, as crystalline solids, they are air- and moisture-stable. The inertness of the trifluoroborate ($-\text{BF}_3$) group under common reaction conditions for direct transformation, using Pd or copper catalysts, enables the preparation of highly functionalized organotrifluoroborates to be performed [53,54]. In this context, Kim et al. [55] have recently described a sustainable MW assisted SMC process which starts from various triazole-containing trifluoroborates and which was successfully prepared via a regioselective, one-pot Cu-catalyzed azide/alkyne cycloaddition (CuAAC) reaction from ethynyltrifluoroborate. Potassium (1-organo-1*H*-1,2,3-triazol-4-yl)trifluoroborates were successfully cross-coupled with various functionalized aryl and alkenyl bromides under MW conditions. Good yields (88%–90%) were described in aqueous methanol for reactions performed at 150 °C for 40 min in the presence of $\text{PdCl}_2(\text{dppf})\cdot\text{CH}_2\text{Cl}_2$ (10 mol %), TBAB (1 equiv.) and K_2CO_3 under MW irradiation at 80 W (Scheme 21). C–C coupling products were achieved in reasonable yields (57%) even when using sterically bulky coupling alkenes, such as 1,2,2-triphenylvinyl bromide.



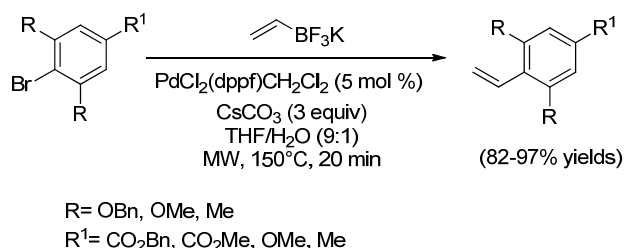
Scheme 21. MW-assisted C–C cross-coupling starting from (1-organo-1*H*-1,2,3-triazol-4-yl) trifluoroborates K salt.

The benzimidazole skeleton is an important heterocycle because of its wide range of pharmacological activities. The formation of a C–C bond at the 6-position of the electron-rich 1-,4-,6-trisubstituted benzimidazole nucleus is challenging and was not obtainable via Kumada, Negishi, Stille or Heck coupling strategies. As a result, Jain et al. [48] have also focused their attention on the advantages of organotrifluoroborate salts as coupling partners for SMC with 4-nitro-6-triflyl benzimidazoles under MW activation in aqueous tetrahydrofuran (THF) [56]. Novel functionalization of 1-,4-,6-trisubstituted benzimidazoles at the 6-position was presented and 37%–70% yields were reported under 1–2 h of MW irradiation at 100 °C in the presence of $\text{PdCl}_2(\text{dppf})\cdot\text{CH}_2\text{Cl}_2$ (1 equiv.) and Cs_2CO_3 (1.5 equiv.) (Scheme 22).



Scheme 22. MW-assisted SMC of potassium organoborates with 6-sulfonate benzimidazoles.

0.091 M with a slight drop in yields). Moreover, the $\text{PdCl}_2(\text{dppf})\text{CH}_2\text{Cl}_2$ catalyst loading was reduced by over three-fold under MW (from 18 to 5 mol %). It maintained good conversions to styrene derivatives, while avoiding side product formation. In addition, it has been observed that vinylation with potassium vinyltrifluoroborate is better fulfilled using ortho and ortho'-substituted aryl halides with at least one electron-withdrawing group present, thus reducing the electron-rich nature of the aromatic halide (as is usual for SMC).

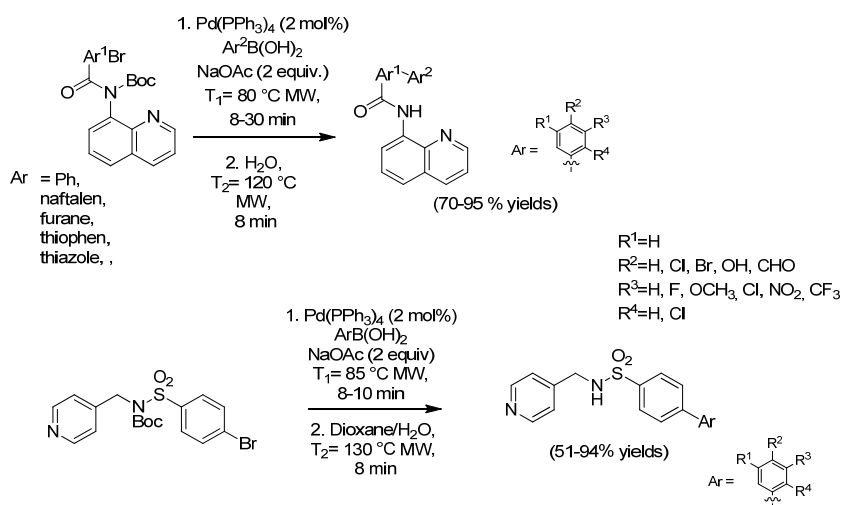


Scheme 24. MW-promoted SMC vinylation of electron-rich, sterically hindered substrates using potassium vinyltrifluoroborate.

2.1.3. MW-Assisted One-Pot Protocols

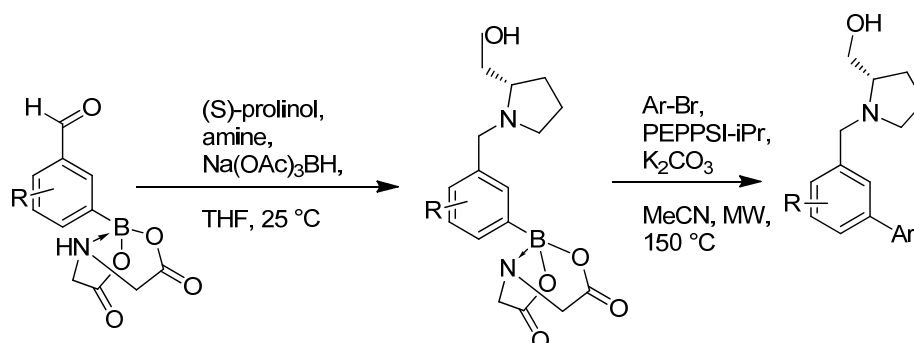
An efficient synthesis of *N*-quinoline 3'/4'-biaryl carboxamides, which avoids the protection/deprotection of the amide function, has recently been described as being based around a one-pot, MW-assisted SMC and *N*-Boc-deprotection sequence [59]. The mixture with 2.0 mol % of $\text{Pd}(\text{PPh}_3)_4$, phenylboronic acid (1 equiv.) and NaOAc (2 equiv.) in dioxane:water was irradiated at 80 °C for 8–30 min. The optimal conditions involved the reaction temperature being increased for the first step and then increased further to 120 °C for 8 min. The reaction proved itself to be well tolerant of valuable, but unstable groups, such as hydroxyl and carbonyl groups, and excellent yields were obtained from the benzamido, naftalen, furane, thiophen and thiazole carboxamidoamido derivatives.

Boc protection of the sulfonamino group also greatly promoted the SMC and, as already described for the Boc carboxamides, MW irradiation in water enabled deprotection to be carried out quickly and efficiently. As depicted in Scheme 25, the one-pot procedure, which combines SMC and Boc-deprotection, can be performed starting with 4-bromo *N*-Boc-benzenesulfonamide via the addition of $\text{P}(\text{PPh}_3)_4$ and arylboronic at 85 °C (MW irradiation) for 8–10 min in the first step, followed by a second step at 130 °C for 8 min [60].



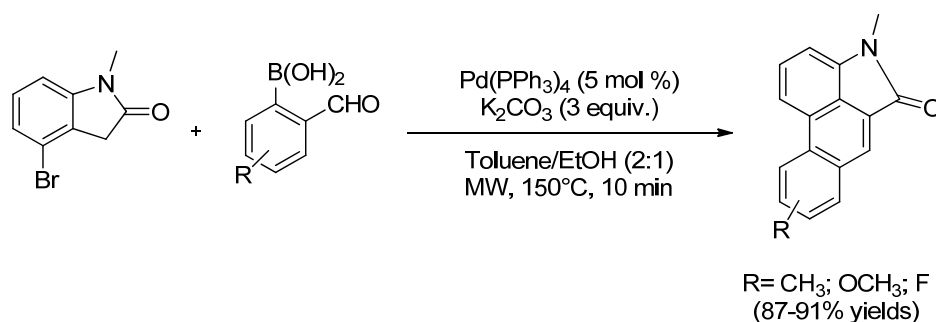
Scheme 25. $\text{Pd}(\text{PPh}_3)_4$ -Catalyzed SMC and *N*-Boc cleavage, one-pot reaction.

The development of synthetic procedures which can perform the parallel synthesis of analogues, where diversity elements are introduced into a multistep sequence, has been the focus of significant interest over the last two decades. This investigation mainly makes use of reactions that are commonly used in the medicinal chemistry, including SMC, one of the most prevalent transformations in drug discovery parallel synthesis. As an application of this approach, a one-pot reductive amination-SMC sequence was proposed by Grob et al. in 2011 (Scheme 26) [61]. Boron-functionalized aryl aldehydes were first subjected to reductive amination and the C–C coupling then gave the diaryl derivative. MIDA (*N*-methyliminodiacetic acid) ligand boronates were selected on the basis of a preliminary screening because of their high stability when undergoing reductive amination. Furthermore, the proposed MW-promoted protocol includes both the deprotection of the MIDA boronate and the subsequent cross-coupling reaction. The authors observed that good yields were achieved with both electron-rich and electron-deficient haloarenes. Interestingly, heteroaryl halides react successfully with examples spanning a wide variation of ring size electronics and substitutions types; the only class that failed in the SMC was the five-membered NH free heterocycles. Relative success was obtained in the assessment of the versatility of reductive amination with amines containing amino-acid derivatives, ethers, esters and heterocycles.



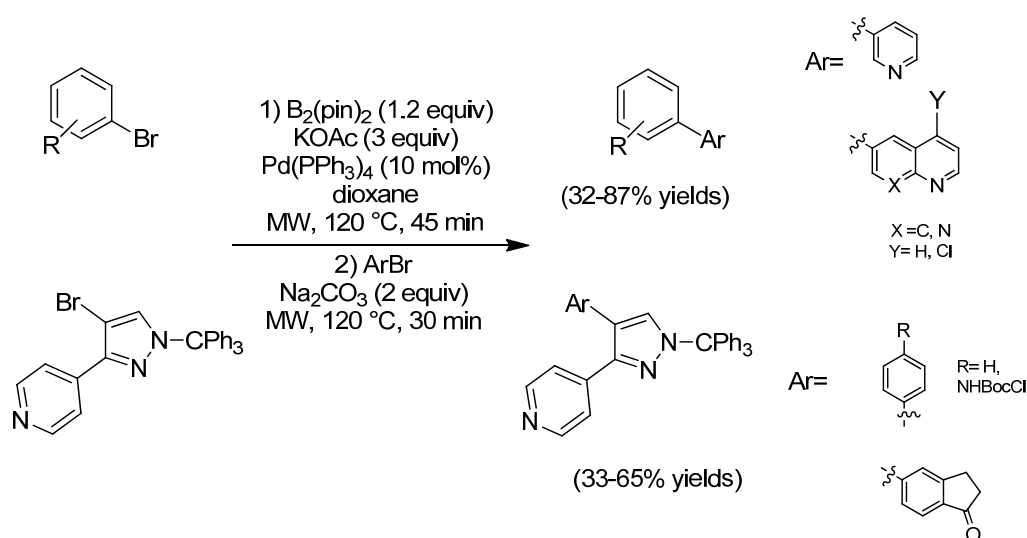
Scheme 26. Preparation of boron-functionalized aryl aldehydes and one-pot synthesis of biphenyl amine.

Park et al. [62] have developed a one-pot method that proceeds via SMC and aldol condensation reactions to obtain naphthoxindoles in good to excellent yields (63%–94%). This reaction afforded an oxindole moiety from 4-bromooxindoles and 2-formylarylboronic acids in 5 min under MW irradiation at 150 °C. Pd(PPh₃)₄ (5 mol %) was used as a catalyst in the presence of K₂CO₃ (1.5 mmol) as the one pot reaction was performed in toluene/EtOH (2:1) (Scheme 27). The described synthetic method was tolerant of various substituents and functional groups, while MW irradiation was used to improve the reaction rate of a wide set of naphthoxindole libraries.



Scheme 27. One-pot synthesis of naphthoxindoles from 4-bromooxindoles by SMC and aldol condensation reactions.

MW irradiation has been applied to a versatile and efficient one-pot borylation/SMC in an attempt to overcome one of the main limitations of the SMC reaction; the lack of availability and/or the instability of certain boronic species [63]. The authors optimized the one-pot model reaction which starts from 5-bromoindanone and 3-bromopyridine to give 3-pyridinylindenone. The transformation is mediated by the formation of the intermediate bis(pinacolato)diboronic (Scheme 28). A change in the base used was crucial to this study. KOAc was used at first to activate the halide within the catalytic complex for the transmetalation step with bis(pinacolato)diboron. Na₂CO₃ was then introduced as a second base, after the formation of pinacolate, to form the biaryl-substituted palladium species. The optimized protocol was performed via the irradiation of a dioxane solution of arylbromide, Pd(PPh₃)₄ and KOAc in a MW oven at 120 °C for 45 min, followed by the addition of a second arylbromide, Na₂CO₃ and further irradiation at 120 °C for 30 min. The author synthesized a large series of diaryl and keto, Boc-protected aniline, halo, aryl, indanone, pyridyl, pyrazole, azaindole and quinoline functional groups to provide a set of hinge-binding fragments. Furthermore, heteroaromatic rings, which either contained a hydrogen bond acceptor, a hydrogen bond donor or both, were coupled in combination with four phenyl halides.

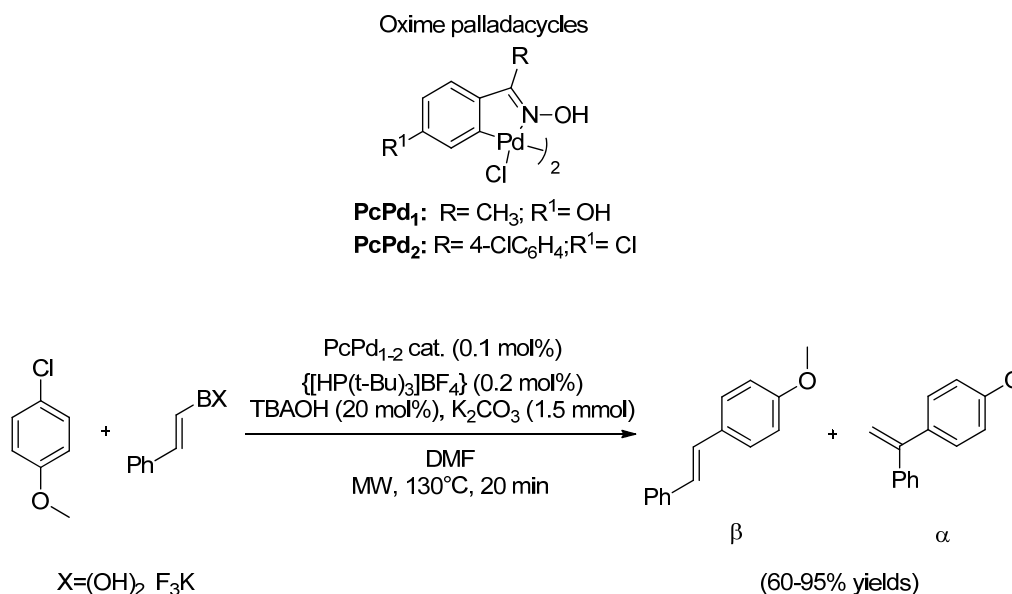


Scheme 28. One-pot borylation/SMC.

2.1.4. Ligands in MW-Assisted SMC

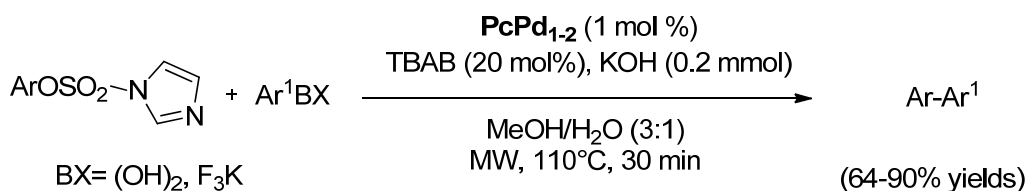
It is well known in literature that palladacycles are efficient pre-catalysts for the SMC reaction. Oxime-derived palladacycles are often chosen because they are known to be (1) stable at high temperature; (2) inert with air and moisture; (3) a pre-catalyst that releases Pd(0) and avoids the formation of large Pd metal particles. In this context, Cívicos et al. [64] have recently demonstrated the high catalytic activity of a number of different oxime palladacycles (Scheme 29) in the SMC of biaryls in aqueous solvents, using both conventional and MW irradiation conditions. The same authors presented a new and simple protocol for the Pd catalyzed SMC alkenylation of deactivated organic chlorides under MW irradiation conditions.

Alkenylboronic acids and potassium alkenyltrifluoroborates are effectively cross-coupled with these aryl and heteroaryl chlorides using the 4,4'-dichlorobenzophenone oxime-sourced palladacycles (**PcPd**₁₋₂) as pre-catalysts at 0.1 to 0.5 mol % Pd loading, tri(*t*-butyl)phosphonium tetrafluoroborate {[HP(*t*-Bu)₃]BF₄} as a ligand, tetra-*n*-butylammonium hydroxide as the co-catalyst and K₂CO₃ in DMF at 130 °C under MW heating (Scheme 29). Alkenylarenes, stilbenes and styrenes were obtained in 60%–95% yields, with high β/α regioselectivity and diastereoselectivity in only 20 min, under these conditions. The reported procedure is also very useful for the regioselective alkenylation of benzyl and allyl chlorides to obtain allylarenes and 1,4-dienes.



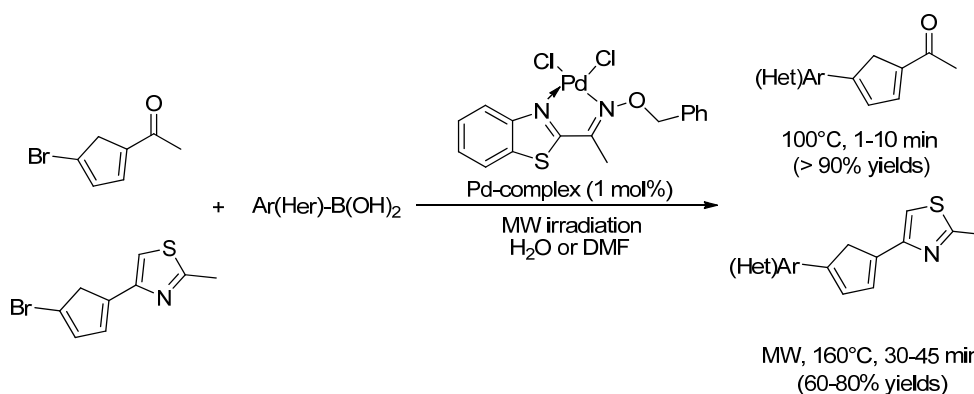
Scheme 29. SMC alkenylation of aryl chlorides.

The same authors proved that the oxime-palladacycle was efficient in arylation and alkenylation when using neutral, electron-rich and electron-poor phenyl imidazolesulfonates (Scheme 30) and also with sterically hindered electrophiles [65]. High isolated yields were obtained. 2-phenylpyridine was synthesized in a high isolated yield (72%) in aqueous conditions from phenylboronic acid and pyridin-2-yl 1*H*-imidazole-1-sulfonate.



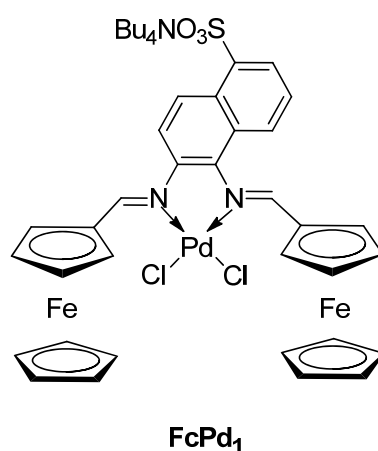
Scheme 30. SMC reaction of aryl imidazolesulfonates with arylboronic acids and potassium aryltrifluoroborates.

The authors underlined the efficiency of MW irradiation in all examples, but in particular with sterically challenging imidazolesulfonate. Remarkable, isolated yields (62%–93%) were also commonly described for the regio- and stereo-selective syntheses of stilbene and styrene compounds, regardless of which nucleophile was used. MW-assisted cross-coupling reactions were performed in the presence of different β -aryl- and β -alkyl-substituted alkenylboronic acids and potassium trifluoroborates. The improved reaction conditions have also proven to be effective in the coupling of electron-deficient electrophiles and heterocycles, such as pyridine-2-yl. Within a bi-functional starting material, the reactivity gap between the C–Br bonds and the C–O imidazolesulfonate bond was exploited by the authors to demonstrate that MW-promoted orthogonal cross-couplings with arylboronic acids primarily afforded the biphenyl-1*H*-imidazole-1-sulfonate via C–Br activation. This product can be subsequently submitted to SMC with phenylboronic acid under aqueous conditions to obtain the desired diarylated derivative (Scheme 31).



Scheme 33. MW-assisted synthesis of 2-acetyl-5-arylthiophenes and 4-(5-arylthiophen-2-yl)thiazoles via SMC.

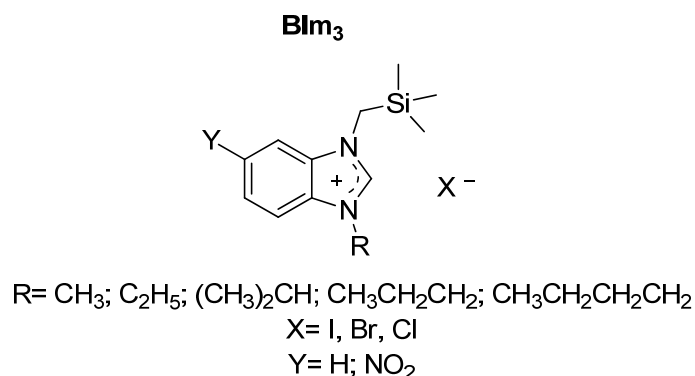
Attempts to exploit aryl chlorides as SMC reaction substrates have led to several catalysts being developed. Of these new catalysts, the use of ferrocene derivatives (**Fc**) as ligands has attracted remarkable attention due to their large size and electron-rich nature. Ferrocene-containing phosphine ligands have been applied, however, the use of other ligands, such as diimines, has gained some limited attention. The use of diimine or pyridylimine ligands, in lieu of phosphine ligands, has major benefits, such as simple synthetic procedures, easy management and easy tuning of the electronic and steric properties of the final catalysts. In this context, Hanhan et al. (2012) [68] have reported the MW assisted SMC, in aqueous media, of different boronic acids with aryl chlorides using a ferrocene-containing Pd(II)–diimine complex as the catalyst. The use of the air-stable diimine ligand, which bears two ferrocene units, was observed to be powerful for SMC reactions due to the sterically demanding character of the ligand and the electron-rich properties of the ferrocene fraction. These features allow the active Pd(0) species to be stabilized in the catalytic cycle and support the reaction. Small amounts of **FcPd₁** (0.1%) (Scheme 34) were found to be powerful in the coupling of different boronic acids with non-activated aryl chlorides to supply sterically hindered ortho-substituted biaryls (yields > 90%) in aqueous medium in the presence of K₂CO₃ (1.5 equiv.) in only 15 min at 800 W. Rather, the use of very low quantities of catalyst (0.0001%) allowed the coupling of aryl iodides and bromides with boronic acids to be carried out in quantitative yields. When **FcPd₁** was compared with other catalysts, that have already been described as used in SMCs, **FcPd₁** did not required any additives, such as TBAB, or solvents other than H₂O.



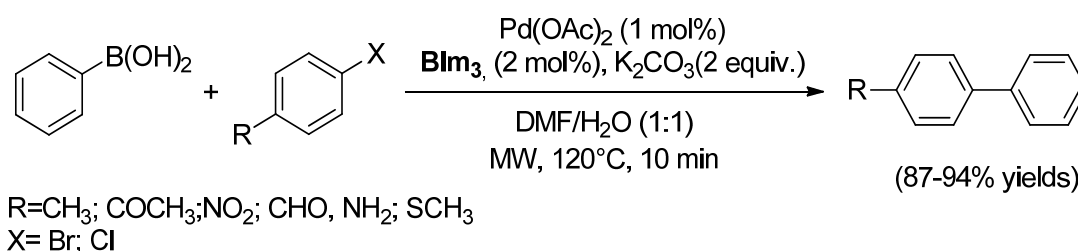
Scheme 34. Ferrocene-based Pd(II)–diimine catalyst.

Palladacycles can possess widespread structural arrangements and synthetic accessibility and, as such, have gained attention as catalytic precursors. In this context, organosulfur ligands are usually

and lower reaction times than under conventional heating. Good reaction yields were also described under optimized MW conditions even when aryl chlorides were used and particularly so with electron withdrawing substituents (94% for $-\text{NO}_2$) (Scheme 38). On the other hand, electron-donating alkyl groups on benzimidazole salts led to better catalytic activity than electron withdrawing groups.

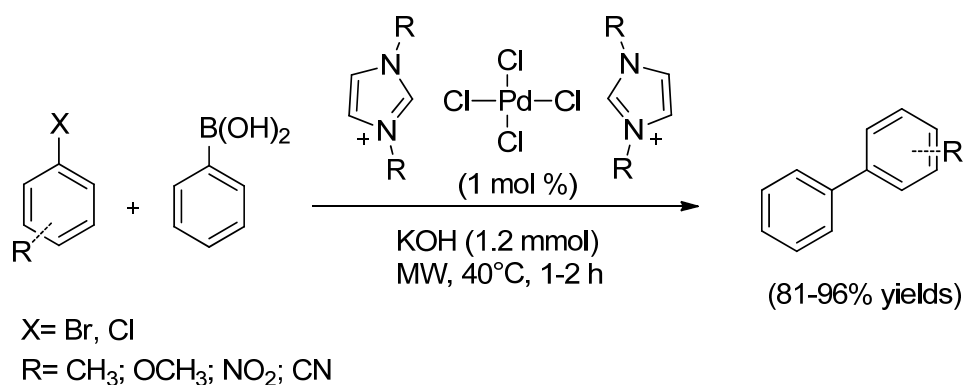


Scheme 37. General structure of benzimidazole salts which contain trimethylsilylmethyl substituent (**Bim₃**).



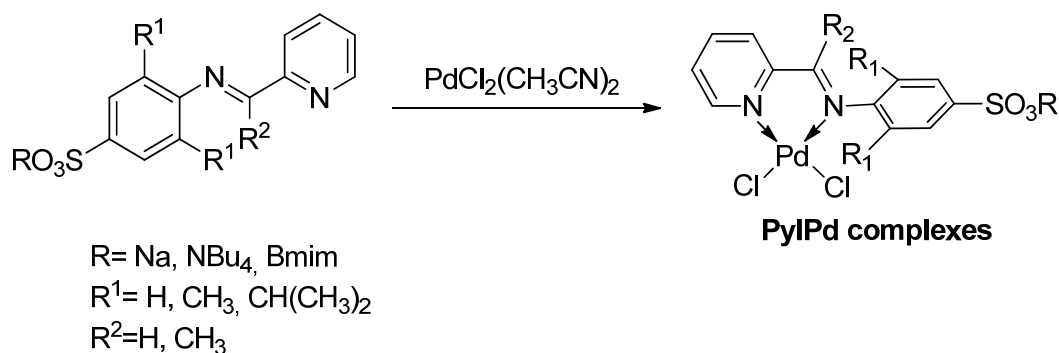
Scheme 38. SMC using **Bim₃** under MW irradiation.

Of the phosphine-free (ligand-free) Pd catalysts available for use, anionic Pd complexes with imidazolium based ionic liquids have recently attracted increased attention. In this context, Pd complexes of the $[\text{IL}]_2[\text{PdCl}_4]$ (IL = imidazolium cation) type have been shown to be effective catalysts when used in the SMC of phenylboronic acid with 2-bromotoluene, in the presence of aqueous or pure 2-propanol at 40 °C under MW. In 2-propanol, the maximum yields (89% and 85%) have been described by Silarska et al. [72] for $[\text{dmiop}]_2[\text{PdCl}_4]$ and $[\text{dmdim}][\text{PdCl}_4]$ (dmiop = 1,2-dimethyl-3-propoxymethylimidazolium cation, dmdim = 3,3'-[1,7-(2,6-dioxheptane)]bis(1,2-dimethylimidazolium) cation) which contain cations with a methyl group at the C2 position. When water was used, all $[\text{IL}]_2[\text{PdCl}_4]$ complexes produced ca. 90% of the 2-methylbiphenyl product. Excellent results were also reported in the C–C cross coupling reaction of various aryl bromides and chlorides (81%–96% yields) (Scheme 39). For instance, the conversion of 2-chlorotoluene was 71% at 70 °C. The formation of Pd(0) nanoparticles during the catalytic reaction was identified by transmission electron microscopy (TEM) and confirmed by mechanistic studies, also involving Hg(0) tests, showing that active soluble Pd species could be generated from Pd(0) nanoparticles in catalytically amounts.



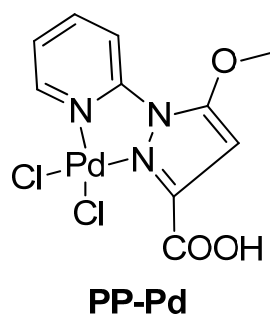
Scheme 39. SMC in the presence of [IL]₂[PdCl₄] complexes, used as efficient catalysts.

Pyridyl-imine and diimine type ligands are very helpful for designing homogeneous catalysts due to their easily switchable properties, but they suffer from rapid decomposition in water. In this context, Hanhan and Senemoglu [73] have prepared a series of unsymmetrical, ionic sulfonated pyridyl imine ligands and their Pd(II) complexes which are suitable for MW-assisted SMC in water (**PyIPd**) (Scheme 40). These ionic Pd(II) complexes proved to be effective when used as 0.1 mol % catalysts in water for SMC reactions in the presence of K₂CO₃ (2 mmol) and tetrabutylammonium bromide (TBAB) (0.5 mmol), used as the phase transfer reagents. Ionic Pd(II) complexes tolerate a broad range of functional groups on the substrate phenyl rings and good yields (71%–98%) were described in all cases, in only 5 min of MW irradiation (850 Watt), and bulky groups on the ligand increased the efficacy of these catalysts. Furthermore, it was possible to use Pd complexes for up to four cycles before decomposition under MW irradiation. The hydrolysis of the imine C=N bonds in water to give aldehydes and Pd-black is probably more easily prevented by the faster MW assisted SMC.



Scheme 40. Water soluble and unsymmetrical sulfonated Pd(II)-pyridyl imine complexes.

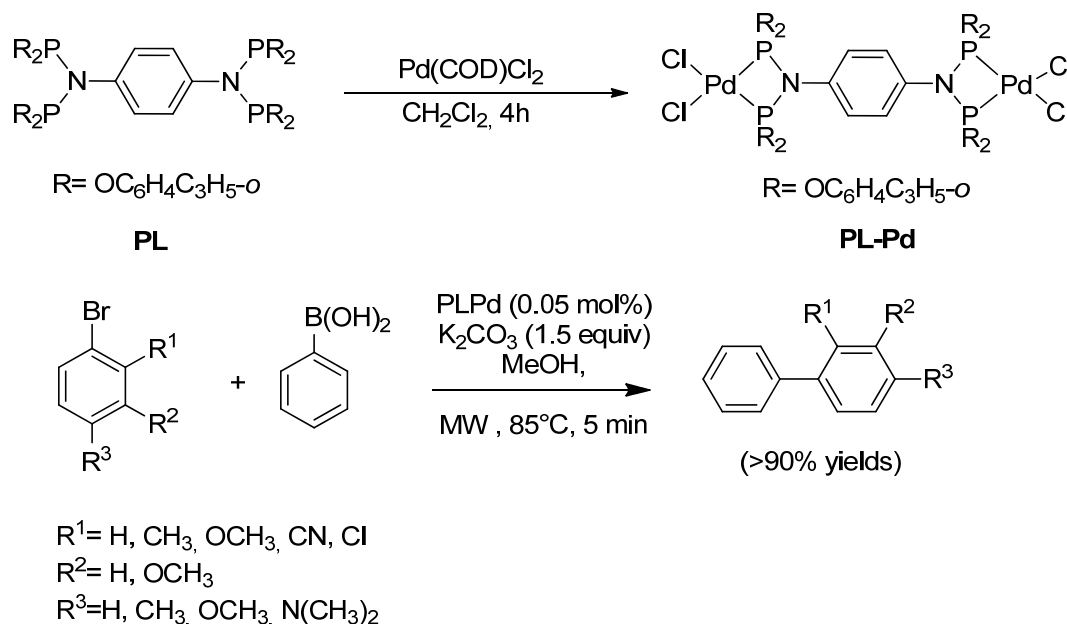
A new and efficient pyridine-pyrazole/Pd(II)catalyst system (**PP-Pd**) (Scheme 41) for MW-mediated SMC reactions has been developed by Shen et al. [74]. To the best of our knowledge, this is the first report of such complexes for the catalysis of SMC. The reactions were carried out under MW irradiation in a water/EtOH mixture and were applied to the synthesis of different biaryls. The MW protocol has the advantage of quick reaction (2 min, 60 W), while also avoiding anaerobic conditions or the use of a nontoxic solvent. The best results (75%–90%) were obtained using KOH as the base, in the presence of 0.1 mol % complex **PP-Pd**. The catalysts were applied for up to five cycles and the methodology is an effective synthetic route to biaryl synthesis.



Scheme 41. New pyridine-pyrazole/Pd(II) species as a SMC catalyst in aqueous media.

In the past decade, the synthesis and design of polyphosphine ligands has been a hot research topic due to the wide structural diversity of their metal complexes.

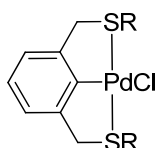
This type of ligand can easily form multinuclear complexes and also lead two metals into close proximity if the bite distances are small. In this context, the bis-amino(diphosphonite) ligand, $p\text{-C}_6\text{H}_4\{\text{N}[\text{P}(\text{OC}_6\text{H}_4\text{C}_3\text{H}_5\text{-o})_2]_2\}_2$ (**PL**), has recently been prepared, by Naik et al. [75], by reacting $p\text{-C}_6\text{H}_4\text{-}\{\text{N}(\text{PCl}_2)_2\}_2$ with *o*-allylphenol (4 equiv.) in an 85% yield (Scheme 42). When the **PL** ligand was reacted with $[\text{Pd}(\text{COD})\text{Cl}_2]$ (2 equiv.) a di-nuclear complex $\{[\text{PdCl}_2]_2\{p\text{-C}_6\text{H}_4\{\text{N}[\text{P}(\text{OC}_6\text{H}_4\text{C}_3\text{H}_5\text{-o})_2]_2\}_2\}$ (**PL-Pd**) was reached which was proven to be suitable for SMC under MW. This was the first example where a dipalladium(II) complex, containing a bis(diphosphonite) ligand, has been used in a MW-assisted SMC reaction. Of the various solvents and bases tested, the best results (>90%) were obtained under MW irradiation in methanol and K_2CO_3 (1.5 equiv.). An excellent turnover frequency (TOF) of 22,800 was obtained with bromotoluene in 5 min at 60 W and at a catalyst loading of 0.05 mol %. Even aryl halides, in particular sterically hindered bromides with *ortho* substituents, reacted with phenylboronic acid in excellent conversions and yields. An enhanced TOF of 24,000 was obtained for acyl and formyl substituents.



Scheme 42. Pd complex synthesis from bis-amino(diphosphonite) ligand.

Morales-Morales [76] have reported the preparation of a family of SCS pincer compounds, of the $[\text{PdCl}[\text{C}_6\text{H}_3\text{-2,6-(CH}_2\text{SR)}_2]]$ $\{\text{R} = t\text{Bu, sBu, iBu}\}$ type, which are suitable for SMC reaction, under both conventional and MW heating. These series of alkyl-substituted SCS-Pd^{II} pincer complexes

(Scheme 43) were prepared via the direct C–H activation of a series of α,α -bis(butylthio)metaxylene proligands (C_6H_4 -1,3-(CH_2SR) $_2$, for R = *t*Bu, *s*Bu, *i*Bu substituents) starting from a PdCl $_2$ suspension in toluene. The C–C coupling reaction between the various aryl halides and phenylboronic acid were then carried out in DMF using a catalyst loading of 0.2 mol % in the presence of Na $_2$ CO $_3$, used as a base. Quantitative conversions were described for all ligands tested under dielectric heating (75 W) in 10 min irradiation while 10 h were required with conventional heating. In addition, a correlation has been established between the Hammett parameter (σ) of the *para* electron-withdrawing substituents on aryl halide substrates used and the SMC conversion.

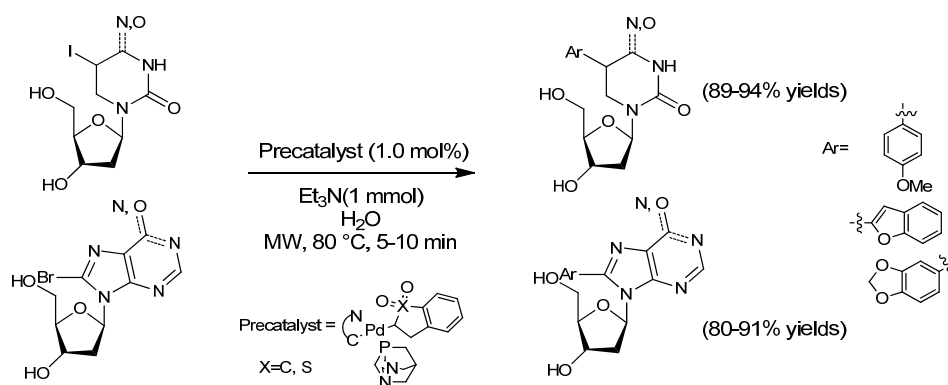


R = *t*-Bu; *s*Bu; *i*Bu

SCS Pd^{II} pincer complexes

Scheme 43. General structure of SCS-Pd^{II} pincer complexes.

Palladacycles have been reported to exhibit weak water solubility. However, an example of a comprehensive study into the use of Pd–PTA–imidate complexes in palladium-catalyzed SMC in water has nevertheless been published by Gayakhe et al. [77]. Four new, water-soluble palladacyclic derivatives [Pd(C[∞]N) (imidate) (PTA)] were prepared via bridge-splitting reactions of the corresponding di- μ -imidate complexes with PTA (1,3,5-Triaza-7-phosphaadamantane). The palladacycles were then tested in SMC with four nucleosides and a wide variety of aryl and heteroarylboronic acids (Scheme 44). Good to excellent yields (89%–94%) were obtained in 5 min under MW irradiation for the pyrimidine nucleosides, while an appreciable increase in product formation was observed for cytidine. Similarly, an improvement in reactivity was observed in the coupling reaction with purine nucleosides (adenosine and guanosine) under MW irradiation, in comparison to conventional heating, albeit in longer reaction times than their pyrimidine analogues (10 min).



Scheme 44. Pd–PTA (1,3,5-Triaza-7-phosphaadamantane)–imidate complexes in palladium-catalyzed SMC.

2.1.5. MW Promoted Ni Catalyzed SMC

The clear advantages such as, cheapness and earth abundance, of the first row transition metals compared to precious metals have moved the scientific community to study Ni catalyzed SMC [78]. A few papers have studied the effect that MW irradiation has on SMC in the absence of Pd [79,80]. The replacement of traditionally used Pd with less expensive Ni-based catalyst systems was approached by Kappe et al. in 2011 [81]. The Ni-catalyzed SMC reactions were performed using aryl carbamates

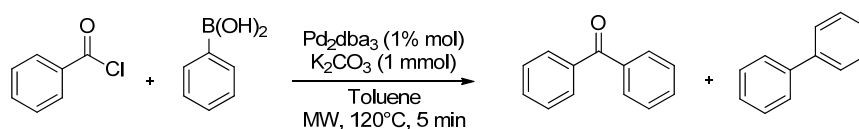
and/or sulfamates as the electrophilic coupling partners for reactions, because they are readily available and more stable under a variety of reaction conditions than the more reactive triflates. The commercially available and air/moisture stable $\text{Ni}(\text{PCy}_3)_2\text{Cl}_2$ catalyst was employed and the coupling was performed in toluene at 150–180 °C for 10 min in a single-mode MW reactor with accurate internal temperature monitoring. 87% of isolated yield was obtained from the *N,N*-diethyl naphthalene carbamate with 5 mol % of the Ni catalyst and boronic acid (2.5 equiv.) at 180 °C for 10 min, whereas the reaction required 20–24 h under conventional heating. The rate enhancement was demonstrated by the authors to be the result of a purely thermal effect as highlighted by control experiments which made use of a reaction vessel made out of strongly MW absorbing silicon carbide (SiC).

2.2. Moving from Homogeneous to Heterogeneous Catalysis in MW Promoted SMC

Supported Pd catalysts (1.0 wt %) and Pd_2dba_3 (1.0 mmol) have been found, by Martins et al. [82], to be active catalysts in the SMC of aryl chlorides with arylboronic acids. Excellent yields, in terms of aromatic ketones, were described (79%–99%) under MW irradiation without the addition of phosphine ligands in 5 min at 120 °C (250 Watt) (Scheme 45).

Selectivity toward benzophenone was not good under optimized conditions in MW when Pd/C was used as the catalyst. Pd/C is as strong MW absorber. The high superficial temperatures reached on the Pd/C surface under dielectric heating probably lead to rapid biphenyl by-product formation. Selectivity toward benzophenone dramatically improved upon reducing the reaction temperature from 120 to 80 °C. Moreover, Pd/C was proven to be more effective when acetonitrile was exploited as reaction solvent under MW irradiation instead of toluene. This improved result can be ascribed to the optimized solubilization of the base ($\text{Na}_3\text{PO}_4 \cdot 12\text{H}_2\text{O}$) in a more polar solvent. This catalytic system gave excellent selectivity, when acetonitrile was used as the solvent and Pd_2dba_3 as the Pd source, but the reaction was slower. In fact, the improved base solubility in acetonitrile was found during the hydrolysis of the benzoyl chloride and the discovery of large amounts of benzoic acid. Better selectivity was finally observed using K_2CO_3 in toluene.

The effect of phase transfer catalysts in the Pd_2dba_3 catalyzed coupling reaction was also investigated. Of the phase transfer catalysts studied, polyethylene glycol 200 (PEG-200) was found to be a good choice probably because it avoids the acyl chloride hydrolysis issue as well as promoting better base solubilization.



Scheme 45. Synthesis of aromatic ketones without the addition of phosphine ligands under MW irradiation.

2.3. Solid Supported Pd Catalyzed MW Promoted SMC

The combination of MW heating, supported metal (mainly Pd) nanoparticles and ligand-free C-C coupling reactions give very high reaction rates using very small catalyst amounts, therefore increasing the sustainability of the processes. However, separating the homogeneous catalyst (generally palladium metal ions) is a challenging requisite, especially from a pharmaceutical point of view. A first example of maintaining high Pd dispersion in the presence of a support can be found in $\text{Pd}(\text{OAc})_2$ species immobilised on mesoporous $\gamma\text{-Al}_2\text{O}_3$ which displayed excellent catalytic activity in the coupling of a number of aryl halides with phenylboronic acid [83]. A DMF/water mixture was employed and it was necessary to heat the reaction via MW irradiation, at 150 °C for 10 min, despite the low catalyst amount (0.2 mol % Pd). It was proposed that the highly dispersed nature of $\text{Pd}(\text{OAc})_2$ coupled with its high affinity for $\gamma\text{-Al}_2\text{O}_3$ render the catalyst both active and very stable. XPS measurements revealed that the original Pd(II) was basically transformed to Pd(0) after reaction. The use of metallic nanoparticles, instead of isolated Pd(II) species, can therefore be advantageous. Indeed, the increase in surface area

that accompanied the decrease in the nanoparticle size implies that more active sites are available for catalysis. Pd is the most investigated metal, however, the introduction of more than one metal allows the tuning of the electronic properties of the material to be carried out by opportunely choosing the metal or alloy.

Novel CuPd bimetallic nanoparticles have recently been synthesized in oleylamine which acted as both surfactant and solvent, therefore avoiding the need for additional surfactants, ligands or reducing agents [84]. Moreover, the introduction of Cu did not only lower costs because of the need for less Pd in preparation, but catalyst recovery was also more efficient as there were no phosphine ligands, which can interact with the reaction product. The alloyed nanoparticles (0.01 mol %) showed high catalytic activity in the SMC reaction of aryl halide and phenylboronic acid with a number of functionalized substrates in the presence of K_2CO_3 using H_2O ; ethanol was used as an environmentally benign solvent system under MW irradiation at $120\text{ }^\circ\text{C}$ for 10 min. The high 92% biphenyl product yield, an excellent TON (6000) and good TOF of $72,000\text{ h}^{-1}$ were achieved. The outstanding activity was explained by the presence of electron transfer from Pd to Cu (as revealed by the co-presence of both Pd and Cu metals and oxides) that allows the conversion of Pd^{2+} to Pd^0 to catalyze the reaction. Furthermore, the CuPd nanoparticles were successfully recycled, giving 95%, 90% and 78% conversions after 3 consecutive runs. The PdCu nanoparticles were easily recovered by centrifugation and washed with ethanol after which the solution was decanted and reused in the subsequent run. Both electron donor and electron withdrawing functional groups, such as methoxy, ethoxy, cyano, aldehyde, thiomethyl and dimethylamino, in both aryl halides and arylboronic acids were used and gave excellent yields.

In order to promote separation, the nanoparticles can be strategically supported on insoluble supports which can stabilize the nanoparticles without decreasing the accessibility of the catalytic sites. In addition, the manipulation of supported nanoparticles further improves the sustainability of the material by facilitating both recovery and reuse. The huge effort made to obtain green protocols for reaction has given rise to the synthesis of water soluble ligands on one hand, and polymer supported ligands or Pd-based catalysts on the other [85]. The research was focused on reactions carried out in mild and ligandless conditions, using water as a solvent and at moderate temperatures, including room temperature. The use of heterogeneous catalysts, instead of homogeneous catalysts, therefore has several advantages, caused by their facility of reusability and good compatibility with flow reactors, which facilitate the effective production of materials using continuous processes [86–88]. Several strategies have been designed to effectively immobilize catalysts on solid supports, which include inorganic oxides, polymers and organic–inorganic hybrid materials, in order to obtain, on one hand, a highly dispersed and stable metal phase and, on the other, an active phase which is able to maintain its catalytic activity under MW irradiation. For example, Soni et al. (2014) [89] have described a suitable heterogeneous catalyst for SMC with the synthesis of a new palladium doped silica (Pd/SiO_2) mesoporous catalyst, which proceeds via the sol–gel route, using the P123 surfactant as a structure directing agent. Of the wide plethora of supports available, ordered mesoporous silica materials are very attractive for immobilizing/doping Pd catalysts, due to their large pore size, high surface area and tunable pore structure. The Pd/SiO_2 catalyst (0.5 wt %) exhibited high activity in the coupling of various aryl bromides and a number of arylboronic acids at $85\text{ }^\circ\text{C}$ in water with KOH after 7 min of MW irradiation at 245 W power. The catalyst was recycled 9 times without a significant loss in activity. It is worth noting that the reactions were completed in 2 h at $60\text{ }^\circ\text{C}$ under conventional heating conditions. In a previous paper, it was shown that SMC was mediated by a 0.5–1 mol % Pd-organosilica heterogeneous catalyst (SiliaCat Pd(0)) at room temperature, with complete conversion of the substrate after 6.5 h [90]. MW heating was needed to convert readily available chloroarenes. Under 200 W power irradiation, aryl chlorides reacted with arylboronic acid in good yields, whilst aryl bromides were coupled in remarkably short reaction times (from 20-to-100 times faster than under reflux).

Verho et al. have observed a 15-fold increase in reaction rate, compared to conventional heating in an oil bath, in the SMC which gave 87%–90% yields in the presence of Pd nanoparticles immobilized

on aminopropyl (AmP)-functionalized siliceous mesocellular foam (MCF) (Pd^0 -AmPMCF) under MW irradiation [91]. The corresponding reaction under conventional heating, employing an oil bath, gave rise to a four-fold decrease in yield. The authors explained such trends in terms of the existence of more proficient heat transfer to the Pd nanoparticles which was achieved by MW irradiation, giving rise to so-called “hot spots” [92] which possess a temperature higher than the neighboring solvent. Additionally, two blank experiments were carried out; the first reaction was carried out in the absence of Pd^0 -AmPMCF and the second was performed with MCF. As expected, no product formation was detected in the absence of Pd.

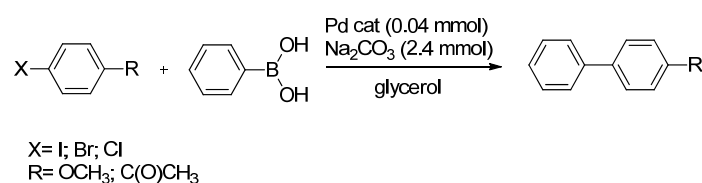
A MW-assisted SMC was also performed which tested two catalysts, Pd/MCM-41 and Pd/SBA-15, under solvent-free conditions and heating at 120 °C for 10 min in the presence of a base (K_2CO_3 , Cs_2CO_3 or CsF) [93]. Phenylboronic acid and phenyl iodide produced biphenyl in a 97.4% yield using Pd/MCM-41, whereas phenylboronic acid and phenyl bromide gave biphenyl in excellent yields with both Pd/MCM-4 and Pd/SBA-15. Nevertheless, the reaction with phenyl chloride gave poor yields in the same experimental conditions.

Zheng et al. [94] have reported the MW-assisted SMC of a series of Pd and Pd/Au alloy nanoparticles (with uniform size 1–3 nm) that had been either encapsulated or stabilized by G4-poly (amido-amine) (G4-PAMAM, G stands for the generation) planted in SBA-15. A water/ethanol (3:2) solvent was heated with iodobenzene (1 mmol), benzenboronic acid (1.2 mmol) and 0.5% mol of catalyst in the presence of K_3PO_4 (3 equiv.) at 100 °C. In conventional conditions, a 97% yield was observed after the first cycle of 8 h, whereas the yield dropped to 31% after the 2nd cycle. However, MW irradiation granted a 97% yield after only 10 min, a 48-fold rate increase, and the reactions were completed after 30 min. In order to clarify the influence of the catalyst in the MW-assisted reaction, the authors performed SMC with and without a catalyst under MW. Almost no product was obtained, which demonstrates that the effect of MW irradiation was limited to the promotion of the catalyzed reactions. Moreover, it was demonstrated that air retained its influence on the reaction as the procedure that was carried out without N_2 bubbling gave a 96% yield. It is worth noting that the presence of a mild base is required to avoid the dissolution of the SBA-15 holding dendrimers in solvent. Interestingly, they found that Pd/Au alloy nanoparticles display higher activity than monometallic catalysts, at similar metal loading values, in catalyzing the coupling between aryl bromide/aryl chloride and arylboronic acid. Although, pure gold gave no catalytic activity, the presence of Au^{3+} in the dendrimer before reduction may be able to decrease Pd^{2+} complexation by internal amine groups or other groups, resulting in the complete reduction of Pd^{2+} to Pd^0 . This feature may justify the higher catalytic activity shown by the Pd/Au alloy catalyst over the monometallic Pd catalyst.

An effective methodology has been developed for the coupling of aryl halides (including aryl chloride) and phenylboronic acid under MW irradiation for 30 min in the presence of Pd/ Fe_3O_4 @ SiO_2 and K_2CO_3 [95]. The catalyst was prepared by simply supporting PdCl_2 on Fe_3O_4 @ SiO_2 in ethylene glycol and it was easily recovered using an external magnet after the reaction and reused without further treatment. The MW-assisted reaction time was shortened and increased yields (99.4% and 99.8%) were achieved, as compared to those obtained for traditional heating (90.6%) in 12 h of reaction time. Interestingly, Pd/ Fe_3O_4 @ SiO_2 exhibited considerable catalytic activity in the SMC involving aryl chlorides and a 68.2% yield was observed in the coupling of chlorobenzene with $\text{PhB}(\text{OH})_2$ under MW irradiation for 90 min. In addition, no deactivation was observed even after 6 runs. At the same time, Nehlig et al. reported the exceptional catalytic performance displayed by palladium (0.01 mol % Pd), immobilised on a maghemite nanoparticle core bearing proline at the surface, in the coupling of 4-tolylboronic acid (0.22 mM) to 4-iodonitrobenzene (0.20 mM) in water–ethanol (1:1), under aerobic conditions and using a base [96]. The TOF values were 1940 and 18,000 mol *p*-I- $\text{C}_6\text{H}_4\text{NO}_2$ (mol Pd) $^{-1}$ ·h $^{-1}$. MW irradiation was used to heat the reaction mixture in accordance with the green chemistry approach and to obtain careful control of the reaction conditions (temperature, stirring, cooling). It was reported that the test reactions performed under thermal heating gave exactly the same results. Moreover, γ - Fe_2O_3 @Cat-Pro(Pd) was reused for seven runs providing total conversion

and contained Pd leaching. The catalyst was also extremely stable; it was still active with the same efficiency after being stored in aqueous solution, under aerobic conditions at room temperature for more than 6 months after its synthesis.

Cravotto et al. have observed the advantages on offer when working under MW irradiation and/or ultrasound irradiation [97]. To our knowledge, this is the sole example found in the literature in which the coupled techniques have been successfully employed. They have performed a comparison of a number of different activation methodologies, such as conductive heating in an oil bath (OB), MW irradiation (MW), US horn irradiation coupled with conductive heating in a thermostated oil bath (US/OB) and contemporary US/MW irradiation (US/MW) (as reported in Table 2) in the study of a series of metal-catalyzed C–C couplings in glycerol, along with the SMC (Scheme 46).



Scheme 46. SMC reaction in glycerol (for specific reaction conditions see the Table 2).

Table 2. Cross-coupling yields in glycerol of 4-iodobenzene and phenylboronic acid via a variety of techniques.

Method ¹	T (min)	Yield (%)		
		Pd(OAc) ₂	PdCl ₂	Pd/C
OB ²	60	85	75	44
US/OB	60	99	98	86
MW	15	57	70	60
MW	60	74	92	67
US/MW	60	100	98	94

¹ Reaction conditions: 4-iodomethoxybenzene (2 mmol), phenylboronic acid (2.4 mmol), Na₂CO₃ (2.4 mmol), ligand-free catalyst (0.04 mmol), glycerol (42 mmol, 4.0 g), 80 °C; ² OB = oil bath.

In particular, they investigated the coupling between 4-iodoanisole and phenylboronic acid employing ligand-free palladium salts or palladium on charcoal as a model reaction. All the reactions were performed at 80 °C, because glycerol guarantees excellent acoustic cavitation even at high temperatures. PdCl₂ and Pd(OAc)₂ were more efficient than Pd/C (see Table 2) and it was found that US/OB, MW and simultaneous US/MW irradiation significantly enhanced the reaction rate, with the US/MW and US/OB methods giving the best results due to enhanced heat and mass transfer. In addition to classic palladium salts, a solid ligand free catalyst, a Pd loaded cross-linked chitosan [98], gave outstanding catalytic activity. Enhanced reaction rates, in the order MW/US > US > MW, were observed in a number of Pd catalyzed SMC in glycerol. It is worth noting that ultrasound and MWs significantly improved the reaction of halobenzenes, such as chloroacetophenone, which are poorly reactive toward C–C coupling. Further modification of the Schiff base chitosan by reaction with 2-pyridinecarboxaldehyde and the subsequent palladium deposition resulted in catalysts that are highly active in the coupling of phenylboronic acid with *p*-bromophenol and *p*-bromoacetophenone giving high product selectivity and yields (>99%) in water under MW irradiation without the need for a phase-transfer catalyst [99].

In order to make any catalytic process “greener”, the catalyst itself should be “green” in nature and the process should not demand harmful solvents. With such an approach in mind, Baran et al. [100] have prepared a green cross-linked-chitosan-cellulose composite microbead-based catalyst support for Pd ions and tested it in the synthesis of biaryl compounds, via an environmentally safe MW irradiation

technique in a solvent free medium. The cellulose particles were incorporated into the chitosan matrix to improve mechanical strength on one hand and the interaction with Pd(II) on the other (see Figure 1).

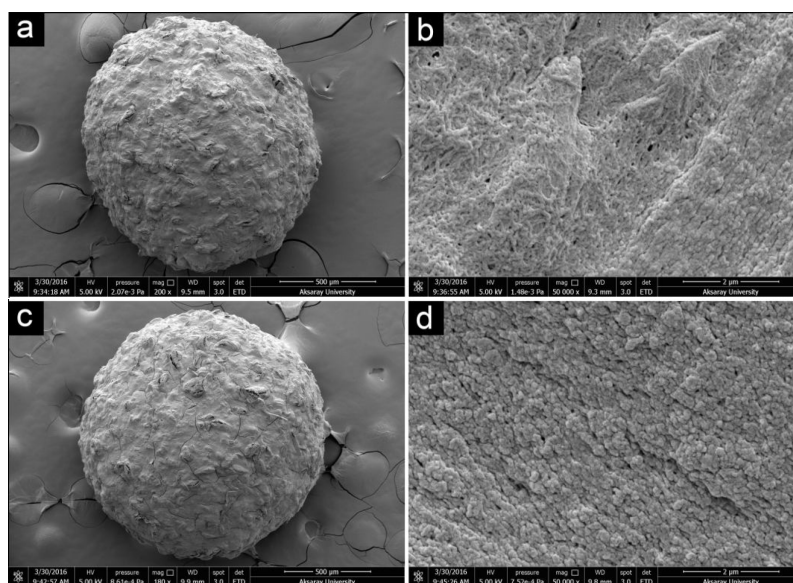


Figure 1. Scanning electron microscopy (SEM) images of (a,b) cross linked-chitosan-cellulose composite micro beads; (c,d) green chitosan/cellulose-Pd(II) catalyst. Reprinted from [100]. Copyright (2016), with permission from Elsevier.

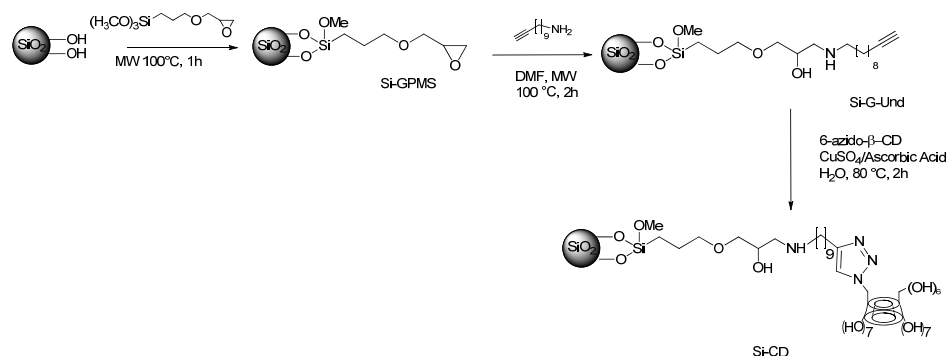
The reactions between phenylboronic acid and 16 different arylhalides were also examined. The 5 min MW-assisted synthesis of biaryl compounds was carried out in a solvent free medium adopting a small amount of catalyst (0.015 mol %) at 50 °C. The activity of the catalyst was compared with that of commercially available Pd salts PdCl₂, PdCl₂(CH₃CN)₂ and Na₂PdCl₄, under the same reaction conditions. In addition, the authors tested the performance of the activation method against a conventional heating reflux system (90 °C, 24 h reaction time). They found TON and TOF values of 6600 and 82,500. Na₂PdCl₄ (the best performing commercial product) gave a 47% yield, whilst a much higher product yield (99%) was obtained using the green chitosan/cellulose-Pd(II) catalyst.

In order to reveal the efficiency of the MW irradiation method, 4-methoxybiphenyl was synthesized in the presence of the chitosan/cellulose-Pd(II) catalyst in a conventional heating-reflux system (24 h, 90 °C) using toluene as the solvent, obtaining a 46% product yield vs. the 99% reaction yield produced by green method (5 min, 50 °C) in solvent-free media. The catalyst worked efficiently for up to nine cycles, giving high TONs (2867) and TOFs (35,837). It was concluded that this environmentally harmless catalyst can be transferred and scaled-up into industrial operations.

A new series of solid cross-linked cyclodextrin (α -, β -, and γ -cyclodextrin) based catalysts that are obtained via reticulation with hexamethylene diisocyanate in solutions containing either Pd(II) or Cu(I) cations was investigated by the same group [101]. Diisocyanates are efficient cross-linking agents for cyclodextrins, due to their high reactivity towards hydroxyl groups. The Pd(II) based catalysts have been successfully tested in C–C couplings (Heck and Suzuki reactions). The catalyst proved to be extremely versatile because of its polar structure and was found to be particularly suitable for MW-assisted reactions. Indeed, both native cyclodextrins and cross-linked derivatives are very sensitive to dielectric heating due to their polar structure. Such effect was further enhanced by the embedded cations.

One of the strategies exploited for the preparation of active catalysts that contain solid supported nanoparticles is the functionalization of the surface with organic ligands. Martina et al. have reported [102] the synthesis of a novel cyclodextrin/silica support to host Pd nanoparticles with enhanced stability and reactivity, according to Scheme 47. The authors ascribed the formation of homogeneously dispersed

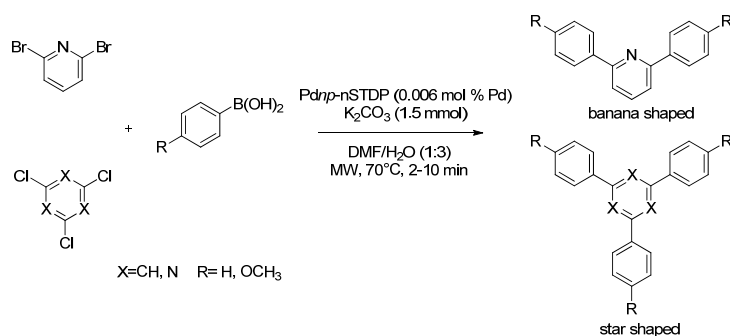
Pd nanoparticles of small size to the presence of a coordinating group. Indeed, the amino alcohol groups and triazole on the spacer are also able to coordinate Pd species and influence metal nanoparticle content, size and distribution on the silica surface.



Scheme 47. Synthetic procedure for the preparation of Si-cyclodextrin [102].

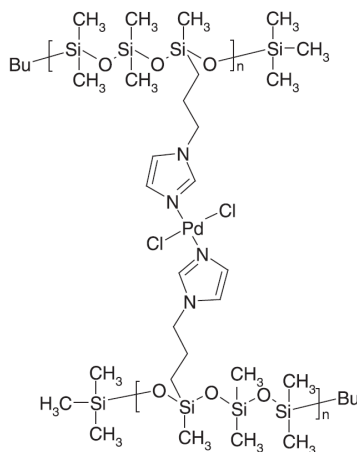
An extensive study of the catalytic performance of a Pd nanoparticle supported hybrid cyclodextrin derivative in ligand-free C–C SMC with a large number of aryl iodides and bromides was also carried out. The catalyst exhibited excellent results and MW irradiation abated reaction times. The catalyst underwent 5 cycles and no appreciable loss in activity was detected. Inductively coupled plasma (ICP) analyses of the catalyst after recycling showed negligible Pd leakage, whereas XRD measurements indicated a slight increase in Pd nanoparticle size after usage.

Isfahani et al. [103] have described, for the first time, the synthesis of a new catalyst which is based on Pd nanoparticle immobilized on a nano-silica triazine dendritic polymer (Pdn_p-nSTDP) and its subsequent application in C–C coupling reactions. This catalytic system showed high activity in the SMC of aryl iodides, bromides and chlorides with arylboronic acids. These reactions were best performed under MW irradiation (200 W, 70 °C) in a dimethylformamide (DMF)/water mixture (1:3) in the presence of K₂CO₃ (1.5 equiv.) and of only 0.006 mol % of Pdn_p-nSTDP (Pd size 3.1 ± 0.5 nm) and gave (2–10 min) the desired coupling products in high yields (>90%). Pdn_p-nSTDP was also applied as an effective catalyst for the MW preparation of a series of star- and banana-shaped compounds, using benzene, pyridine, pyrimidine or 1,3,5-triazine units as the central core, via a SMC reaction (see Scheme 48). 2,6-dibromopyridine (for banana-shaped) or 1,3,5-tribromobenzene, 2,4,6-trichloropyrimidine and 2,4,6-trichlorotriazine (for star-shaped) were used as the starting materials. The Pdn_p-nSTDP catalyst was easily recovered and reused without significant loss in catalytic activity making this a sustainable process. The analysis of palladium leaching from the Pdn_p-nSTDP catalyst by ICP pointed out that only a trace amount of palladium leached in the first two runs.



Scheme 48. Star- and banana-shaped compounds with benzene, pyridine, pyrimidine or 1,3,5-triazine units as the central core.

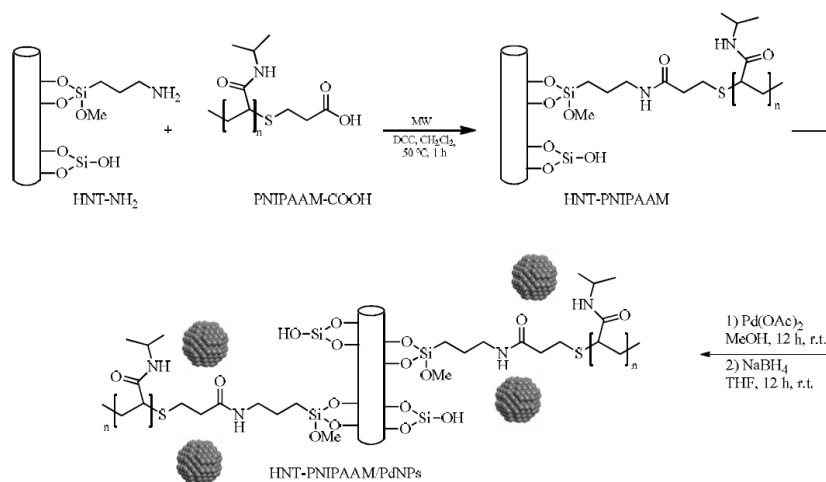
Following a similar approach, Borkowski et al. [104] achieved very good results using Pd supported on a siloxane polymer functionalized with imidazole groups (Scheme 49) in a SMC model reaction between 2-bromotoluene and phenylboronic using conventional heating and MW energy. Environmentally friendly solvents, such as H₂O and a 2-propanol/H₂O mixture, were employed.



Scheme 49. Proposed structure of Pd catalyst supported on a siloxane polymer functionalized with an imidazole group. Reprinted from [104], Copyright (2016), with permission from Elsevier.

The Pd supported catalyst showed very good recyclability (eight runs) and high activity at 40 or 60 °C. However, even better results and yields of 90%–100% were obtained after 1 h in three sequential runs with the same catalyst when MW heating was used instead of conventional heating. Interestingly, the application of MW conditions enabled the less reactive 4-chlorotoluene and 1-chloro-4-nitrobenzene to react.

Ceramic materials, based on aluminosilicates, react quickly under MW irradiation with consequent rapidity and uniformity of heating. MW irradiation was very recently employed during a SMC reaction between phenylboronic acid and a broad range of aryl halides in the presence of K₂CO₃ (1.12 equiv.), TBAB as an additive (0.05 mmol) and 0.016 mol % (0.7 mg) of Pd nanoparticles immobilised into Poly(*N*-isopropylacrylamide) (PNIPAAm), which had previously been grafted onto halloysite nanotubes (HNT) using water as the solvent [105] (see Scheme 50).



Scheme 50. Representation of the synthesis of Pd nanoparticles immobilised into Poly(*N*-isopropylacrylamide) (PNIPAAm) previously grafted onto halloysite nanotubes (HNT). Reprinted from [105]. Copyright (2016), with permission from Royal Society of Chemistry.

The reactions were performed at varying temperatures (between 25 and 120 °C) under MW irradiation. The catalyst was recuperated via centrifugation and used again for five cycles (Figure 2). Yields ranged from 73% to 99% and no by-products were formed. Nevertheless, aryl chlorides gave almost no conversions under the same reaction conditions.

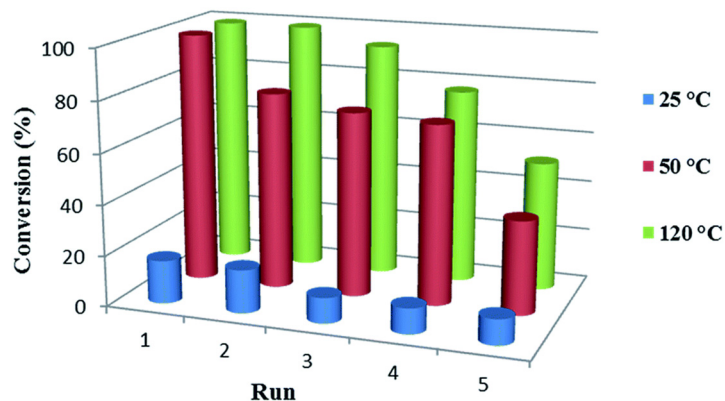


Figure 2. Effect of temperature on the SMC between 4-bromoacetophenone and phenylboronic acid (reaction conditions: phenylboronic acid (0.547 mmol), 4-bromoacetophenone (0.55 mmol), K_2CO_3 (0.615 mmol), EtOH/ H_2O 1:1 (1.2 mL), catalyst (0.16 mol %, 7 mg) under MW irradiation). Reprinted from [105]. Copyright (2016), with permission from Royal Society of Chemistry.

The good results may well be due to the thermo-responsive behavior of PNIPAAm. When recycling tests were carried out at temperatures above the lower critical solution temperature (LCST > 32 °C) of PNIPAAm, the system catalyzed the formation of the desired biphenyl-4-acetophenone product in good yields, even after 4 runs, ranging from 99% to 77%. On the other hand, very low conversions (about 10%) were obtained at 25 °C as expected for the thermo-responsive behavior of the polymer. It was proposed that, the PNIPAAm chains collapse, at above the LCST, to form a dense hydrophobic layer covering the surface of HNTs hence promoting the mass-transfer of the hydrophobic reagents (Figure 3). However, it was observed that prolonged MW irradiation induced a decrease in both conversion and yield, due to homocoupling, dehalogenation products and the degradation of both reactants and products.

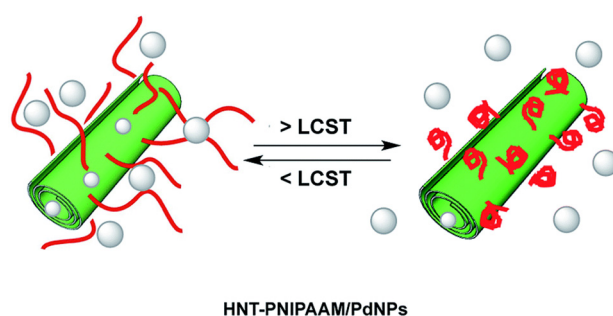


Figure 3. Sketch representation of the swelling behavior of HNT-PNIPAAm/Pd nanoparticles at the critical solution temperature (32 °C). Reprinted from [105]. Copyright (2016), with permission from Royal Society of Chemistry.

Environmentally friendly halloysite-dicationic triazolium salts (HNT-IL) were used as supports for palladium catalysts and used in the SMC between phenylboronic acid and a set of aryl halides. The reaction was carried out in water at 120 °C and using K_2CO_3 [106]. All the reactions were run for 10 min. HNT-IL/Pd was used at 0.1 mol % loading. Conversions were high with yields up to 99% in the case of anisole derivative substrates. On the other hand, the conversion of other substrates increased

when the H₂O/EtOH (1:1) mixture was used, due to the good solubility of the organic reactants and of the inorganic base in the co-solvent. It was proposed that the impressive conversions for anisole derivatives may be justified by a synergic effect caused by the ethereal alkyl chains, or the aromatic rings, of the support and by MW irradiation on the cross-coupling of anisole in water. The catalyst was recovered via centrifugation and reused for 5 runs, affording biphenyl-3-anisole in 99%–90%. The same authors [107] found that the use of MW irradiation cut down the reaction time and enhanced the conversion, with respect to traditional heating, when using the same catalyst, for which the modification of the external halloysite nanotube surface with octylimidazolium moieties (HNT-IL) was performed using MW irradiation under solvent-free conditions. The HNT-IL/Pd catalyst (1 mol %) was tested in the SMC of a number of different kinds of aryl bromides, iodides and less reactive aryl chlorides with phenylboronic acid in under 10 min MW irradiation at 120 °C in the presence of K₂CO₃. No by-products were detected in all cases and the conversions reported in Table 3 correspond to yields. Full conversions were obtained when aryl bromides and iodides were used, whilst less reactive aryl chlorides gave lower yields. The authors pointed out that no product was detected when traditional heating was used on aryl chlorides. Moreover, comparable results were achieved with both electron-donating and electron-withdrawing substituents on aryl halides.

Table 3. SMC reaction of phenylboronic acid with a number of different halides under optimized reaction conditions under MW irradiation ¹.

Ar-X	Yield (%) ²
4-Bromoacetophenone	>99
3-Bromoacetophenone	80
4-Bromobenzaldehyde	>99
3-Bromobenzaldehyde	>99
4-Bromoanisole	>99
3-Bromoanisole	90
4-Bromotoluene	>99
2-Bromotoluene	>99
4-Bromoaniline	78
2-Bromobenzonitrile	>99
3,5-Bis(trifluoromethyl)bromobenzene	>99
1-Bromo-2,4,6-triisopropylbenzene	<5
1-Bromo 4-nitrobenzene	>99
4-Iodoacetophenone	>99
4-Iodotoluene	>99
Methyl 4-iodobenzoate	>99
2-Chlorobenzaldehyde	14
4-Chlorobenzaldehyde	33

¹ Reaction conditions: aryl halide (1.01 mmol), phenylboronic acid (1 mmol), K₂CO₃ (1.12 mmol), solvent (1.2 mL), HNT-IL/Pd (1 mol %), 10 min MW irradiation at 120 °C; ² Determined by ¹H NMR.

It was therefore shown that MW irradiation can decrease the reaction time and improve conversion when compared to traditional heating (50 °C for 19 h). The outstanding reactivity was explained by the introduction of an ionic liquid onto the external surface of the halloysite nanotubes. Such a small amount was able to induce a dramatic change in the heating profiles by changing the overall dielectric properties of the reaction mixture, which consequently led to improved yields.

The biogenic synthesis of cellulose supported Pd(0) nanoparticles (NPs) employing the hearth wood extract of *Artocarpus lakoocha* Roxb and their use as a flexible and effective catalyst in Suzuki and Heck couplings under MW heating has been reported [108]. Catalyst synthesis was followed by the observation of color changes (Figure 4); the aqueous solution C, containing oxyresveratrol, PdCl₂ and cellulose initially displayed a light brown color and then gradually turn to black (Figure 4D). The black solid deposited on the bottom of the test tube was solid Pd(0) NPs@cellulose (Figure 4E). In a 10 mL MW glass vial, 0.5 mol % (0.028 g) Pd(0) NPs@cellulose, 0.5 mmol 2-bromobenzaldehyde,

0.75 mmol phenylboronic acid and 1.5 mmol K_2CO_3 were mixed in 5 mL H_2O . The mixture was stirred at 80 °C for the stipulated time in a MW oven. It was found that the $PdCl_2$ salt gave disappointing results (yield < 30%) as a catalyst, compared to $Pd(0)$ NPs@cellulose (product yield > 90%), under the same reaction conditions. In addition, the catalyst was filtered off and simply washed with acetone and stored for further reactions. Its reusability was proven for up-to 10 runs without measurable Pd leaching.

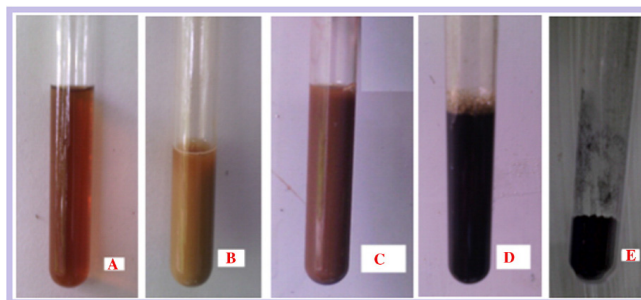
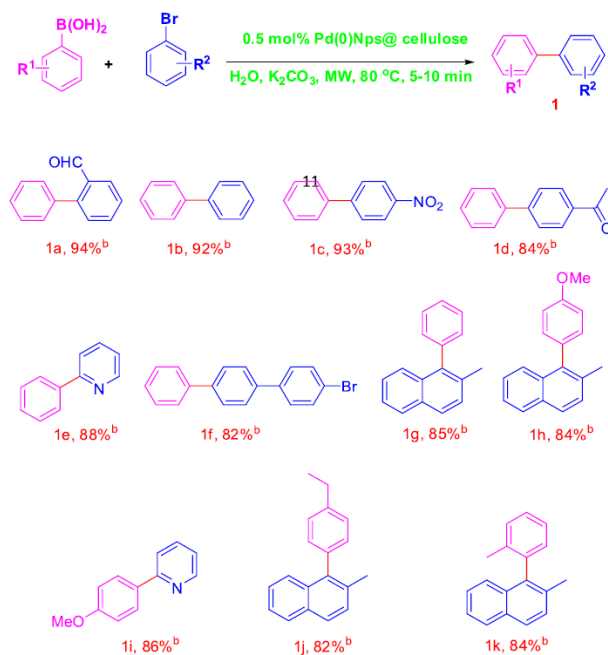


Figure 4. Photograph of (A) hearth wood extract of *A. lakoocha* Roxb in water; (B) solution A with cellulose; (C) Solution B with $PdCl_2$; (D) Solution C after 15 min warming in heating bath at 60 °C; (E) solid recyclable $Pd(0)$ NPs@cellulose. Reprinted from [108]. Copyright (2015), with permission from Elsevier.

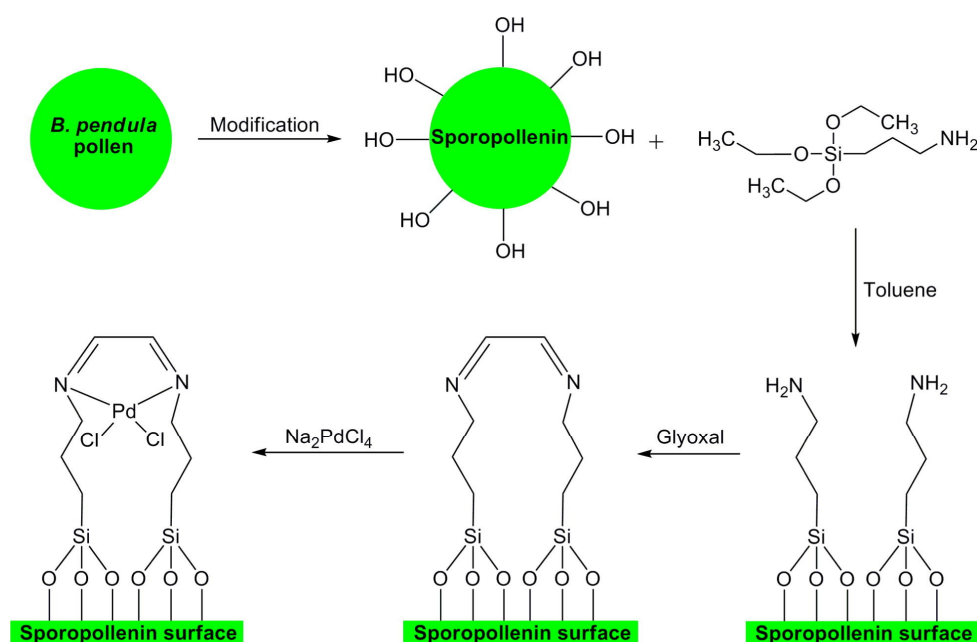
Furthermore, two comparative cross coupling reactions were carried out using the same substrates, the former was performed in MW heating and the latter using an oil bath at 100 °C. It was shown that the MW-assisted reaction required shorter times and gave higher yields than conventional heating. The SMC was then carried out on a large number of substituted arylbromides (0.5 mmol) and arylboronic acids (0.75 mmol) as substrates using $Pd(0)$ NPs@cellulose (0.5 mol %) in the presence of K_2CO_3 (1.5 mmol), H_2O (5 mL) at 80 °C under MW irradiation. The results are reported in Scheme 51.



Scheme 51. SMC reaction between phenylboronic acid and substituted arylbromides under MW heating. Reaction conditions: arylbromides (0.5 mmol), phenylboronic acid (0.75 mmol), $Pd(0)$ NPs@cellulose (0.5 mol %), K_2CO_3 (1.5 mmol), H_2O (5 mL), 80 °C, under MW irradiation (isolated yield). ^b Isolated yields. Reprinted from [108], Copyright (2015), with permission from Elsevier.

Generally, all reactions provided excellent coupling product yields under MW heating (yields in the 82%–94% range). However, aryl bromides, containing electron withdrawing groups (**1a**, **1c**), gave yields that were higher (93%–94%) than those obtained with their electron donating counterparts. It was found that the coupling reaction occurred also in the case of hetero aryl bromides (**1e**, **1i**) and ortho substituted aryl bromide (**1a**, **1g**, **1h**, **1j**, **1k**) as substrates. In conclusion, substrate steric and electronic factors did not markedly influence the product yield, due to the high activity of the cellulose supported Pd(0) catalyst.

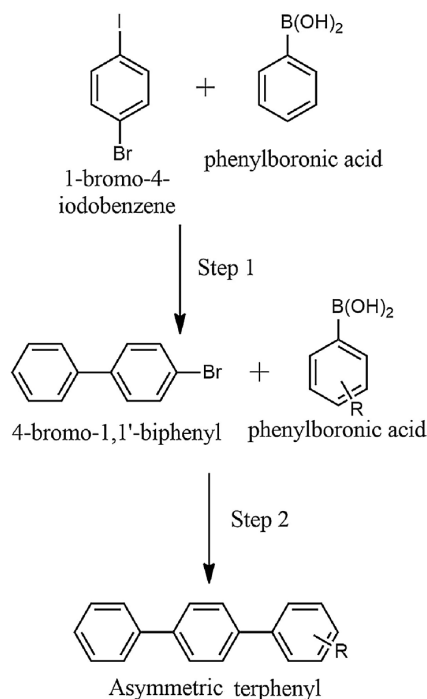
Baran et al. [109] have very recently reported the design of highly thermally stable silane and Schiff base-modified sporopollenin microcapsules as a support for Pd(II) catalyst (see Scheme 52). This catalyst displayed high selectivity towards SMC reactions by producing TONs and TOFs as high as 40,000 and 400,000. In order to prove the efficiency of MW heating, the authors tested the behavior of the catalyst on the reaction in a reflux heating setup at 100 °C for 48 h in toluene and found that MW irradiation proved to be more efficient than reflux-heating.



Scheme 52. Design of sporopollenin microcapsule supported Pd(II) catalyst. Reprinted from [109]. Copyright (2016), with permission from Elsevier.

In a related paper, where a chitosan-pyridil-based Pd(II) catalyst was investigated in the MW-assisted synthesis of biaryls in SMC reactions [110], outstanding TON and TOF values were obtained with very low catalyst loading values (5×10^{-3} mol %) in 5 min and catalytic activity was retained up to 7 cycles. In addition, the authors demonstrated that the catalyst was more suitable for MW irradiation than for a conventional reflux-heating system, for which low reaction yields, TON and TOF values were found. In another very recent paper [111], *Ulva* sp. (a fast growing macroalga) particles were incorporated into a chitosan matrix to favor interactions with Pd ions. The presence of functional groups, such as thiol, hydroxyl, carboxyl, amino and imidazole moieties, on the cell surface, mean that the biomass derived from such macroalga can be used to uptake metal ions. Moreover, Pd ions can coordinate with the imine groups belonging to the glutaraldehyde cross-linked chitosan Schiff base. The catalytic performance of chitosan-*Ulva* supported Pd(II) green catalysts was investigated in the biaryl synthesis via the SMC reaction without using any solvent under MW irradiation. High selectivity and efficiency were found in the reactions of phenylboronic acid with a number of aryl halides under MW irradiation in only 4 min at 50 °C (TON and TOF values: 4950 and 75,000) without showing any activity drop for 8 cycles.

Shah et al. [112] have compared the time and yield benefits of MW heating reactions with those carried out under conventional heating. The authors prepared and employed Pd nanoparticles supported on cross-linked polystyrene resins to successfully catalyze the one pot synthesis of asymmetric terphenyls, a useful industrial commodity, starting from 1-bromo-4-iodobenzene via the sequential addition of various boronic acids, according to Scheme 53:



Scheme 53. Synthesis of asymmetric terphenyls. Reprinted from [112]. Copyright (2016), with permission from Elsevier.

The reaction was carried out according to a two-step procedure. Step 1: 4-iodo bromobenzene (1.0 mmol) phenyl-boronic acid (1.0 mmol) sodium carbonate (2.0 mmol), Pd catalyst (200 mg), ethanol (1.5 mL) and water (1.0 mL) were added into a 10 mL vial. Then the mixture was heated at 140 °C under microwave irradiation (100 W). Step 2: 1.0 mmol of substituted phenylboronic acid (1.0 mmol) was added after 10 min and the mixture was further heated under the same conditions for 10 min. The same reaction was also performed under conventional heating and the authors contrasted reaction times and yields with those found upon MW heating. Heating with MW was not only very effective, but is also green. Indeed, the reaction time was reduced (8 min) compared to conventional heating (12 h). The yields obtained were 75% and 82%, respectively. It is worth noting that the continuous purging of inert gas was not required during MW heating. The authors did not observe any side products. The excellent reactivity was explained by the choice of non-functional resin, which probably rendered the reaction sites more accessible and less than 0.1% palladium was sufficient to carry out the C–C coupling reactions. The presence of permanent pores and the hydrophobic nature of the resin can favor the mass transfer of the materials inside the resin matrix. Effective contact among the reactants and the catalyst leads to high reaction rates (TOFs in the order of >103) for bromo derivatives.

Kaur et al. [113] have optimized a very simple procedure for a simple, robust, efficient and recyclable material that is based on Pd nanoparticles encapsulated inside the matrix of Amberlite XAD-4 (a commercial polystyrene–divinylbenzene cross-linked macroporous resin). XAD-4 can be employed in a variety of solvents, due to the low degree of cross-linking, it guarantees facile mass transfer and, above all, is chemically and mechanically stable under MW heating. Encapsulated Pd nanoparticles were successfully tested in the ligand-less SMC reactions of a variety of aryl bromides

under MW heating conditions giving high yields. The reaction conditions were reported as the following; phenylboronic acid (1.8 mmol), aryl bromide (1.5 mmol), sodium carbonate (2.0 mmol), ethanol (1.5 mL), water (1.0 mL) and catalyst (200 mg wet resin) were heated in a 10 mL vial using a CEM MW (140 °C, 100 W) for 8 min. Interestingly, catalytic activity was maintained even in the presence of a thio-containing substrate and a 54% yield was obtained with chlorobenzene.

There are few examples in the literature in which a supported Pd catalyst shows higher activity than a homogeneous system [114,115]. An explanation for this behavior can be found in the improved stability of the active Pd species in the heterogeneous catalyst. Giacalone et al. [116] have adopted a synthetic strategy to achieve the efficient stabilization of very small Pd nanoparticles and therefore grant enhanced catalytic activity. They prepared a C₆₀-ionic liquid hybrid covalently linked to three different solid supports (amorphous silica, SBA-15 and Fe₂O₃@SiO₂) and the resulting materials were used to immobilize and stabilize the metal active phase. The synthetic approach was successful as outstanding catalytic activity was achieved in SMC both under classical heating and under MW irradiation (TOFs up to 3,640,000 h⁻¹) and the silica-based catalyst showed full recyclability even after 10 cycles. The modular synthesis of these supported catalysts, depicted in Figure 5, started from the reaction between triethoxy-3-(2-imidazolin-1-yl)propylsilane and the C₆₀ hexakis-adduct **1** to form compound **2**. **2** was then grafted onto varying supports to obtain compounds **3a–c**, which reacted with 1-methylimidazole and gave the corresponding **4a–c**. The obtained C60-IL hybrids **4a–c** were used for the immobilization of palladium nanoparticles via anion metathesis with tetrachloropalladate ions. Further reduction with NaBH₄ supplied catalysts **5a–c**.

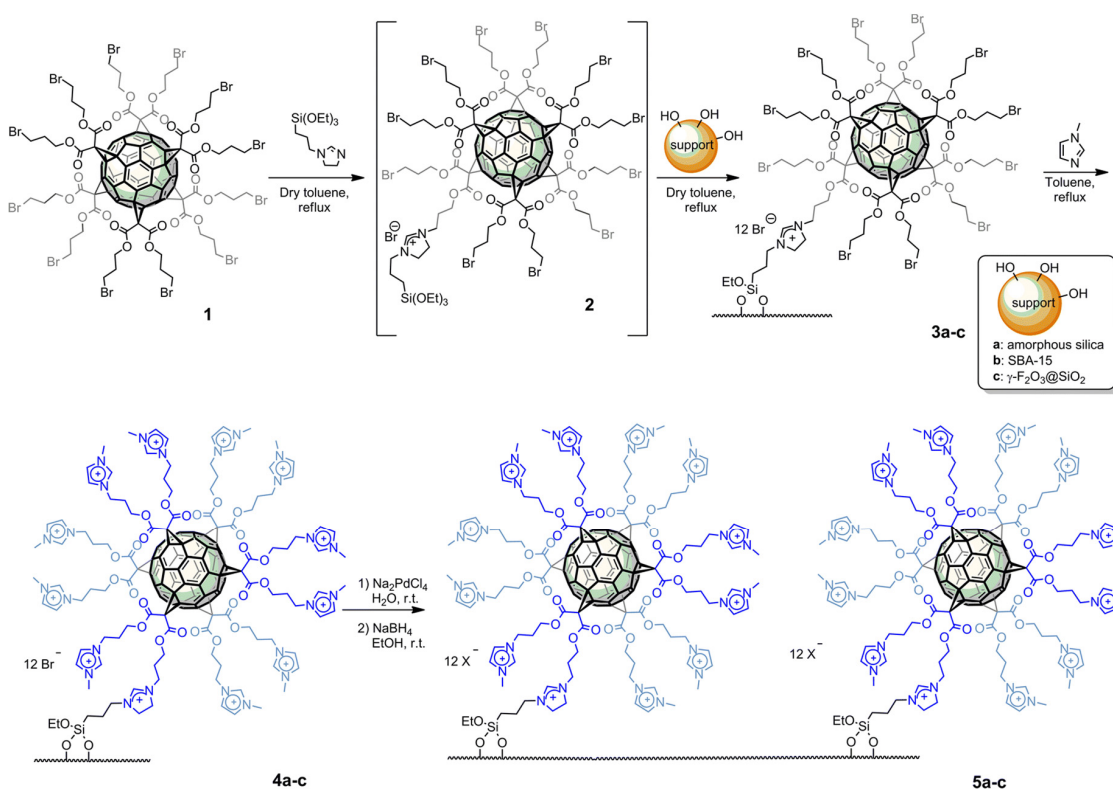
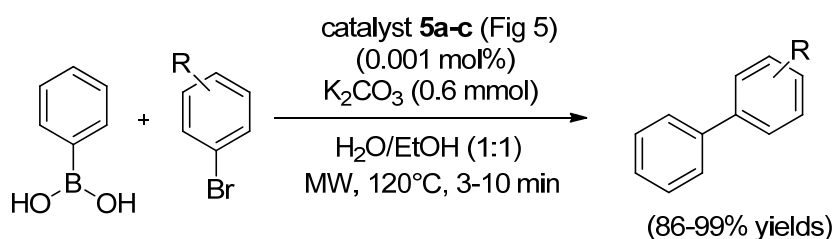


Figure 5. Synthesis of catalysts **5a–c**. Reprinted from [116]. Copyright (2016), with permission from the Royal Society of Chemistry.

Catalysts **5a–c** were also tested at just 0.01 mol % loading in a SMC carried out between various aryl bromides and phenylboronic acid at 50 °C in a mixture of ethanol and water (1:1) in the presence of K₂CO₃. High yields were obtained in short times (1–2 h) in almost all cases. The silica-containing catalyst **5a** was less active than the corresponding SBA-15 and γ -Fe₂O₃@SiO₂ based catalysts **5b** and **5c**.

Interestingly, catalysts **5a** and **5b** were chosen to carry out experiments at higher temperatures (120 °C) both under MW irradiation and conventional heating, according to Scheme 54, in order to investigate the occurrence of any benign effect that may be due to the use of MWs during the reactions.



Scheme 54. Reaction conditions used for the SMC reaction performed in the presence of the **5a-c** catalysts.

The results of the comparative catalytic tests are summarized in Table 4. In more detail, the reactions between 4-bromoacetophenone or 3-bromoanisole and phenylboronic acid were performed in the presence of catalyst **5b** (0.001 mol %), which was the most active at 120 °C. The authors found no specific effect on the formation of the 4-phenylacetophenone product when the reaction was carried out for 10 min using MWs, since both reactions reached 100% conversion within this time (Table 4, entries 1 and 2).

Table 4. SMC catalysed by materials **5a-b** at 120 °C¹.

Entry	Catalyst	R	T (°C)	T (min)	Conv. ² (%)	TON ³	TOF ⁴ (h ⁻¹)
1	5b	4-COCH ₃	120 Δ ⁵	10	>99	100,000	600,000
2	5b	4-COCH ₃	120 MW	10	>99	100,000	600,000
3	5b	4-COCH ₃	120 Δ	3	88	88,000	1,760,000
4	5b	4-COCH ₃	120 MW	3	>99	100,000	2,000,000
5	5a	4-COCH ₃	120 MW	3	>99	100,000	2,000,000
6	5b	3-OCH ₃	120 Δ	10	56	56,000	336,000
7	5b	3-OCH ₃	120 MW	3	73	73,000	1,460,000
8 ⁶	5b	4-COCH ₃	120 MW	3	91	182,000	3,640,000

¹ Reaction conditions: phenylboronic acid (2.2 mmol), 4-bromobenzaldehyde or 3-bromoanisole (2 mmol), K_2CO_3 (2.4 mmol), EtOH (0.8 mL), H_2O (0.8 mL), and catalyst (0.001 mol %) were stirred under MW irradiation (11 W) or under conventional heating for the indicated time; ² Determined by ¹H NMR; ³ TON defined as mol of product/mol of catalyst; ⁴ TOF = TON/h; ⁵ Δ, conventional heating; ⁶ Phenylboronic acid (4.4 mmol), 4-bromobenzaldehyde (4 mmol), K_2CO_3 (4.8 mmol), EtOH (1.6 mL), H_2O (1.6 mL), and catalyst (0.0005 mol %).

However, a small difference between the two activation methods was observed when the heating time was decreased to 3 min (see entries 3 and 4). This was probably due to the faster and uniform heating of the reaction mixture during MW irradiation, as compared to conventional heating. It was proposed that the higher heating ability of the MW irradiation is the discriminating factor that led to a quantitative yield in such a short time. On the other hand, 10 min was enough time to mitigate any difference between the two methods and a quantitative yield was also obtained when conventional heating was adopted (Table 4, entries 1 and 2). In addition, the less active catalyst SiO_2 -C60-IL-Pd (**5a**) also efficiently catalyzed the reaction under MW irradiation giving the coupling product in a quantitative yield in 3 min (entry 5).

A TON of 100,000 and a TOF of 2,000,000 h⁻¹ were reached in **5b** (entry 4). Nevertheless, the MW-assisted reaction of the less reactive 3-bromoanisole substrate, for 3 min at 120 °C, led to improved conversions as compared to the same reaction carried out under conventional heating for 10 min, proving that there was a beneficial effect (entries 6 and 7). Finally, a further decrease in catalyst **5b** loading, to 0.0005%, gave the outstanding TON and TOF values of 182,000 and 3,640,000 h⁻¹, respectively (entry 8).

A novel $Fe_3O_4@SiO_2/N$ -[3-(trimethoxysilyl)propyl] ethylenediamine-Pd(II) catalyst was successfully synthesised and tested in the Suzuki cross-coupling reaction between phenyl boronic acid and

4-iodoanisole [117]. The authors proposed an elegant multivariate approach to optimise the reaction by varying different parameters. In the first stage, the effects of time and temperature, as well as of the interaction between them were evaluated by using factorial design. In the second step, the Doehlert matrix was used to find the optimal reaction conditions, as the choice of the solvent, the nature of the base and the catalyst loading for the Suzuki cross-coupling. The authors claimed that the optimized protocol can be applied to many substrates, with yields ranging from 71% to 96% after 6 min under microwave irradiation. In addition, the catalyst was recovered and reused for 3 runs with restrained activity loss [117]. Moussa et al. [118] have reported the optimization of an easy laser reduction method to synthesise Pd nanoparticles immobilised on partially reduced graphene oxide (PRGO) and have demonstrated their high activity in Suzuki, Heck and Sonogashira cross-coupling reactions. The strategy adopted in improving this procedure makes use of the photogenerated electrons in GO that can reduce the Pd ions and, at the same time, can partially reduce GO, thus forming PRGO-supported Pd nanoparticles. It was shown that it is possible to modify the reducing environment by tuning the composition of the solvent, thus controlling the growth kinetics of the Pd nanoparticles. The authors compared the catalytic activity of the Pd-PRGO nanocatalysts A (20 μ L of Pd(NO₃)₂ added to 6 mL of GO solution in 2 mg of GO/10 mL of deionized water), B (in 50 vol % ethanol–water), and C (in 50% methanol–water mixtures) in the SMC reaction of bromobenzene and phenylboronic acid in a mixture of H₂O/EtOH (1:1) at room temperature. In more detail, A and B show comparable reactivity and result in high conversions of 100% and 95%, respectively, after 45 min at room temperature. Catalyst C displays only 88% conversion in 45 min. The same trend was noted when the catalyst loading was decreased to 0.008 mol % after 8 h at room temperature (A, B, and C result in 95, 92, and 80% conversions, respectively).

Interestingly, the reaction was surprisingly fast for catalyst A in the presence of the same Pd loading at 120 °C under MW irradiation, converting 62% of the bromobenzene after 2 min. The complete formation (100%) of the biphenyl product was observed after 5 min under the same reaction conditions. The authors also claimed that MW heating at 120 °C was needed to reach full conversion with this very low catalyst loading. An outstanding turn over number (TON) of 7800 and a turnover frequency (TOF) of 230,000 h⁻¹ were obtained for catalyst A.

It is worth noting that a small conversion (5%) was observed after 6 h in refluxing conditions at 120 °C when a similar SMC reaction was carried out under conventional thermal heating, using 0.008 mol % of catalyst A. This finding definitely proves the beneficial effect of MW irradiation. Indeed MW, as a direct and rapid heating source, can increase the cross coupling reaction rates. This is in agreement with recent studies on the non-uniform heating at the surface of heterogeneous catalysts and on the production of hot spots by MW irradiation, resulting in non-equilibrium local heating localized at the surface of the metal nanoparticles present on the catalysts. This phenomenon was observed as occurring to the dimethylsulfoxide (DMSO) molecules in the proximity of Co nanoparticles under MW irradiation by real-time in situ Raman spectroscopy [119]. Interestingly, non-equilibrium local heating was only induced under MW irradiation, not under conventional heating. The Raman spectra collected for dimethylsulfoxide (DMSO) under MW heating at 0.25 s intervals, in the temperature range of 300–500 K, are shown in Figure 6a. The T_r (temperatures measured by the intensity ratios of Stokes to anti-Stokes lines employing in situ Raman scattering measurements) and T_f (temperatures determined by the fiber-optical thermometer) plotted vs. t (time) are reported in Figure 6b,c. Some spikes were detected in the measured temperatures, as defined by Raman, demonstrating that abnormally high temperatures occurred at 3.4 min (433 K), 5.8 min (473 K), and 7.3 min (423 K).

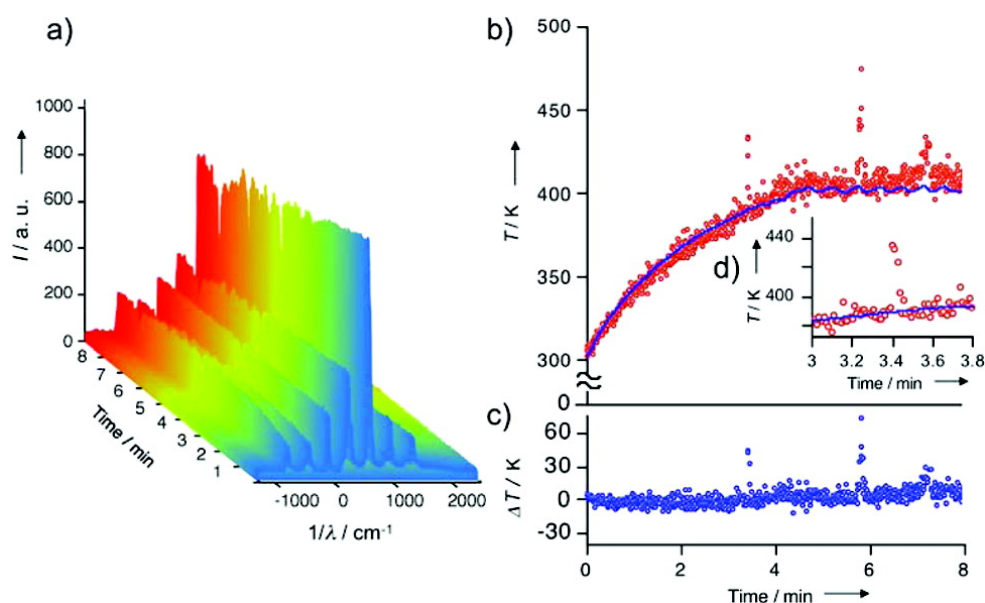


Figure 6. Non-equilibrium local heating induced by MW irradiation. (a) Time-dependent Raman spectra of DMSO heated by MW irradiation at 0.25 s intervals for 8 min in the temperature range 300–500 K; (b) T_r (temperatures determined by the intensity ratios of Stokes to anti-Stokes lines using in situ Raman scattering measurements) (red circles) and T_f (temperatures monitored by the fiber-optical thermometer) (blue line) vs. t (time) plot; (c) ΔT ($\Delta T = T_r - T_f$) vs. t (time) plot; (d) Enlarged view of Figure 6b in the range 3.0–3.8 min. Reprinted from [119]. Copyright (2010), with permission from American Chemical Society.

Horikoshi et al. [120] investigated the hot-spot generation on Pd nanoparticles supported on activated carbon during the synthesis of 4-methylbiphenyl by a Suzuki coupling reaction occurring in a nonpolar solvent by recording the events with a high-speed camera. The authors found that the hot-spots are produced during reaction under exposure to the microwave electric field, whilst they are scarcely formed under magnetic field conditions. It was demonstrated that the efficiency in hot-spot generation is related to the type of microwave generator (semiconductor or magnetron) that is employed. Interestingly, the microwave H-field originated by a semiconductor generator has a positive effect on the reaction, resulting in enhanced yields. On the contrary, the authors claimed that the formation of hot-spots on the activated carbon under E-field conditions negatively influences the product yields, due to the Pd nanoparticle aggregation. Therefore, hot-spots can have both positive and negative effect and it is of pivotal importance to control the formation of hot-spots under E-field conditions when the reaction is performed in the presence of a heterogeneous catalyst in a nonpolar solvent. Nevertheless, the reaction can be carried out with microwaves under H-field conditions. It is worth noting that hot-spots also play an important role in the synthesis of heterogeneous catalysts, as will be discussed in detail in the following. Pd nanoparticles supported on graphene platelets have been successfully employed in a SMC between 4-bromoanisole and potassium phenyltrifluoroborate using 1 mol % of Pd and K_2CO_3 , used as a base, in MeOH/ H_2O as the solvent at 80 °C under conventional and MW heating [121]. The separation of the catalyst from the reaction mixture after each run was easily achieved by washing with a solvent mixture (EtOAc/MeOH/ H_2O) and further centrifugation. Interestingly, Pd/graphene was reused at least 8 times without losing activity when MW irradiation (MW) conditions were adopted (first row of Table 5). However, the activity significantly dropped after 5 cycles under conventional heating (Δ) reaction conditions (second row of Table 5).

Table 5. Pd/graphene recyclability and yields in the SMC across different cycles.

Cycle		1	2	3	4	5	6	7	8
Yield (%)	MW ¹	>99	>99	>99	>99	91	95	97	>99
	Δ ¹	>99	>99	>99	90	83	58	44	40

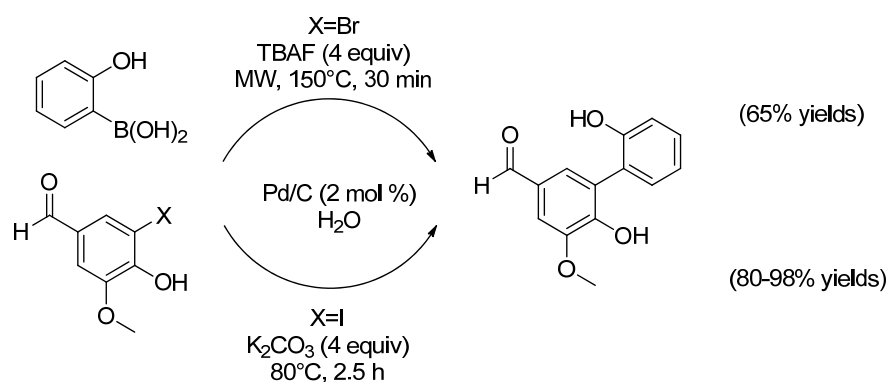
¹ MW irradiation for 2 h or Δ for 20 h.

The authors performed an inductively coupled plasma mass spectrometry (ICP-MS) analysis of the washings after the 1st cycle under both reaction conditions (MWs and conventional heating), and found varying Pd leaching levels. In particular, 1103 ppb of leached Pd were detected under MW irradiation conditions, whilst 15 ppb of Pd were found after the 1st run using conventional heating. Pd leaching was therefore not the cause of the activity decrease observed after 5 cycles under conventional thermal conditions. Transmission electron microscopy (TEM) measurements highlighted that the average diameter of the nanoparticles after 8 cycles (originally 4.5 nm) increased significantly under conventional heating compared to MW heating (13.4 nm vs. 6.6 nm), explaining the lower reactivity of the recycled catalyst after being tested under conventional heating reaction conditions. It was elegantly demonstrated that the Pd leached for the duration of the reaction is largely re-deposited on the solid support after the reaction and that centrifugation facilitated this recovery process.

García-Suárez et al. have compared conventional and MW heating in the use of Pd nanoparticles that are immobilised on mesoporous carbon bead catalysts were evaluated in the aqueous SMC reactions between phenylboronic acid and arylhalides, which contained a number of different electron withdrawing and donor substituents [122]. Excellent activity was obtained at short reaction times (5–10 min) while TOF values of up to 3000 h⁻¹ were reached under MW heating.

It was found that it was possible to recycle catalysts up to 10 (conventional heating) and to 5 (MW irradiation) reaction runs without any loss in activity. The reaction media was found to have a strong influence on the recyclability of the catalysts, which could be improved in the presence of polyethylene glycol. The conditions of a typical experiment, under an open atmosphere, are reported as follows; catalyst (1.5 or 0.375 mol % of Pd), arylhalide (0.25 mmol), phenylboronic acid (1.4 equiv.), either K₂CO₃, NaOH or KOAc (2 equiv.), internal standard (*n*-decane; 25 μL) and solvent (3 mL), namely distilled H₂O or a PEG in H₂O mixture (50 wt %). The reaction mixture was stirred at 50 °C for 5–30 min. As for the reactions performed under MW conditions, the reaction medium was heated in a CEM-DISCOVER reactor for 5 min at a power output of 100 W, reaching a maximum temperature of 150 °C. Very good conversion values, >90%, were achieved in polyethylene glycol/H₂O mixtures after 10 min of reaction with all catalysts. It was found that the catalytic activity is influenced by the chemical surface and porosity of the carbon supports. SMC reactions were also attempted under MW irradiation using para-arylbromides and phenylboronic acid in the polyethylene glycol/H₂O mixture solvent in the presence of a reduced amount of catalyst (from 1.5 to 0.375 mol %). A comparison of the results obtained under MW irradiation and conventional heating lead to the conclusion that that MW heating considerably enhanced the reaction rate for all the catalysts, particularly when using para-bromobenzaldehyde as the substrate. Moreover, the trend for the activity of the catalysts is the same irrespective of the activation method used. Almost complete conversion (96%) was achieved after 5 min of reaction time using Pd supported on mesoporous carbon beads previously heated at 2000 °C for 1 h, while a TOF of 3236 h⁻¹ was found, which is higher than the 650 h⁻¹ obtained under conventional heating. Interestingly, MW heating provided beneficial effects in the cross coupling of para-bromoanisole, with significantly improved conversions as compared with bromobenzene. A similar trend was also reported by Gomez et al. and explained by the interaction between the methoxy group and the metallic surface which induces higher C–Br bond activation than expected for the intrinsically electronic factors behind para-bromoanisole [123]. Finally, coupling reactions were also attempted using the more challenging *p*-chlorobenzaldehyde, but, unfortunately, very low conversions were achieved after 5 min of reaction.

Schmidt et al. [124] have investigated the protecting group-free synthesis of 2,2'-biphenols via heterogeneously catalyzed SMC under MW irradiation (see Scheme 55). Palladium on charcoal was adopted as the simple and conveniently available heterogeneous catalyst. Because of its nature, this catalyst can be recycled and reused and, at the same time, the contamination of the reaction products by metal residues can be diminished. A plethora of o-halophenols and o-boronophenols underwent SMC in high yields (85%–98%) and selectivity, in terms of 2,2'-biphenols. The reactions proceeded in H₂O in the presence of simple additives, such as K₂CO₃, KOH, KF and TBAF and 2 mol % Pd catalysts. The described protocol was simple and extremely sustainable, because no elaborate pre-catalysts and ligands were needed to achieve synthetically useful yields and short reaction times. While iodophenols successfully reacted in 2.5 h in excellent yields even under thermal conditions, the coupling of the analogous bromophenols only proceeded effectively under MW irradiation in 0.5 h.



Scheme 55. Synthesis of 2,2'-Biphenols via protecting group-free MW-promoted SMC in water.

Continuing investigations into catalyst immobilization onto varying supports have led Al-Amin et al. [125] to obtain a low-leaching Pd-catalyst supported on a sulfur-modified Au supported material (SAPd). This immobilized Pd-catalyst has proven to be very feasible in both C–C and C–N bond-forming reactions. SAPd was able to release a trace of highly active Pd into the reaction mixture, which enabled it to be used in the MW-assisted SMC reactions.

In this context, the reported SAPd-mediated reactions proceeded under ligand-free conditions under the coupled use of two different MW irradiation chambers; a leaching chamber, in which traces of the active Pd phase would leach from SAPd via the effects of arylhalides under single-mode MW irradiation and a catalytic reaction chamber, in which the catalytic reaction would occur towards the desired transformations under multi-mode MW irradiation. The combined use of two MW reactors employing differing irradiation methods made the protocol very effective, due to the easy control of the leaching throughout the 2 step process.

The considerable accomplishment of this MW protocol was that less reactive arylbromides (i.e., bromobenzene, 4-bromoanisole, p-bromotoluene, 4-bromonitrobenzene and 4-bromobenzonitrile) were effectively coupled to the desired products in ethanol, a feat which has not yet been reached under conventional heating conditions, with such catalytic system, while the reaction time for aryl iodide coupling was decreased from 12 to 2 h in a toluene/water solvent mixture. In addition, the low leaching characteristics of SAPd make it recyclable for more than 10 runs meaning that the reaction can be simply scaled up.

Use of MWs for the Synthesis of the Catalysts for the SMC Reaction

MW-assisted reactions are considered to be a very interesting approach and one which rapidly prepares uniform and phase pure materials. MW irradiation has been proven to be effective in the synthesis of a variety of nanomaterials, which are prepared with controlled size and shape without the need for high temperatures or high pressures. Heinrich et al. [126] have synthesized two new square-planar *trans* Pd

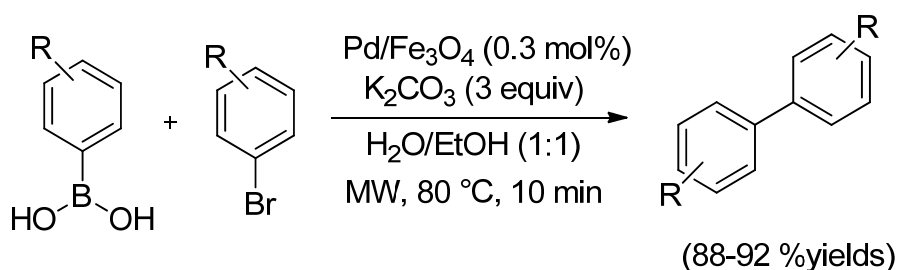
complexes, $[\text{Pd}(\text{MEA})_2\text{Cl}_2]$ and $[\text{Pd}(\text{MEA})_2\text{Br}_2]$ [MEA = (2-methoxyethyl)amine], by reacting 2 equiv. of MEA with either PdCl_2 or $[(\text{cod})\text{PdBr}_2]$ (cod = cycloocta-1,5-diene). The complexes were then used as precursors to the preparation of Pd nanoparticles by MW-assisted synthesis.

The authors investigated the effect of the reaction temperature, irradiation time and surfactant (polyvinylpyrrolidone) amount on the size of the produced particles (5–40 nm). It was found that the growth mechanism of the nanoparticles depended on the type of halide ligand used. The Pd particles were embedded in carbonized wood and tested as a catalyst in C–C cross-coupling Heck, Suzuki and Sonogashira reactions, resulting in TON values of 4321 (Heck), 6173 (Sonogashira) and 8223 (Suzuki).

Pd nanoparticles supported on graphene (G) and graphene oxide (GO) have been prepared using the MW irradiation method [127]. The uniform and fast temperature rise produced by MWs in the presence of hydrazine hydrate, used as a reducing agent, offered a facile and efficient procedure to effectively reduce Pd(II) and GO into a dispersion of metallic nanoparticles supported on graphene sheets with large surface area. Power and time irradiation can be optimized to yield the nearly complete reduction of both GO and the Pd salt precursor. Therefore, it was claimed that, unlike conventional thermal heating, activation by MW provides better control of the extent of graphene oxide reduction by hydrazine hydrates. On the contrary, Pd/GO was synthesized by the MW-assisted deposition of $\text{Pd}(\text{NO}_3)_2$ in a GO dispersion and no reducing agent was added.

The SMC of variously substituted aryl bromide and phenylboronic acid reagents was performed in the presence of 0.3 mol % Pd/G and K_2CO_3 (3 equiv.) in $\text{H}_2\text{O}/\text{EtOH}$ (1:1), used as environmentally benign solvents. The reactions were carried out at room temperature or heated under MW irradiation at 80 °C for 10 min. It was observed that the rapid temperature rise during MW heating in H_2O induced quick Pd nucleation and consequently produced small uniform nanoparticles with sizes of 7–9 nm. As revealed by TEM measurements, the nanoparticles produced were well dispersed on the graphene sheets, explaining the great reactivity displayed by the Pd/C catalyst.

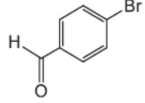
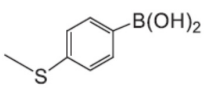
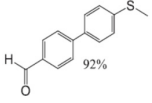
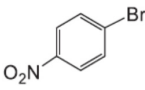
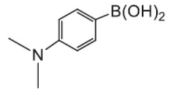
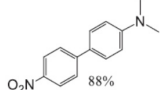
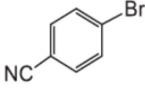
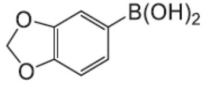
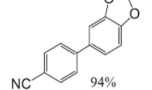
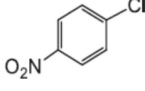
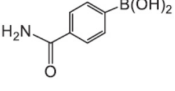
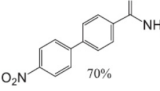
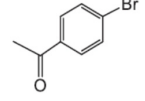
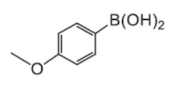
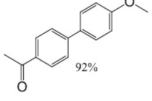
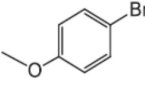
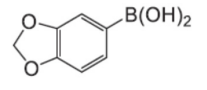
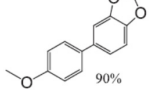
Elazab et al. have reported a simple MW-assisted (1000 W, 2.45 MHz for 120 s) one-step synthesis of Pd/ Fe_3O_4 nanoparticles supported on graphene nanosheets (Pd/ Fe_3O_4 /G) that display extraordinary catalytic activity in Suzuki and Heck coupling reactions [128]. The SMC reaction is reported together with the reaction conditions in Scheme 56.



Scheme 56. MW-assisted SMC with Pd/ Fe_3O_4 /C nanoparticles catalyst.

The catalyst was magnetically separated from the reaction mixture and recycled many times without losing activity. The synthetic procedure envisaged the reduction of palladium and ferric nitrates in the presence of graphene oxide (GO) nanosheets under MW irradiation. Hydrazine hydrate was employed as the reducing agent. It was found that the most active and recyclable catalyst (7.6 wt % Pd loading) was made up of Pd(0) nanoparticles with sizes in the 4–6 nm diameter range which strongly interacted with the 30 wt % Fe_3O_4 nanoparticles, with 12–16 nm diameters, on highly reduced GO containing a C/O ratio of 8.1. Such a combination was proven to have a synergic effect on the catalytic activity of SMC reactions under MW irradiation. The reactions tested in the presence of the 7.6 wt % Pd/ Fe_3O_4 catalyst are summarized in Table 6.

Table 6. SMC reactions using 7.6 wt % Pd/Fe₃O₄¹.

Aryl-Halide	Boronic Acid	Isolated Yields
		 92%
		 88%
		 94%
		 70%
		 92%
		 90%

¹ Aryl halide (0.32 mmol), boronic acid (0.382 mmol), potassium carbonate (0.96 mmol) and Pd/Fe₃O₄/G (0.3 mol %) in 4 mL (H₂O/EtOH) (1:1) was heated at 80 °C under MW for 10 min. 1st and 2nd reactions were completed at r.t. after 30 min.

Indeed, extremely high TON (9250) and TOF (111,000 h⁻¹) values were attained at 80 °C. The magnetic properties caused by the Fe₃O₄ component guaranteed easy separation, as illustrated in Figure 7, thus greatly simplifying the purification of the reaction products and increasing the economic value of the catalyst.

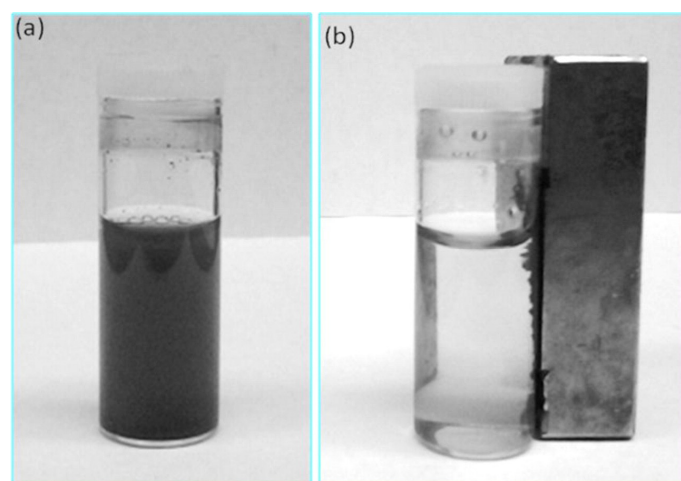


Figure 7. (a) Image of the reaction mixture using 0.3 mol % Pd/Fe₃O₄/G catalyst after reaction; (b) Separation of spent catalyst from reaction mixture using a simple magnet. Reprinted from [128]. Copyright (2015), with permission from Elsevier.

Indeed, the synthesis of materials under MW irradiation is a relatively novel method that can be used in many applications, such as the preparation of nanoporous structures. The synthesis of metal-organic frameworks (MOFs) under MW irradiation not only extensively reduces reaction time,

but also can grant control of the size and shape of the crystals [129]. Li et al. [130] have developed an efficient MW assisted procedure to synthesize UiO-66 in high yields in the presence of benzoic and acetic acids. They found that MW irradiation not only shortened the reaction time, but also improved the surface area of UiO-66. Recently, Dong et al. [131] have successfully synthesized UiO-66 under MW irradiation and then used the MOF as a support for Pd nanoparticles. A 0.075 mol % amount of the obtained catalyst was able to efficiently catalyze the SMC reaction between bromobenzene and phenylboronic acid in ethanol–water mixture (1:1) at 30 °C. Moreover, the complete reaction was achieved in 0.5–1.5 h with moderate or excellent yields, in the presence of substrates that bore electron-donating groups and electron-withdrawing groups. Pd@UiO-66 proved to be very stable since it was separated via filtration and recycled 5 times without significant loss in catalytic activity. Unfortunately, the authors only observed a 29% yield using aryl chlorides.

A novel heterobimetallic Pd/Y-MOF catalyst was synthesized using MW irradiation as reported by Huang et al. [132]. This catalyst was proven to be very active in the water-medium SMC reactions of a number of aryl halides with 4-methylphenylboronic acid and in the Sonogashira reaction. It was found that the catalytic activity of Pd/Y-MOF is as good as that of the traditional Pd(OAc)₂ homogeneous catalyst. This was due to, on one hand, the cooperative effect of Y(III) coordination and, on the other hand, to the highly dispersed and accessible Pd(II) active sites present in the layered structure. More interestingly, besides high activity, the Pd/Y-MOF catalyst was also able to select the size of the reactant molecules because of the diffusion limit within the micropores. The coordination of Pd(II) and N atoms with 2,2'-bipyridine-5,5-dicarboxylate acid blocked the leaching of Pd(II) active species under the reaction conditions. Moreover, it can be successfully recycled and reused repetitively thanks to excellent MOF framework stability, which is derived from the strong interaction between Y(III) and carboxyl, and therefore shows great potential in practical applications. This study demonstrated that the MW-assisted synthetic strategy can be considered a general procedure for developing MOF-based heterogeneous catalysts by building homogeneous counterparts inside MOFs frameworks for practical catalytic applications.

A simple MW assisted technique was recently used to prepare Cu₂O microcubes decorated with nano Au and Pd [133]. The SEM and TEM images, together with Energy-dispersive X-ray Spectroscopy (EDXS) analyses, are shown in Figure 8.

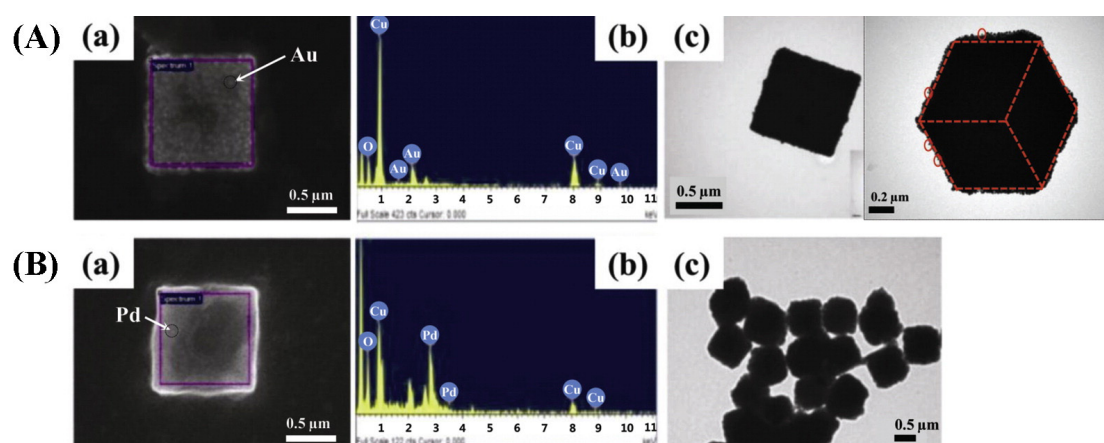


Figure 8. (a) SEM; (b) EDXS; and (c) TEM images of (A) Au and (B) Pd nanoparticle decorated Cu₂O microcubes. Reprinted from [133]. Copyright (2014), with permission from Elsevier.

More specifically, Cu₂O microcrystals were synthesized by adding 0.03 g of polyvinylpyrrolidone to 5.0 mL of a 10.0 mM CuCl₂ aqueous solution, followed by the addition of 0.18 mL 1 N NaOH and 0.38 mL deuterium-depleted H₂O under stirring. Glucose (0.0072 g) was subsequently added as a reducing agent and the solution was placed into a MW oven for 3 min at 100 W. 1.0 mL of

10.0 mM HAuCl_4 was subsequently added to the Cu_2O colloidal solution, which then had a brick red color, and underwent 100 W MW irradiation for 1 min, forming a blackish, winered colloidal solution of $\text{Cu}_2\text{O}/\text{Au}$. A $\text{Cu}_2\text{O}/\text{Pd}$ catalyst was synthesized by following the same procedure, but using 1.0 mL of 10.0 mM H_2PdCl_4 . A dark greenish brown color $\text{Cu}_2\text{O}/\text{Pd}$ colloid was obtained and was tested in the coupling reaction synthesis of phenylboronic acid and 4-iodobenzonitrile (see Figure 9 for all the synthetic steps). The SMC was performed overnight, using water as the solvent in the presence of 8.0 mg $\text{Cu}_2\text{O}/\text{Pd}$ colloid and K_2CO_3 at 80 °C. 4-cyanobiphenyl was produced with good selectivity and a satisfactory yield (over 85%). Moreover, the authors verified the versatile nature of $\text{Cu}_2\text{O}/\text{Pd}$ catalyst in the coupling reactions of iodoarenes by performing reactions with electron donating and withdrawing groups. The results of this paper demonstrate that the MW-assisted technique successfully simplifies the synthesis process for metal/metal oxide catalysts.

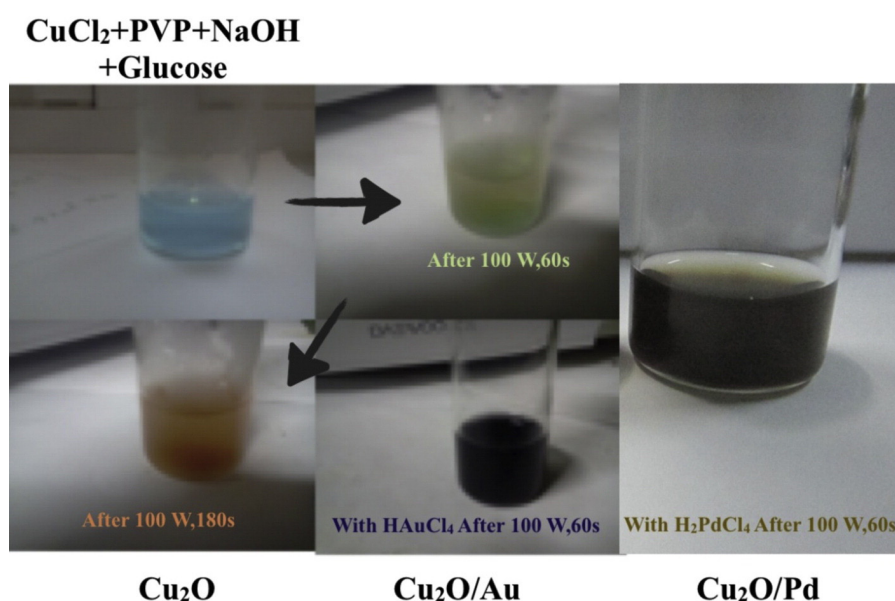


Figure 9. Digital photographs of reagents involved during the preparation of Cu_2O based catalyst. Reprinted from [133]. Copyright (2014), with permission from Elsevier.

Veerakumar et al. [134] have reported the preparation of highly dispersed palladium nanoparticles (average size of ca. 5 nm, PdNPs) immobilized on carbon porous materials (CPMs) via a MW assisted procedure, during which the Pd^{2+} ions were successfully reduced to Pd^0 and extremely well dispersed onto the carbonaceous support. These heterogeneous Pd/CPM catalysts (5.0 mg) exhibit high activity for C–C coupling reactions of various aryl halides with phenylboronic acid in aqueous dimethylformamide ($\text{DMF}/\text{H}_2\text{O} = 1:1$) with desirable product yields of >88% in the presence of K_2CO_3 (2 mmol) when irradiated for 10–15 min in MW at 100 °C. The reported catalyst can be easily recovered from the reaction mixture by centrifugation and reused in a few reaction cycles.

Along with supplying robust, stoichiometric and complex compounds, MW preparation routes have also proven to be suitable for the synthesis of complex substituted oxides, where a dopant ion resides on a metal cation site. Misch et al. [135] have recently reported a rapid MW-assisted combustion/sol–gel preparation as a suitable procedure for the preparation of noble metal-substituted perovskites. The authors performed a detailed investigation of the phase formation process thanks to the very brief and controllable heating times enabled by MWs. It was also demonstrated that substituted perovskites were able to provide a Pd source for SMC catalysis. The La containing perovskites were more active than the Y containing perovskites (the structures are represented in Figure 10), and the authors proposed that a varying inductive effect on the perovskite can occur depending on the differing A-site cation, resulting in differing Pd ion stability in the material.

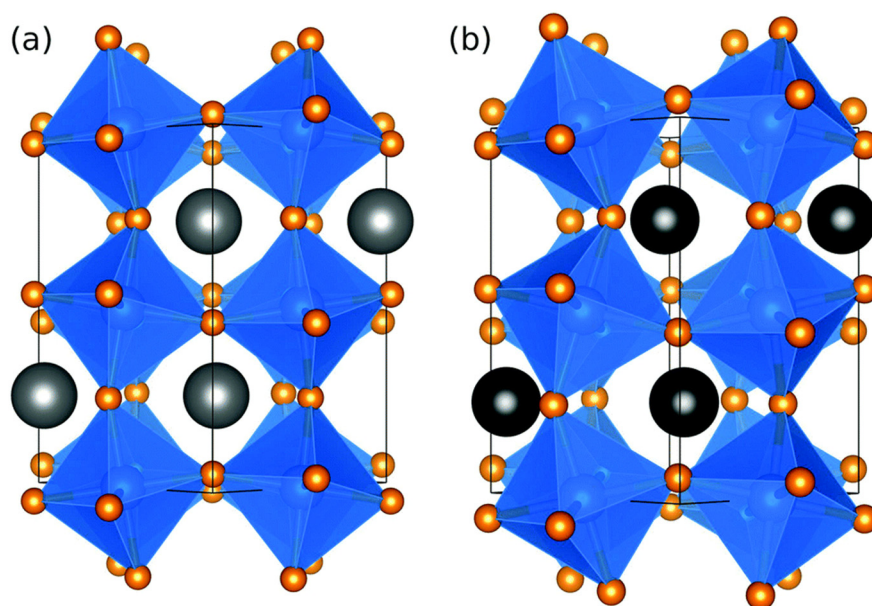


Figure 10. Crystal structures for (a) LaFeO_3 ; and (b) YFeO_3 . The A site cations are displayed as grey spheres and FeO_6 octahedra in blue. Reprinted from [135]. Copyright (2013), with permission from Royal Society of Chemistry.

Furthermore, it was unambiguously established, using the 2-dicyclohexylphosphine-2',6'-dimethoxybiphenyl ligand, that catalytic activity does not originate from the perovskite itself, but from reduced Pd^0 that is liberated and then bound by the ligand. Interestingly, these materials were proven to be suitable for aryl chloride coupling under more mild conditions than had previously been described. The reported method may furthermore allow the synthesis of materials with even higher surface areas to be carried out, thereby regulating their properties.

3. Ultrasound-Assisted SMC Reactions

3.1. Ultrasound-Assisted SMC Reactions

Among the wide range of US application in organic chemistry, a great number of US promoted SMC reactions have been reported in literature in the last decade. [136] An US-induced continuous flow technique has been developed by Shil et al. [137] for the gram scale SMC reaction of haloarenes (chloro, bromo and iodo) with phenylboronic acid catalyzed by solid supported $\text{Pd}(0)$ nano/microparticle (SS-Pd). They previously reported [138] a facile process for the in situ generation of $\text{Pd}(0)$ nano- and microparticles and their stable deposition over the amberlite IRA 900 resin. The hydrophobic and hydrophilic combination of the borohydride exchanged polymer used for SS-Pd preparation played a crucial role in reducing the $\text{Pd}(\text{II})$ ion to $\text{Pd}(0)$, and impregnating it into the hydrophobic pockets of the polymer matrix as nano- and microparticles. The obtained SS-Pd catalyst was noted as being extremely stable in aqueous media, easily separable and recyclable for up to five runs in SMC without relevant loss in activity under mild basic conditions (Figure 11). Furthermore, ultrasonication provided enough excitation energy to perform the reaction in methanol-water and increased the solubility of K_2CO_3 to supply the extraordinary basic conditions, which drove the reaction into products at ambient temperature with satisfactory yields (~80% for 3 mol % of Pd). Furthermore, the simple isolation of the crude products with negligible metal contamination and recyclability of the SS-Pd catalyst can furnish huge green impact and lead to industrial interest.

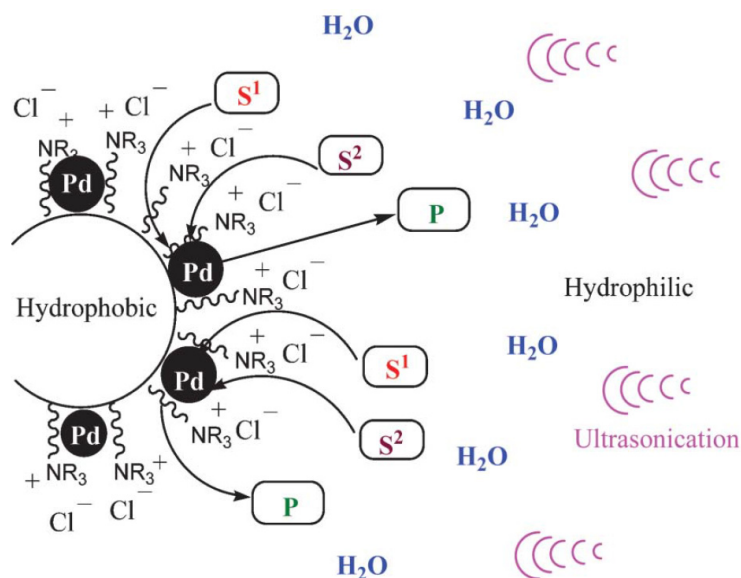


Figure 11. A schematic diagram of the reaction outline on the catalyst surface; S¹ = aryl halide, S² = phenylboronic acid and P = product (Reproduced from [137]. Copyright (2013), with permission from Royal Society of Chemistry).

Azua et al. [139] have reported the synthesis of novel Pd *N*-heterocyclic-carbene (NHC)-based complexes with 3,4,5-trimethoxybenzyl, alkyl and sulfonate *N*-substituents, suitable for SMC (Figure 12). The new complexes were exploited as pre-catalysts (1 mol % of Pd) in the cross-coupling reactions of various aryl halides/boron moieties in glycerol under pulsed-US activation. US activation allows scientists to overcome one of the major drawbacks of the application of glycerol; its high viscosity, which limits mass transport and the efficient mixing of the reaction mixtures. High yields (70%–85%) were obtained in 30 min under pulsed US activation, without the production of undesired by-products. Catalyst fate was investigated by the author using TEM and X-ray Photoelectron Spectroscopy (XPS) analyses. Not quite rigidly classifying the transformation as a homogeneous or heterogeneous process, they preferred to postulate that different active catalytic species (cocktail of compounds) were present in solution.

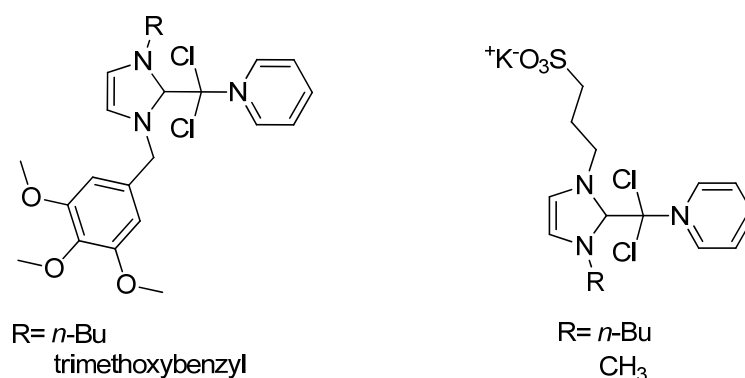


Figure 12. Pd(II)-NHC (*N*-Heterocyclic-Carbene) based complexes.

A series of 1-(α -aminobenzyl)-2-naphthols have been prepared, by Chaudhary and Bedekar, [140] from 2-naphthols using an aromatic Mannich reaction [141] and screened as air-stable phosphine-free ligands for Pd-catalyzed US assisted SMC. The amino phenol structure, as reported in Figure 13, has a suitable arrangement of heteroatoms to form a six-membered stable chelate, a prerequisite for use as a ligand in metal-catalyzed reactions. The results of the Pd(AcO)₂ catalyzed SMC, in the presence of

1-(α -aminobenzyl)-2-naphthols, showed very efficient conversion with aryl iodides and aryl bromides when using a small quantity of TBAB and aqueous dioxane as the solvent. Chlorobenzene was considerably less reactive after a long reaction time but iodobenzene gave biphenyls with good conversion amounts even at very low catalyst quantities. Varying the amount of catalyst, to as low as 0.01 mol % of Pd, resulted in the US assisted formation of biphenyl in high yields and TON values.

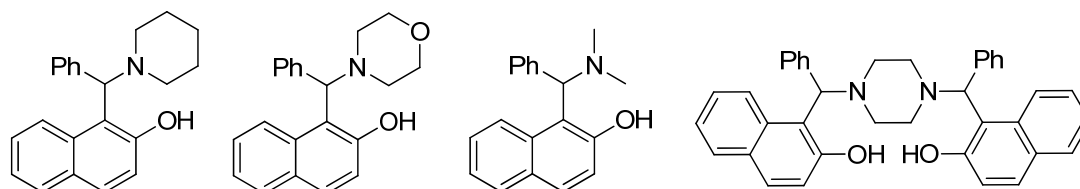


Figure 13. Air-stable phosphine-free ligands used for SMC based on 1-(α -aminobenzyl)-2-naphthol structure.

A new and extremely stable Pd(EDTA)²⁻-salt has been prepared as a catalyst by Ghotbinejad et al. [142] employing a counter-cation of *N*-methylimidazolium bonded to 1,3,5-triazine-tethered superparamagnetic iron oxide nanoparticles (SPIONs) (Figure 14). This complex efficiently catalyzed SMC reactions between various arylbromides and arylboronic acids in the presence of K₂CO₃, used as a base, in an aqueous solution of DMF. The cross-coupled products were synthesized under conventional heating (70 °C) and US irradiation (160 W, 30 °C) using a very low catalyst loading (as low as 0.032 mol % Pd). Results indicated that conventional preparation took longer (4 h) and gave moderate yields, while the reaction occurred quickly (10 min) in the presence of US irradiation and gave high to excellent yields (95%). The SPION-A-Pd(EDTA) catalyst was quickly recovered using an applied external magnetic field and was reused for several cycles without any loss in its high catalytic performance (TOF $1.1 \times 10^5 \text{ h}^{-1}$).

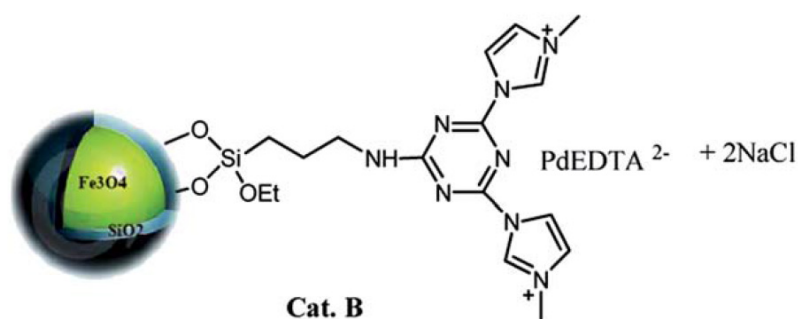


Figure 14. General structure of SPION-A-Pd(EDTA) nanocatalyst. (Reproduced from [142]. Copyright (2014), with permission from Royal Society of Chemistry).

A heterogeneous catalyst, involving Pd embedded within porous carbon (CMK-3), has been prepared by Wang et al. (2014) [143] via a three-step method: immersion, ammonia hydrolysis and heating. Accurate characterization of the Pd@CMK-3 catalyst showed that Pd(0) and Pd(II) species co-exist and were embedded inside the matrix of the porous carbon CMK-3 (Figure 15). This catalyst has shown high activity toward standard SMC in the presence of K₂CO₃. Resistance to mass transfer in the pore channels was significantly reduced when the reaction mixture was homogenized by two minutes of ultrasonication rather than magnetic stirring before heating. As a result, the reactions proceeded quickly and a four-fold increase in the turnover frequency ($\sim 2800 \text{ h}^{-1}$) was described. When ultrasonication (40 kHz, 150 W, 30 °C) was used throughout the total reaction process, conversion exceeded 90% even without the protection of an inert gas.

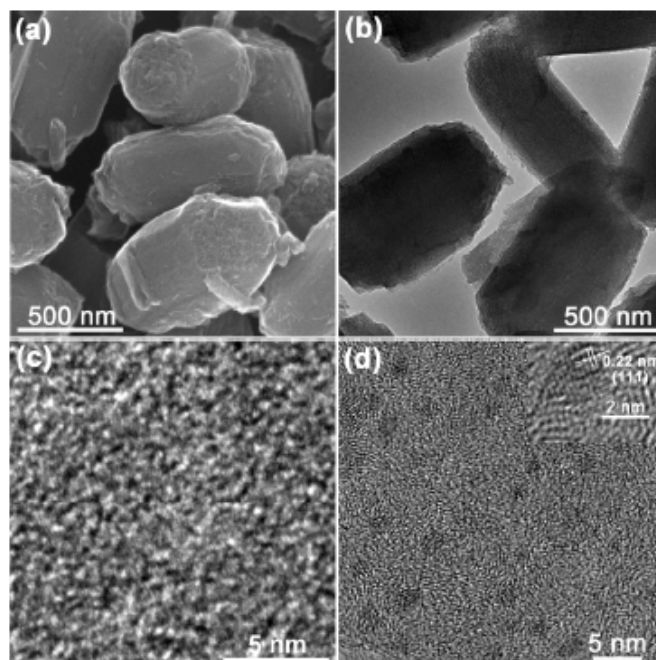
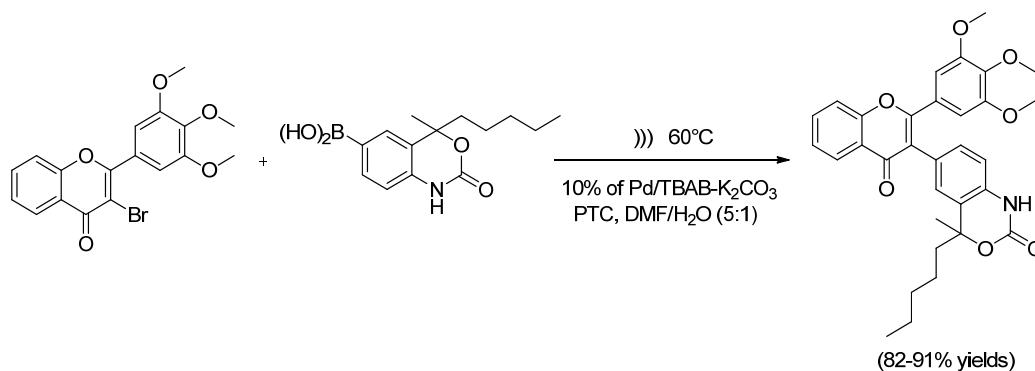


Figure 15. Electron microscope images of Pd@CMK-3. (a) SEM image; (b) TEM image; (c) typical HRTEM image; (d) HRTEM image of the sample after 30 min irradiation (300 keV), and the inset showing the lattice fringe of a typical Pd NP (Reproduced from [143]. Copyright (2014), with permission of Springer).

Pd/C has been identified, by Suresh et al. [144], as an efficient catalyst for the US-assisted SMC coupling of 2-aryl-3-bromoflavones with 4,4-disubstituted (1,4-dihydro-2-oxo-2H-3,1-benzoxazin-6-yl)boronic acids. The coupling reactions were performed in aqueous DMF, without the need for expensive phosphine ligands in the presence of 10% Pd/C and TBAB-K₂CO₃, and afforded the desired 6-flavonyl substituted 1,4-dihydro-benzo[d][1,3]oxazin-2-ones in good yields (82%–91%) and short reaction times (20 min) (Scheme 57). Studies have shown that both catalyst and US played a key role in the faster coupling reaction. The recyclability of Pd/C was documented at four cycles when the reactions were executed under 35 kHz at 55–60 °C. A reaction mechanism describing the generation of actual catalytic species is presented followed by the catalytic cycle. Overall, the methodology may find wide applications in constructing a diverse library of small molecules containing the 6-flavonyl substituted 1,4-dihydro-benzo[d][1,3]oxazin-2-one framework, which would be of potential pharmacological interest.



Scheme 57. US assisted 6-flavonyl substituted 1,4-dihydro-benzo[d][1,3]oxazin-2-ones synthesis via Pd/C catalyzed SMC strategy.

Kulkarni et al. [145] have described the application of an energy-efficient surface acoustic wave (SAW) device for driving SAW-assisted, ligand-free SMCs in aqueous media. SAWs of well-defined wavelength and frequency (19.50 MHz) were generated on a piezoelectric substrate (LiNbO_3). The reactions were performed in a closed vessel using a high boiling point, low viscosity fluid as the liquid couplant. Under these conditions, the SAWs are transmitted into the paraffin oil as a bulk sound wave at a Rayleigh angle of 22.2 degrees. As the bulk wave approaches the glass vessel, a Lamb wave is formed in the base of the vessel which transmits the acoustic energy into the reaction solution within. The reactions were performed on a mmolar scale using low to ultra-low $\text{Pd}(\text{AcO})_2$ catalyst loadings (0.08%–0.0008%). The reactions were boosted by the heating which resulted from the acoustic energy penetration, derived from the radio frequency (RF) Raleigh waves generated by the piezoelectric chip via a renewable fluid coupling layer. The yields were uniformly high (>90%) when starting from a variety of aryl bromides and phenylboronic acid, while the reactions were executed without the addition of ligands in water. In terms of energy density, this new technology was labeled as being roughly as effective as MW and superior to US (Table 7).

Table 7. Surface acoustic wave (SAW), ultrasound (US) and MW energy density comparison for SMC reactions between bromoanisole and phenylboronic acid.

Energy Source	Reaction Time (min)	Power (W)	Energy Density (kJ/mmol)	Catalyst Loading (mol %)	Yields (%)
SWA	25	8	12	0.08	89
MW	17	5	5.1	0.8	72
US	10	120	144	0.9	85

Cravotto et al. [97] have compared results obtained from metal-catalyzed SMC reactions performed under MW, US and conventional thermal conditions. The coupling between 4-iodoanisole and phenylboronic acid, using either ligand-free Pd salts or Pd on charcoal, was used as a model reaction in glycerol. Both US and MW irradiation strongly improved the reaction rate in glycerol. Only by combining these two enabling technologies was it possible to achieve quantitative conversions in 60 min at 80 °C in the presence of 0.04 mmol Pd catalyst. Under these conditions, glycerol showed excellent acoustic cavitation even at high temperatures. In all cases, the Pd salts used were more efficient than Pd on charcoal, but less effective than previously reported Pd-loaded cross-linked chitosan for the SMC of various aryl halides (86% reaction yields).

3.2. Ultrasound Assisted Heterogeneous Preparation of Catalysts Suitable for SMC Reactions

The US assisted synthesis of new palladium nanoparticles (Pd NP) that are supported on cobalt ferrite magnetic nanoparticles (Pd– CoFe_2O_4 MNPs) has been introduced by Senapati et al. [146] (Figure 16). The CoFe_2O_4 MNPs were prepared in aqueous medium (under alkaline pH) without using surfactant or organic capping agents via a combined sonochemical and co-precipitation technique. The catalytic activity of the Pd incorporated cobalt ferrite nanoparticles was evaluated for standard SMC reaction in ethanol at reflux in the presence of Na_2CO_3 under ligand free and aerobic conditions. The cross coupling was performed with low catalyst loading (1.6 mol %) and gave high reaction yields (81%–92%) (TON value = 6250). The recyclability of this magnetic catalyst was also assessed in the SMC reaction of phenylboronic acid and 4-methyl iodobenzene. After each cycle, Pd– CoFe_2O_4 MNPs were magnetically recovered and reused with no significant loss in activity. Moreover, the morphology of the recovered MNPs (40–50 nm) was unaltered, even after four consecutive cycles.

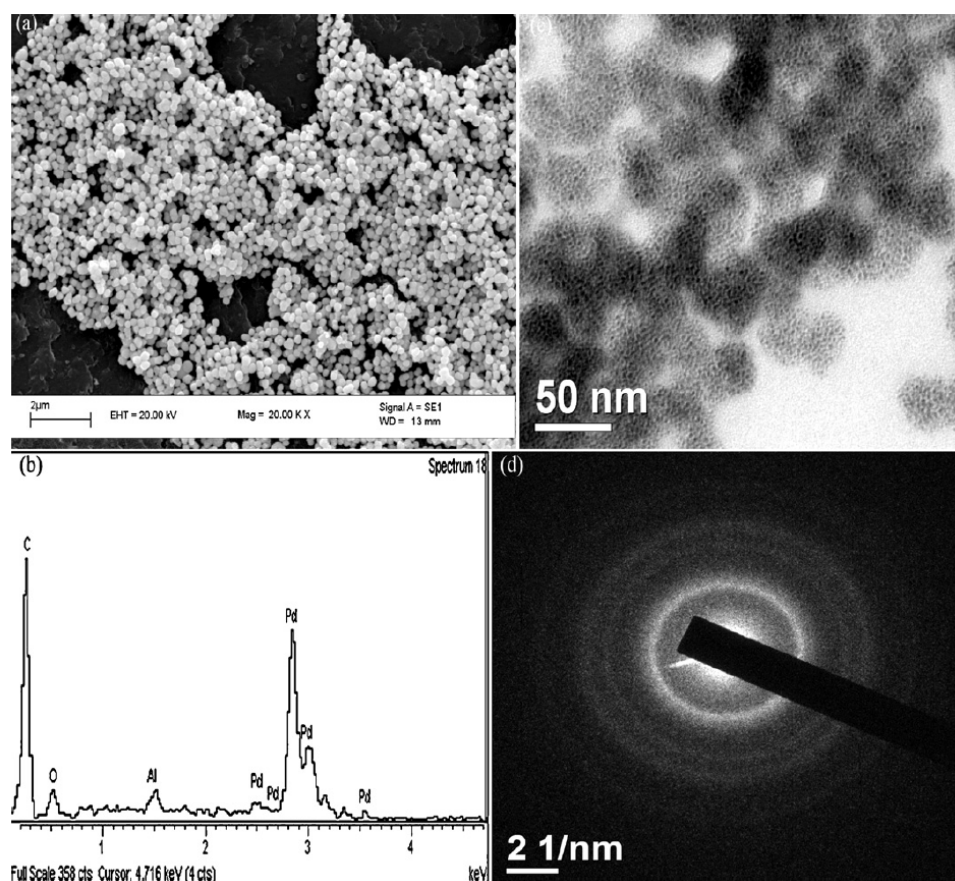


Figure 16. SEM with EDX (a,b) and TEM image with Selected Area Electron Diffraction (SAED); (c,d) of ferrite magnetic nanoparticles (Pd–CoFe₂O₄ MNPs) (Reproduced from [146]. Copyright (2012), with permission from Elsevier).

Magnetic nanoparticles (MNPs) have recently been used as catalyst supports for different organic transformations due to their high surface area and their easy recovery. In this context, an efficient super-paramagnetic solid catalyst, which is suitable for SMC reaction, has been prepared by Singh et al. [147]. Pd(0) species were loaded onto the paramagnetic catalyst support during the synthesis of zinc ferrite nanoparticles using a co-precipitation technique in aqueous medium under ultrasound irradiation, without the need for additional surfactants or organic capping agents. The crystallite size for the Pd–ZnFe₂O₄ nanoparticles was determined by X-ray diffraction and was found to be 10 ± 5 nm, whereas the iron/zinc ratio, measured by EDAX analysis, was found to be 2.05. The activity and stability of this Pd–ZnFe₂O₄ nanocatalyst was proven in model SMC reactions. Good yields (>85%), in terms of the C–C coupling product, were reported for reactions performed under reflux in pure ethanol in the presence of K₂CO₃ and 4.62 mol % of Pd–ZnFe₂O₄–MNPs, for a broad range of aryl halides and phenylboronic acid. Moreover, the super-paramagnetic nature of the catalyst meant that it was recovered using an external magnet and reused without any appreciable loss in activity for five cycles.

Of all the supports available for metal nanocatalyst preparation, widespread attention has recently been paid to so-called g-C₃N₄ which is the most stable allotrope of carbon nitride. In this context, highly uniform Pd NPs, with an average size of 4 nm, were supported on the g-C₃N₄ surface by means of an ultrasound assisted solution-reduction method by Su et al. (2015) [148]. This supported catalyst (Figure 17) was very efficient in SMC and provided isolated yields of up to 99% in aqueous ethanol at 80 °C when used with a 1 mol % Pd content combined with K₂CO₃. Good results were reported for aryl bromides bearing both electron-withdrawing and donating groups, with a TOF value

of 378 h^{-1} , whereas no C–C couplings were detected using aryl chlorides. The results denoted that the electronic transfer from N atoms to the $\gamma\text{-C}_3\text{N}_4$ framework and finally to Pd NPs improved the interaction between the Pd NPs and the support. It was established that the interaction is useful for improving the Pd NPs dispersion and stability on the $\gamma\text{-C}_3\text{N}_4$. The catalyst may be easily recycled without any leak in activity and selectivity at least 3 times showing negligible metal leaching ($<0.5\%$). The outstanding performance of the catalyst, in terms of activity and recyclability, may be ascribed to the considerable interaction between $\gamma\text{-C}_3\text{N}_4$ and Pd NPs and the robustness of the CN framework.

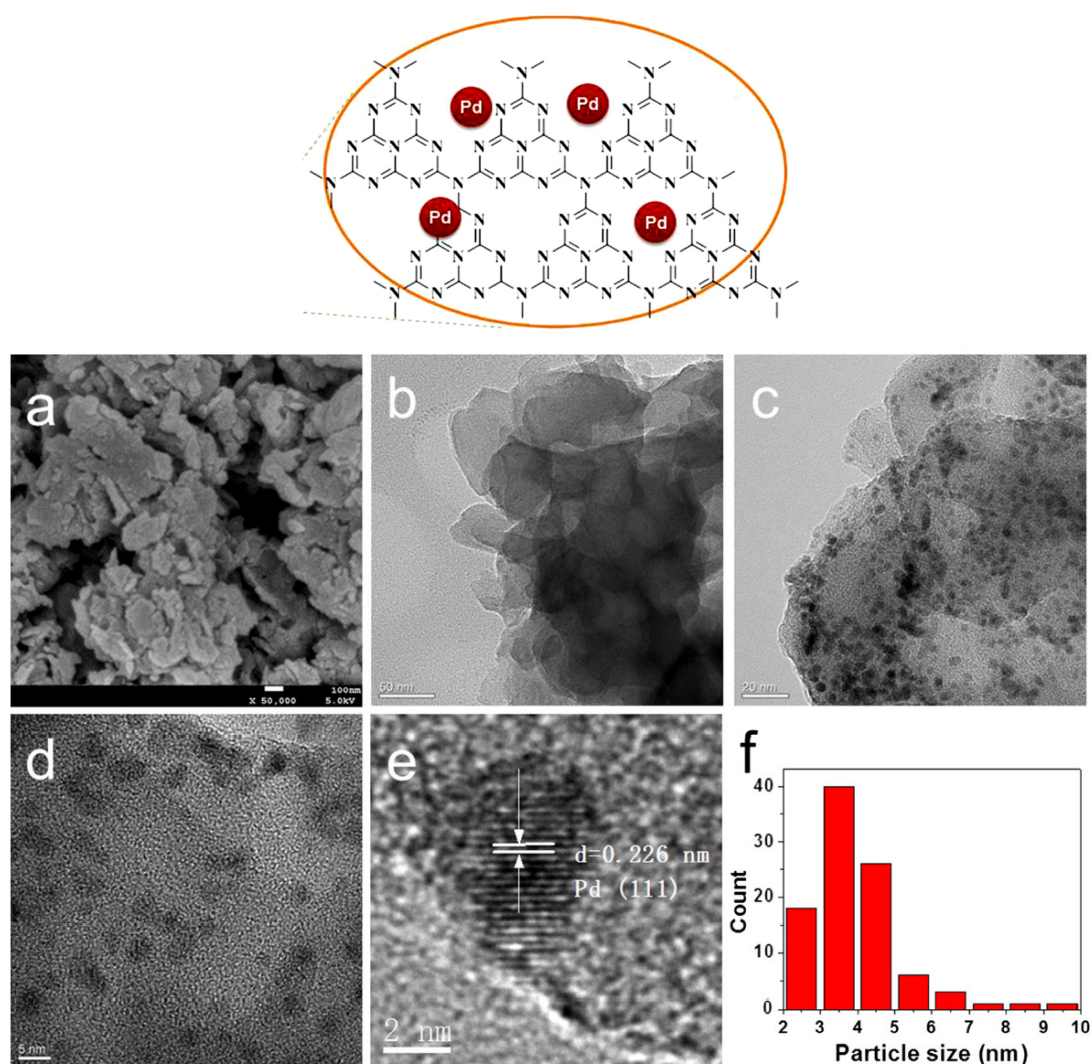


Figure 17. Top: Pd NPs, supported on the $\gamma\text{-C}_3\text{N}_4$ surface. Bottom: SEM image of $\gamma\text{-C}_3\text{N}_4$ (a); TEM images of $\gamma\text{-C}_3\text{N}_4$ (b); and Pd/ $\gamma\text{-C}_3\text{N}_4$ (c); HRTEM images of Pd/ $\gamma\text{-C}_3\text{N}_4$ (d,e); and size distribution of Pd NPs (f) (Reproduced from [148]. Copyright (2015), with permission of Springer).

Supported Pd NPs play a crucial role in SMC reactions. Nevertheless, some issues, such as aggregation and the leaching of Pd NPs onto the support's surface, are still great challenges to be addressed. The uniform dispersion of Pd NPs may well be the first step towards a solution to these problems. Layered double hydroxides (LDHs), also famous as hydrotalcites, have recently fostered increasing attention as they can play a role as a new support for the most profitable layered crystals applied in the synthesis of nanocomposites; this interest is due to some specific features of LDHs, such as their capability to exchange anions and undergo reconstruction ("structure memory effect"). Focusing on this topic, Li and Bai [149] have synthesized, using a one-step ultrasonic method, new Pd

NPs supported on the surface of sodium dodecylsulfonate (SDS)-intercalated LDH nanocomposites that are suitable for SMC. The Pd NPs described were uniformly dispersed on the SDS-LDH surface and showed an average size of 3.56 nm (Figure 18).

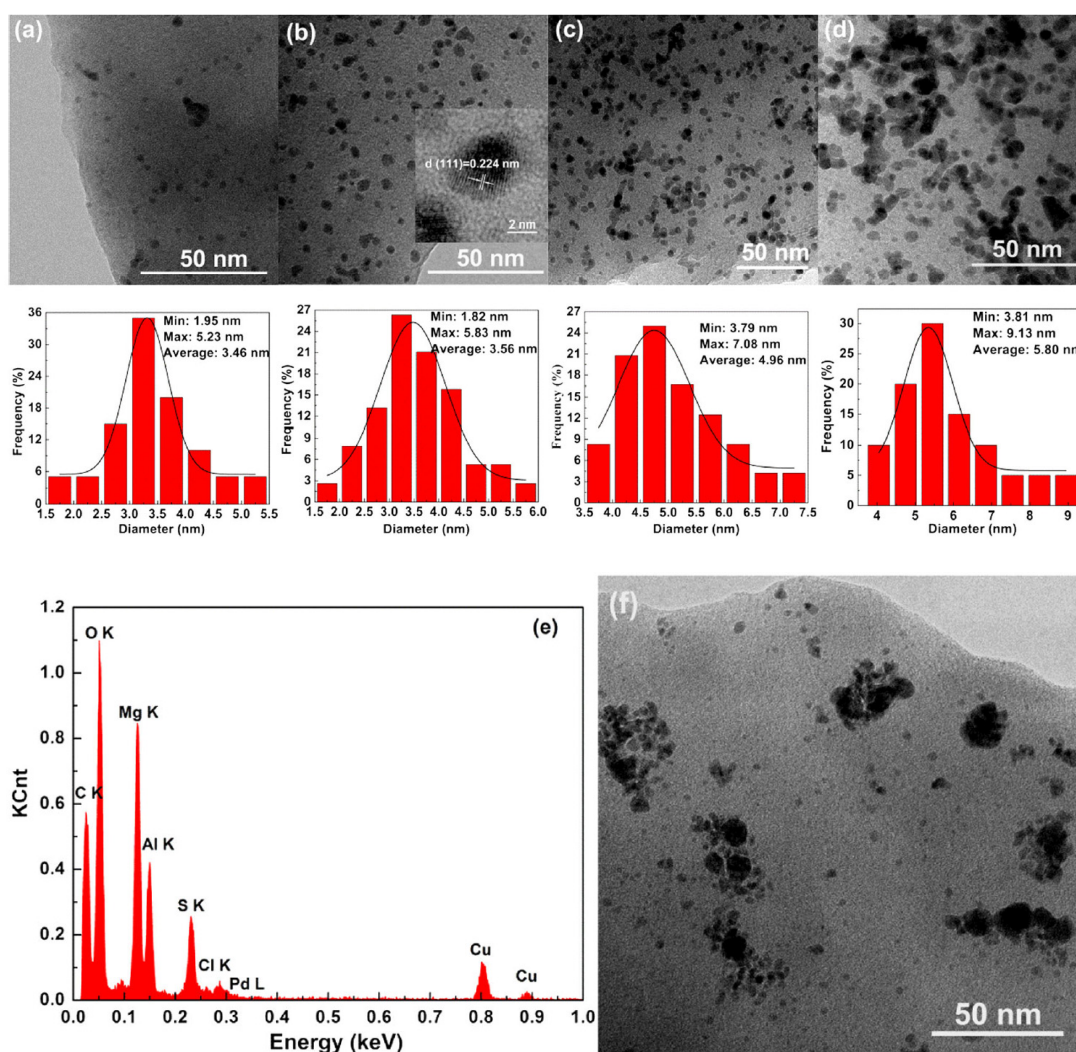


Figure 18. TEM images and corresponding size distributions of the Pd_{0.005}/SDS-LDHs (Sodium Dodecylsulfonate-Layered double hydroxides) (a); Pd_{0.02}/SDS-LDHs (b) (HRTEM images (inset)); Pd_{0.05}/SDS-LDHs (c); and Pd_{0.10}/SDS-LDHs (d); EDS profile of the Pd_{0.02}/SDS-LDHs (e); Pd_{0.02}/SDS-LDHs prepared in the absence of US (f). (Reproduced from [149]. Copyright (2016), with permission from Springer).

The conversion of 4-bromotoluene was catalyzed by Pd/SDS-LDHs in the presence of boronic acid, reaching 98.16% yield with 0.1 mmol % catalyst in EtOH/H₂O at room temperature without any phase transfer agents (Figure 19). Moreover, the conversion was much higher than that of the Pd/SDS-LDHs that were synthesized without US. This enhancement was ascribed to Pd/SDS-LDH's size uniformity and high dispersion. In particular, Pd/SDS-LDHs showed greater catalytic activity than Pd/C catalysts with the equivalent Pd content due to the considerable interaction between the Pd species and SDS-LDHs within the Pd/SDS-LDH nanocomposites. These catalysts were easily separated and recycled five times without any significant leak in activity.

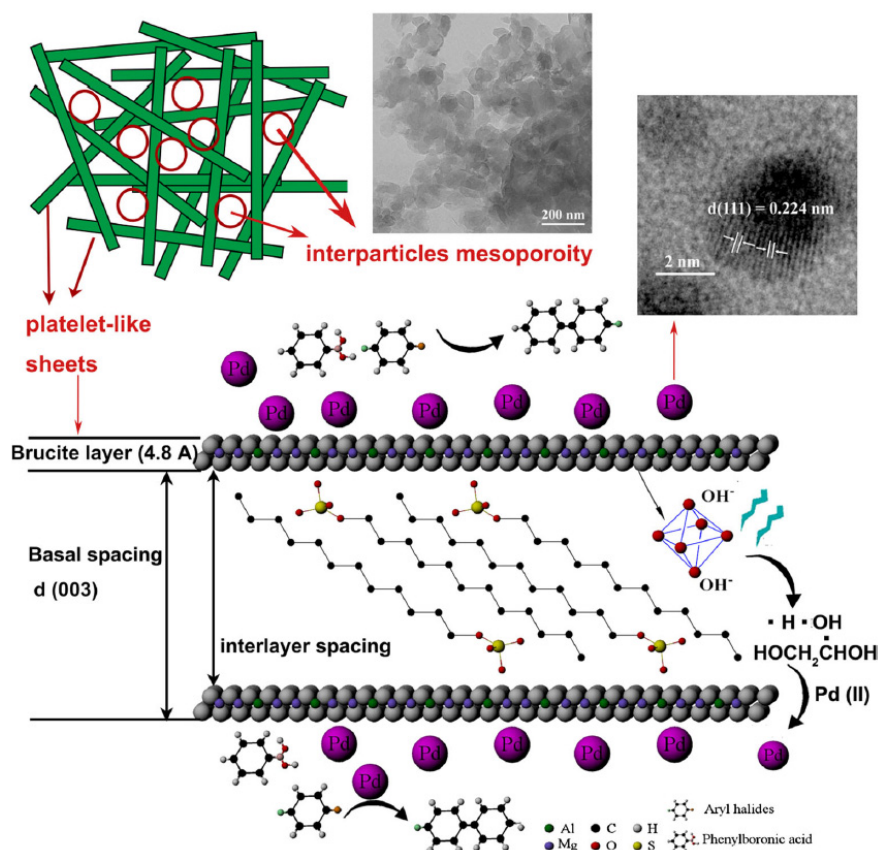


Figure 19. Schematic representation of the Pd/SDS-LDH nanocomposites. (Reproduced from [149]. Copyright (2016), with permission from Springer).

3.3. Ultrasound Assisted Heterogeneous Catalyst Preparation for MW Promoted SMC Reactions

Martina et al. [98] have reported a simple US-assisted procedure to prepare solid supported Pd(II) catalysts on chitosane (CS). They synthesized cross-linked chitosan derivatives (CS-Pd) by reacting chitosan in the presence of hexamethylene diisocyanate and the corresponding metal salt. The in situ polymerization, carried out in water under sonochemical conditions (90 min under 19.5 kHz irradiation at 30 W), was extremely fast and efficient. The activity of these cross-linked CS-Pd(II) catalysts (1 or 0.5 mol %) was tested on a model reaction between 4-bromoacetophenone and phenylboronic acid in a H₂O/dioxane 9:1 mixture. Satisfactory biaryl product yields (90%) were reported to have occurred under MW irradiation in 1 h at 90 °C without the addition of a phase transfer catalyst. The recovered CS-Pd(II) catalyst was reused several times in SMC reactions with a minimal loss in activity.

Cravotto et al. [101] have described the use of a new series of solid cross-linked cyclodextrin (α -, β - and γ -CD) based catalysts that were obtained via US-assisted reticulation with hexamethylene diisocyanate (HDI) in solutions containing Pd(II). Their polar structure makes both native CDs and their cross-linked derivatives very sensitive to dielectric heating. Moreover, this property is strongly enhanced in the Pd(II)-CD cross-linked catalyst by the embedded Pd(II) cations, rendering them extremely active in MW assisted SMC reactions. Best yields (75%–99%) were described as occurring under MW irradiation in water for 45 min using aryl bromides as the C–C coupling partner at 65 °C in the presence of Na₂CO₃. Metal leaching from the Pd(II)-CD catalyst is negligible (0.5%–1.5% less), which allows it to be recycled.

Silica has always found widespread application in the synthesis of solid-supported PdNPs because of its remarkable chemical and thermal stability, mechanical robustness and high accessibility. Silica is a remarkably versatile support and one that is able to host metal nanoparticles (NPs) and improve their reactivity and stability. Martina et al. [102], have recently prepared a novel cyclodextrin/silica

support for Pd NPs (Pd/Si-CD) (Scheme 45). Cyclodextrin (CD) grafting into an inorganic silica framework provided a hybrid organic/inorganic material suitable for further metal impregnation. It displayed modified surface reactivity, with respect to material bulk properties, due to its new hydrophilic/hydrophobic profile. The extremely efficient and homogeneous impregnation of small Pd NPs into this support was successfully carried out under US irradiation at 20.4 kHz (90–100 W) for 1 h. The Pd/Si-CD catalyst exhibited excellent activity in ligand-free C–C SMC with different aryl iodides and bromides (both electron rich and electron deficient).

4. Mechanochemical Activation of SMC

Several publications have recently reported upon the solid-state grinding route for the preparation of new types of supported Pd catalyst. An example of environmentally friendly preparation of PdCl₂ with a bidentate 1,5-bis(diphenylphosphino)-pentane has been described in the Journal of Chemical Education; this procedure consists of grinding a mixed powder against the side of a 50 mL round-bottomed flask so to achieve high metal loading and high particle dispersion capacities [150]. Many other supports with high pore volume have been used, such as mesoporous silica, carbon and one reported example of Pd dispersed in ascorbic acid. Based on our knowledge, some examples of the preparation of Pd supported catalysts by mechanochemical activation are reported in Table 8.

Table 8. Preparation of supported Pd catalyst by mechanochemical activation under solvent-free conditions.

Catalyst	Loading Conditions	Technology	Pd Loading (wt %)	SMC Synthetic Protocol	Reference
Magnetically separable mesoporous SBA-15 nanocomposites	1. SBA-15 silica support, Fe(NO ₃) ₃ ·9H ₂ O 10 min at 350 rpm. 2. propionic acid at 85 °C for 3 h	Retsch PM-100 planetary ball mill 18 stainless steel balls (10 mm)	19.2%	Bromobenzene, phenylboronic acid, Pd catalyst K ₂ CO ₃ , H ₂ O, MW 150 °C, 20 min (59% yield)	[151]
Palladium nanoparticles supported on carbon nanotubes	MWCNT powder/Pd(OAc) ₂ (10:1) mechanical shaking for 30 min	Ball-mill mixer (SPEX CertiPrep 8000D), two ceramic balls (d ¼ 1.3 cm), 1060 lateral cycles per minute.	9%	Bromobenzene, phenylboronic, Pd/MWCNT (Multiwall Carbon Nanotubes) (0.5 mol %) K ₂ CO ₃ , H ₂ O–EtOH (1:1), MW 80 °C for 10 min (100% conv.)	[152]
Monodispersed Pd in ascorbic acid	Pd(NO ₃) ₂ ·2H ₂ O, and Ascorbic Acid (1.0568 g, 6 mmol) 10 min	Mortar	-	Phenyl iodide, phenylboronic acid, Na ₂ CO ₃ , TBAB, Pd (10 mol %), H ₂ O, 80 °C, 24 h (Yield 97%)	[153]

Examples in the literature also address the topic of using mechanochemical activation in solvent free SMC [154,155]. Cravotto et al. have reported the use of a new catalyst, based on chitosan that is cross-linked with hexamethylene diisocyanate using Pd(OAc)₂, in solid-state SMC with aryl chloride. The reactions were carried out in a planetary ball mill for 120 min at 600 min^{−1} and high yields were obtained with unsubstituted and *p*-nitro chloro benzene [11].

The advantage of the strongly basic nature of KF–Al₂O₃, which can replace organic bases in a number of reactions, was explored by Braga et al. in 2004 in solvent free SMC under mechanochemical activation [156]. Stolle et al. have reported the same approach and reactions were performed in a mechanical manner via the co-grinding of the reactants with agate milling balls using a planetary ball mill as the source for alternative energy input. A model reaction was performed with bromo acetophenone and phenylboronic acid and the inherent basicity of the aluminas proved to be beneficial for the reaction, as compared to MgO, SiO₂, TiO₂, CeO₂ and Fe₂O₃. In contrast to the results obtained by Saha et al., who studied a MW assisted Pd(PPh₃)₄-catalyzed solid-state SMC [157], neutral γ-Al₂O₃, and not the basic α-Al₂O₃, yielded the best results with the tested aryl bromides. The reaction was effective in the presence of Pd-loadings higher than 1 mol % and high yields were obtained when KF loading was higher than 20 wt % on aluminas. In addition, KF–Al₂O₃ activity strongly depends on the residual water content, while the extent of water influence on the performance of the coupling reaction is related to the polarity of the aryl bromides [158].

The effect of liquid-assisted grinding has recently been studied using mechanical SMC for the coupling of aryl chlorides as the model reaction [159]. Catalytic systems that used Davephos and PCy₃ were tested and the author demonstrated the strong influences that various liquids had, added at the amount of 0.045 μL/mg. Alcohols produce unexpected improvements in yield, when used as additives. This is perhaps due to the in situ formation of alkoxides and their participation in oxidative addition, while the reactions performed neat gave the worst results. Based on this evidence, the authors proposed a mechanism and the reaction was optimized over a series of chloro benzene reactions to reduce the amount of catalyst to 2% (chloro benzene derivative, phenylboronic, Pd(OAc)₂ (2 mol %), PCy₃·HBF₄ (4 mol %), K₂CO₃ (5.0 equiv.) and MeOH (η = 0.045 μL/mg, two stainless steel balls (ø = 1.4 cm), 30 Hz, 99 min).

5. When the SMC Reaction Is Driven by Light

Solar light is a copious and safe source of energy that is attracting huge interest in efforts to figure out the matter of growing energy demands and environmental concerns. The ultimate aim for us here is to carry out visible light driven photocatalytic reactions. Indeed, solar light absorption is a convenient and sustainable means for generating electronically excited states in photocatalysts. In fact, plasmonic metal nanoparticles are able to transform solar energy into chemical energy via localized surface plasmon resonance (LSPR) [160]. In particular, many advantages, in terms of light harvesting and energy of the electrons, can be achieved when metal NPs are immobilized on insulating solids [161]. Indeed, the photo-excited electrons of NPs attain energy and gather on the surface, therefore aiding the molecule activation for chemical reactions. Higher photon efficiency can be achieved since the light harvesting and reaction occur at a single site [162]. Pd is judged as one of the most active metals for many reactions, among which the SMC is counted. However, its inability to show plasmonic absorption inhibits the utilization of visible light energy, whereas other metals, such as Ag nanoparticles, display a marked light harvesting ability due to their size-dependent plasmonic absorption [163]. Plasmonic Pd/Ag bimetallic catalysts supported on mesoporous silica SBA-15 have recently been used in the SMC coupling of iodobenzene and phenylboronic acid in the presence of K₂CO₃, used as a base, with ethanol as the solvent for 6 h (Figure 20) [164]. Pd nanoparticles were synthesized by LSPR-assisted deposition on the highly dispersed Ag nanoparticles under visible light irradiation. It was found that the integrated system, made up of Pd and plasmonic Ag nanoparticles, favored the formation of an efficient light harvesting system with unique photocatalytic reactions. It is worth noting that no catalytic activity (yield < 1%) was observed under dark conditions at room temperature (at 25 °C) due to the lack of the LSPR effect induced by silver and to the very low amount of Pd NPs. The authors observed that the yield of biphenyl was determined by the color of the Ag catalysts, according to the following order; Pd/Ag/SBA-15 (yellow) (2.16) < Pd/Ag/SBA-15 (red) (3.00) < Pd/Ag/SBA-15 (blue) (3.33), the values in brackets are the rates of activity enhancement. It was supposed that the occurrence of the reaction under visible light irradiation was related to the heating effect of the infrared component of light. Indeed, a 10 °C temperature increase in the reaction mixture was observed under light irradiation. The reaction was therefore performed at 35 °C and the contribution of the conversion efficiency under light irradiation was evaluated.

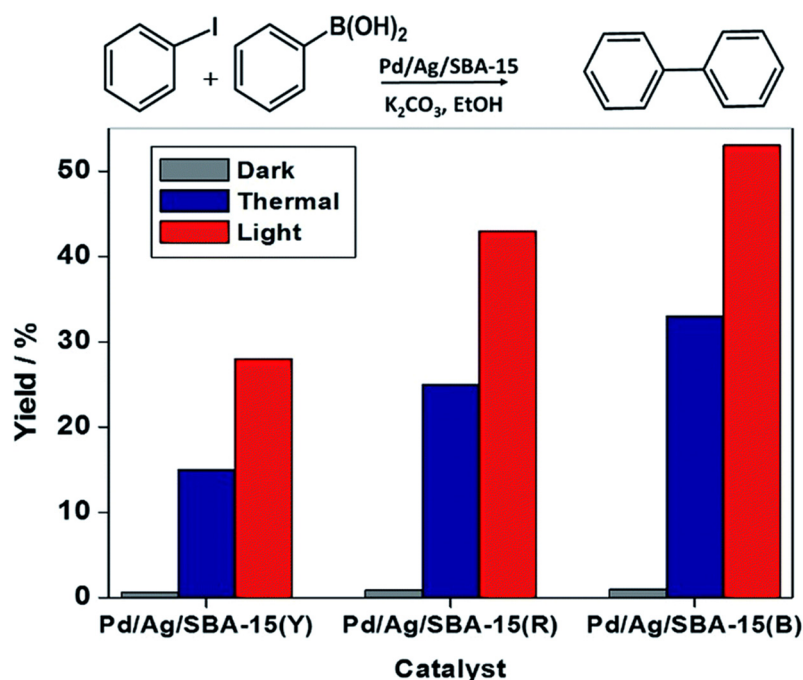


Figure 20. SMC for Pd/Ag/SBA-15 catalysts under dark, thermal (35 °C) and light irradiation conditions. Reprinted from [164]. Copyright (2015), with permission from Royal Society of Chemistry.

Superior performance was observed under light irradiation, followed by thermal conditions and then the reactions in the dark. This clearly indicates that the enhanced activity was strictly connected to the synergistic effect between Pd and Ag nanoparticles which mutually interact with the assistance of the LSPR effect. It was proposed that, due to the charge heterogeneity at the interface between the two metals, the energetic electrons generated on the silver transfer to the Pd nanoparticles upon irradiation with visible light. This can be understood if we consider that the work function of Pd metal is 5.00 eV in a vacuum, which is larger than the work function of Ag metal, which is 4.30 eV in a vacuum. The amount of energy required to eject the electron determines the position of the Fermi level, suggesting that the position of the Fermi level of Pd is lower to that of Ag, making the electron transfer process achievable [165,166]. Activated Pd species can therefore accelerate the oxidative addition step, resulting in an increase in the intrinsic catalytic activity of palladium. The energetic electrons also release energy into the surrounding environment, leading to an increase in temperature, which also contributes to the improvement in activity. All Pd/Ag bimetallic catalysts were active in the coupling reaction under visible light irradiation which was emitted at $\lambda > 420$ nm.

In a very recent paper by Yamashita et al. [167], bimetallic Pd/M (M = Ag, Au) nanoparticles embedded into a SBA-15 (20 mg) matrix have been tested in the coupling of aryl halides and boronic acid in ethanol and in the presence of K₂CO₃ (41.5 mg) and phenylboronic acid (36.6 mg) at room temperature for 2 h under a Xe lamp irradiation with a glass filter cutting out the ultraviolet portion of light. In these systems, Pd (0.5 wt %) was deposited onto M/SBA-15 (M = Au, Ag) using an LSPR assisted deposition method under visible light irradiation. Interestingly, both Au and Ag (1 wt %) were incorporated into the mesoporous silica by the MW (500 W, 2450 ± 30 MHz, 3 min) polyol method using either ethylene glycol or 1-hexanol as the solvent and reducing agent.

PdAg/SBA-15 and PdAu/SBA-15 were proven to be more active than the monometallic Pd-containing catalyst, while the beneficial effects of photoactivity are higher in the presence of gold than in the presence of Ag, according to the results of the photocatalytic tests reported in Figure 21.

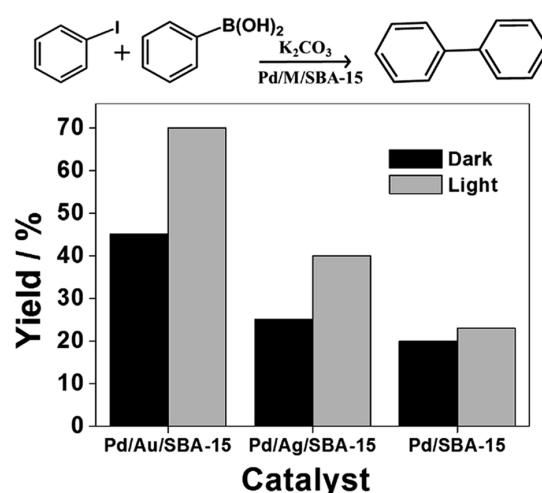


Figure 21. Results for Pd/M/SBA-15 in the SMC reaction under dark and visible light irradiation conditions. Reprinted from [167]. Copyright (2016), with permission from Royal Society of Chemistry.

A supposable mechanism has been proposed to explain the tentative reaction pathway that may occur under visible light irradiation. The resonant excitation of plasmonic nanoparticles, which is accomplished by matching frequencies with those of the incident electromagnetic radiation, undergoes relaxation within tens of femtoseconds [168–170]. Relaxation can occur via either radiative or non-radiative emission. The possible relaxation mode for metal nanoparticles with a diameter < 30 nm is the non-radiative Landau damping process, which causes the formation of electron–hole pairs [171,172]. The electron–hole pairs are generated by the elevated electric fields caused by the resonance condition between the plasmonic metal nanoparticles and the electromagnetic radiation [173]. These energetic electrons, or so-called hot electrons, are available at the surface of the Pd sites in the bimetallic catalysts due, as explained before, to the considerably higher work function values of Pd (5.0 eV) than Ag (4.3 eV) and Au (4.7 eV), making the electron transfer process quite feasible. These energetic electrons can be accumulated in the lowest unoccupied molecular orbital (LUMO) of the reactant arylhalide, through the Pd nanoparticles, which is a transformed ionic/transient species and leads to bond weakening, as illustrated in Figure 22.

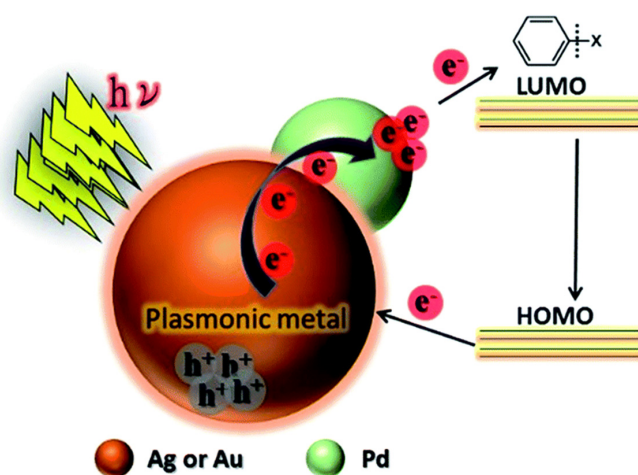
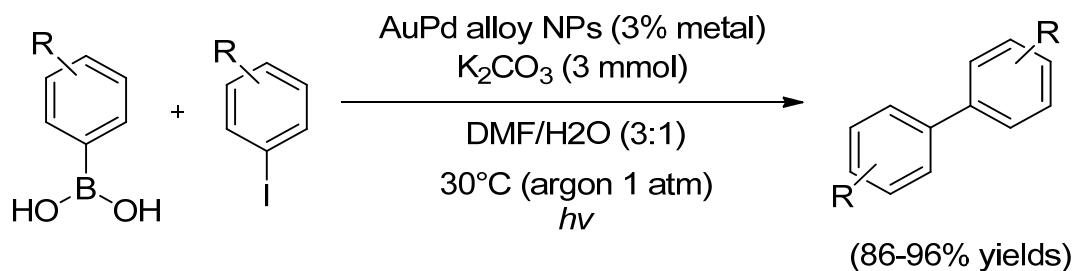


Figure 22. Proposed mechanism for enhanced catalytic activity under visible light irradiation in the presence of plasmonic metal NPs. Adapted from [167]. Copyright (2016), with permission from Royal Society of Chemistry.

The electrons return to the HOMO and ultimately back to the plasmonic metal nanoparticles after the activation of the reactants. The differing behavior of Ag and Au was explained on the basis of their tunability sensitivity upon electron injection. Ag is much more sensitive than Au towards the plasmonic tunability of wavelength, however both showed significant damping of intensity.

Sarina et al. [174] have observed that in reactions, such as the SMC (see Scheme 58), where the catalytic activity is driven by Pd, the intrinsic catalytic activity of palladium in PdAu alloy nanoparticles is significantly enhanced by light irradiation, even at room temperature. On the other hand, AuPd alloy nanoparticles did not perform better than mono metallic Au in other reactions in which the activity is dominated by gold.



Scheme 58. SMC under light irradiation.

Additionally, catalytic performance was found to be strongly dependent on Au/Pd molar ratio in both the presence and the absence of light, as demonstrated by the data reported in Table 9.

Table 9. SMC catalyzed by Au–Pd@ZrO₂ with different Au/Pd molar ratios under visible light irradiation and in the dark¹.

R ₁	R ₂	Au/Pd ¹	Yield (%)		Selectivity (%)		TON		TOF (h ⁻¹)		Q.Y. ⁷ (%)
			Light	Dark	Light	Dark	Light	Dark	Light	Dark	
3-CH ₃	4-H	1:1.86	96 ²	37	99	99	87	34	14.5	5.7	2.7
		1:1.00	55 ²	17	98	99	56	17	9.3	2.8	1.7
		1:5.58	40 ²	10	99	99	34	8	5.7	1.3	1.4
		1:0.62	28 ²	6	99	100	33	6	5.5	1.0	1.0
		1:0	2 ²	0	100	-	3	0	0.5	0	0.1
		0:1	26 ²	11	98	99	18	8	3.0	1.3	0.7
4-CH ₃	4-H	1:1.86	94 ²	46	98	97	95	46	15.8	7.7	2.2
2-CH ₃	4-H	1:1.86	86 ²	30	98	98	87	30	14.5	5.0	2.6
4-OCH ₃	4-H	1:1.86	96 ³	41	98	99	97	41	19.4	8.2	2.5
4-H	4-OCH ₃	1:1.86	99 ⁴	58	99	99	100	99	50.0	0.0	1.9
4-H	4-CHO	1:1.86	98 ⁵	65	99	96	99	67	24.8	0.0	1.5
4-H	4-N(CH ₃) ₂	1:1.86	80 ⁶	55	68	60	81	56	3.0	0.0	0.3

¹ Molar ratio; ² Reaction time 6 h; ³ Reaction time 5 h; ⁴ Reaction time 2 h; ⁵ Reaction time 4 h; ⁶ Reaction time 22 h.

⁷ Q.Y., quantum yield. Reaction conditions: 1 mmol of aryl iodide, 1.5 mmol of arylboronic acid, 50 mg (containing 3% of metals) of catalyst and 3 mmol of base K₂CO₃ in DMF/H₂O = 3:1 (solvent) at 30 °C and 1 atm of argon. TON and TOF values were calculated based the total amount of metal(s).

AuPd nanoparticles are able to absorb light energy and photo-excited conduction electrons are generated at the surface of Pd sites where the reactant molecules are activated. Moreover, the increase in light intensity produced a linear increase in conversion, while the reaction temperature was carefully checked and kept at 30 ± 1 °C in order to avoid the influence of thermal effects on performance. It was observed that the largest contribution (>64%) to the catalytic activity came from radiation with wavelengths in the 490–600 nm range, which is where the LSPR peak of gold nanoparticles is usually observed. This suggests that Au atoms present in the alloy nanoparticles work as an antenna for visible light absorption. Furthermore, the apparent activation energy of the SMC was calculated both in the dark (~49.2 kJ/mol) and under visible light illumination (~33.7 kJ/mol). It was found that the

activation energy is reduced by 15.5 kJ/mol under visible light irradiation, which represents a 31% decrease in activation energy.

It was proposed that the intrinsic catalytic activity of these alloy AuPd nanoparticles is related to charge heterogeneity at the surface of the alloy nanoparticles, hence to the Au/Pd ratio of the alloy, resulting in an enhanced interaction between the alloy nanoparticles and the reactant molecules. The catalytic activity's observed dependence on alloy composition was believed to be related to electron redistribution between the two metals. Using a free electron-gas model, the same authors found that the number of transferred electrons (ΔN) is at its highest when the ratio of the electrons of the two metals in the alloy NPs is approximately equal [175]. In more detail, the electron transfer (ΔN) predicted by the model is a function of the Au electron concentration (%) in the AuPd alloy nanoparticles and/or of the Au/Pd molar ratio. A strong correlation between ΔN and the conversion efficiency of reactants was observed, as illustrated in Figure 23. The alloy nanoparticles which possess an Au/Pd electron ratio near to 1:1 (corresponding to the Au/Pd molar ratio 1:1.62) have the largest electron transfer number and displayed significant Au–Pd ionic bond character because of the Pd rich surface of the NP.

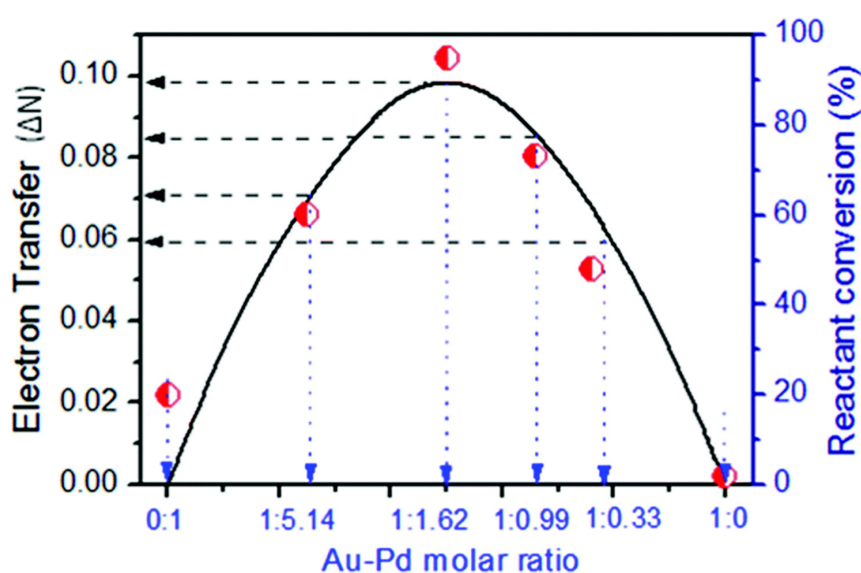


Figure 23. Electron transfer from gold to palladium in the alloy NPs, expressed as ΔN , varies with the composition of the alloy NPs (the curve). ΔN reaches a maximum when the Au/Pd molar ratio is 1:1.62. The Au/Pd molar ratio in the alloy NPs (horizontal axis) and photocatalytic conversions (red symbols) of the SMC in the present study (vertical axis on the right) are given respectively, reaction conversions are based on the average values of three runs for each experiment. Reprinted from [175]. Copyright (2014), with permission from Royal Society of Chemistry.

These papers highlight the fact that the intimate interaction between light-absorbing plasmonic and catalytically active components plays a key role in achieving efficient light harvesting as well as catalytic activity. Following the same idea, Wang et al. [176] has proposed different Au–Pd plasmonic metal nanostructures with synthetically tunable absorption wavelengths to efficiently harvest light. According to Figure 24, the most promising new nanostructures were made up of gold nanorods decorated with small Pd nanoparticles that had previously been heteroepitaxially grown on the nanorods [177,178].

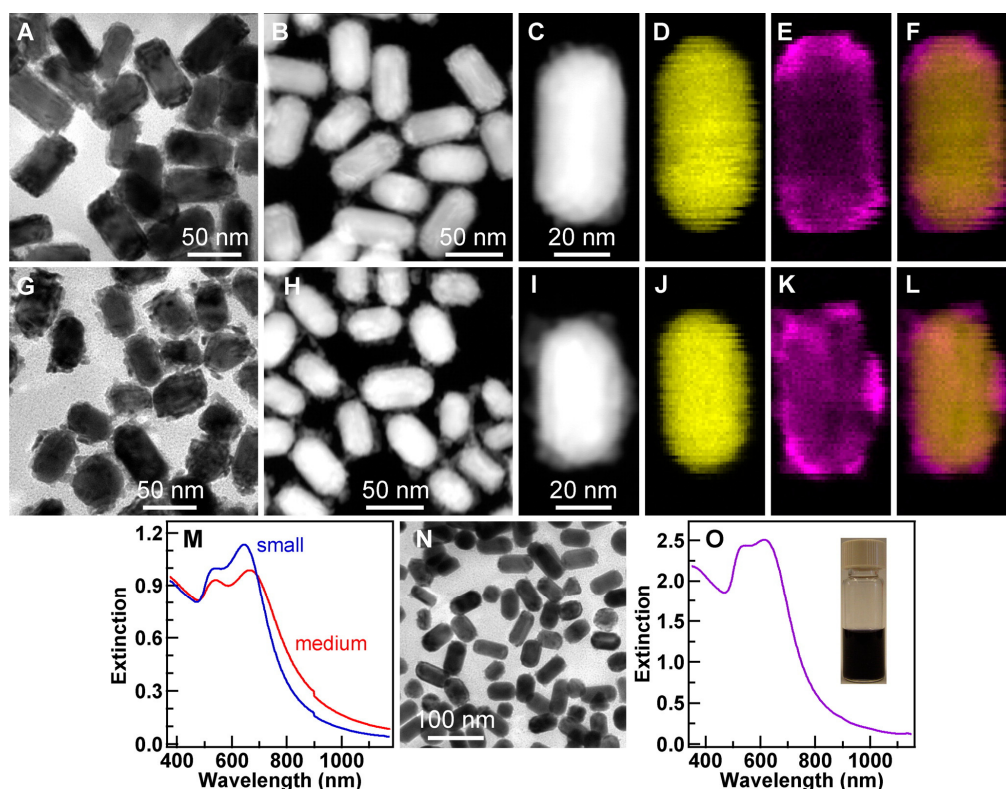


Figure 24. Nanostructures for catalytic reactions under solar radiation. (A–F) Medium Au–Pd nanostructures: (A) TEM image; (B) high-angle annular dark-field scanning transmission electron microscopy (HAADF-STEM) image; (C) HAADF-STEM image of a single nanostructure; (D) elemental map of gold for the nanostructure shown in (C); (E) corresponding elemental map of palladium; (F) merged elemental map; (G–L) Corresponding imaging results for the small Au–Pd nanostructures; (M) Extinction spectra recorded in 0.5 cm cuvettes for the medium and small Au–Pd nanostructure samples; (N) TEM image of the mixture of the medium, small and spherical nanostructure samples; (O) Extinction spectrum of the mixture at 1 cm path length. The inset shows the digital photo of the reaction solution containing the nanostructure mixture in a glass vessel for experiments under solar radiation. Reprinted with permission from [176]. Copyright (2013), with permission from American Chemical Society.

The authors demonstrated that the use of a mixture of these nanostructures, of varying size and shape (medium, small and spherical), guaranteed the maximum exploitation of sunlight and the best photoactivity. In particular, it was proposed that the Au nanorods can function as the light-harvesting component, because of their synthetically tunable longitudinal plasmonic absorption. At the same time, the Pd nanoparticles are active catalysts for the C–C cross coupling reaction. The strong interaction between the two metals means that the chemical potentials of the electrons in the Pd nanoparticles and in the Au nanorods are in equilibrium [179]. The electrons belonging to the Pd nanoparticles are therefore involved in the plasmon resonance occurring across the entire nanostructure upon light irradiation. As a consequence, plasmon excitation promotes the Pd-catalyzed SMC reaction. The authors also synthesized a similar nanostructure with a 25-nm-thick TiO_x shell that plays the role of separating the Au nanorod from the Pd nanoparticles. A comparison of the photocatalytic performances of these two nanostructures, i.e., Au–Pd and Au– TiO_x –Pd, further confirmed the key role played by the longitudinal plasmon of the Au nanorods. Several reactions (involving the coupling of mainly arylbromides with different arylboronic acids) performed under solar radiation gave quite satisfying yields, of above 50% even >90% with nine of them. The catalyst used in these catalytic tests contains 326 μg of gold and 16.6 μg of palladium.

More recently, a very interesting paper [180] reported the intriguing possibility of extending the plasmonic absorption of Pd nanoparticles into the visible-NIR (Near-Infrared) region of the spectrum. This was exploited by synthesizing Pd hexagonal nanoplates with well-defined and tunable longitudinal localized surface plasmon resonance (LSPR). As shown in Figure 25, each Pd nanoplate is indeed a twin crystal, with its top and bottom faces enclosed by {111} facets with stacking faults and with side surfaces surrounded by a mixture of six {111} and six {100} facets. These new nanostructures efficiently catalyze the SMC reaction of iodobenzene and phenylboronic acid under light irradiation. Experimental and theoretical results proved that the increase in catalytic activity granted by the Pd hexagonal nanoplates was due to the photocatalytic effect of plasmon induced hot electrons.

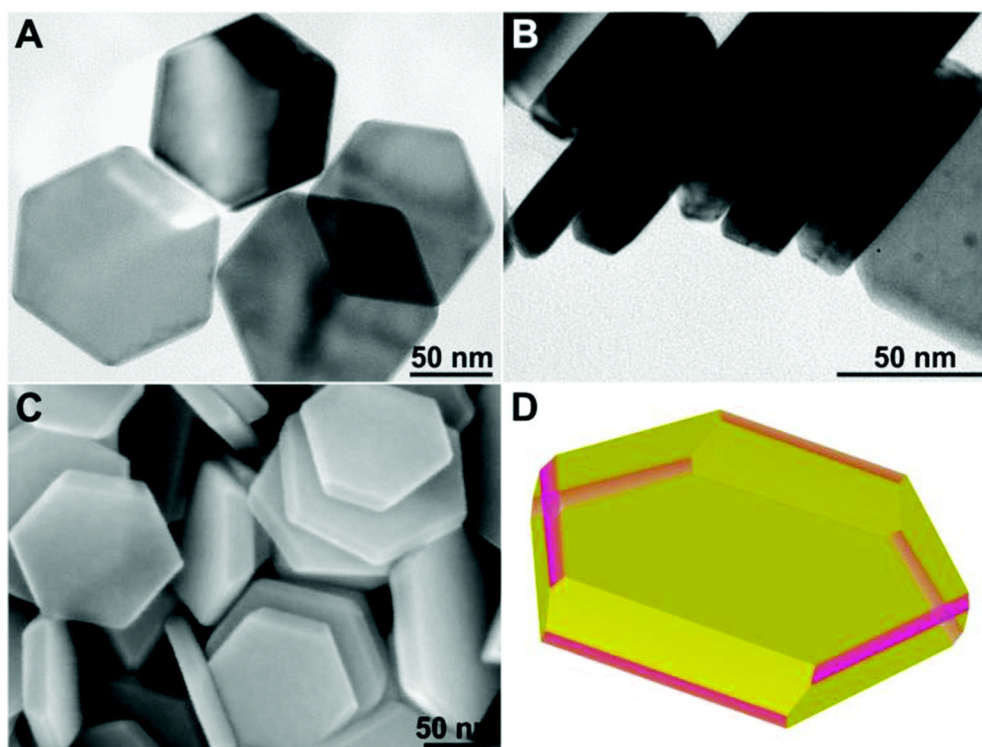


Figure 25. (A) Top-view; and (B) side-view TEM; (C) SEM images; and (D) sketch of the Pd hexagonal nanoplates. Yellow and pink represent the {111} and {100} planes, respectively. Reprinted from [180]. Copyright (2015), with permission from Royal Society of Chemistry.

As shown in Figure 26, the obtained TOF values were 2.5 and 2.7 times higher than those related to non-plasmonic {111}-enclosed Pd nano-octahedra and to {100}-enclosed Pd nanocubes, respectively, under illumination with a Xe lamp ($\lambda = 300\text{--}1000\text{ nm}$, $176\text{ mW}\cdot\text{cm}^{-2}$) and 1.7 times higher than the value obtained when the reaction was thermally heated to the same temperature.

Basing on the mechanism of activation of homogeneous Pd-containing catalysts which depend on the electron-enrichment caused by the introduction of special ligands, Li et al. [181] were interested in increasing the activity of heterogeneous Pd nanoparticle-based catalysts by increasing their electron density via support effects. The authors employed the stimulated electron transfer at the metal-semiconductor interface from optically active mesoporous carbon nitride (g-C₃N₄) nanorods to Pd nanoparticles. It was proposed that the presence of noble metal nanoparticles on the surface or inside of the pores of mesoporous g-C₃N₄ would give rise to metal-semiconductor contact (Mott-Schottky heterojunction). Charge transfer can be envisioned at the interface and would result in a positively charged region (the depletion region with a thickness of a few nanometers measured from the interface) and a nanoparticle with negative charge, due to the Schottky effect [182]. Theoretically, the energetic electrons located at the noble metal NPs and the holes placed at the g-C₃N₄ plane

would be able to activate two substrates, towards electron-rich and electron-deficient intermediates respectively, to facilitate C±C coupling reactions. The Schottky effect can also be amplified by photo-excited electrons under irradiation, simultaneously amplifying the effective charge transfer at the interface towards the metal nanoparticle. It was found that mesoporous g-C₃N₄ nanorod supported Pd nanoparticles are highly efficient in the Mott-Schottky accelerated SMC of aryl halides with various coupling partners under photo irradiation and very mild conditions. The wavelength-dependence of the activity, which corresponded to the optical absorption spectrum of carbon nitride, was elegantly demonstrated, as shown in Figure 27.

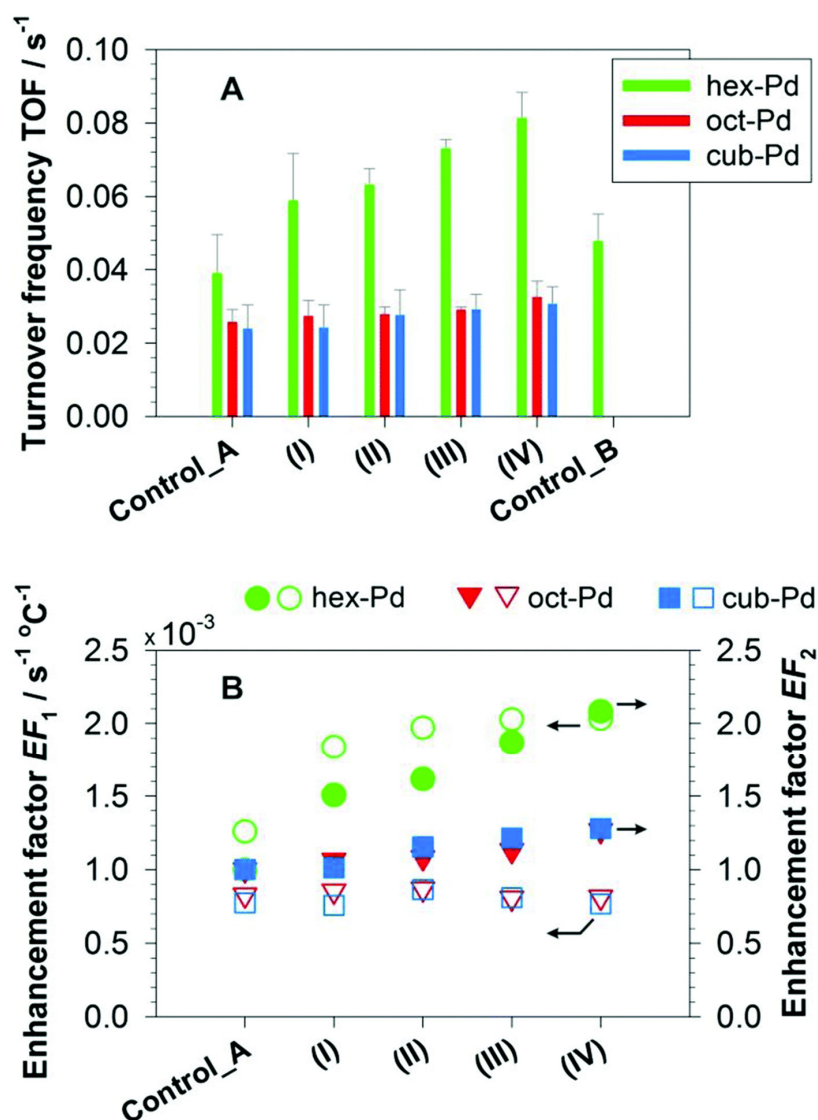


Figure 26. (A) Turnover frequencies (TOFs) per surface Pd atom of hexagonal-Pd were compared with octahedral-Pd and cubic-Pd in SMC reactions carried out using different light sources: 350 nm, 2.6 mW·cm⁻² (I); 380 nm, 3.4 mW·cm⁻² (II); 420–1000 nm, 84.0 mW·cm⁻² (III); and 300–1000 nm, 176.0 mW·cm⁻² (IV); (B) The enhancement factors EF_1 (open symbols) and EF_2 (solid symbols) for hexagonal-Pd were estimated from the data in (A); Control_A was performed without light illumination in a dark room and Control_B was performed under isothermal heating at 40 °C. All reactions were performed in an isothermal environment (25 °C) for 3 h. Reprinted from [180]. Copyright (2015), with permission from Royal Society of Chemistry.

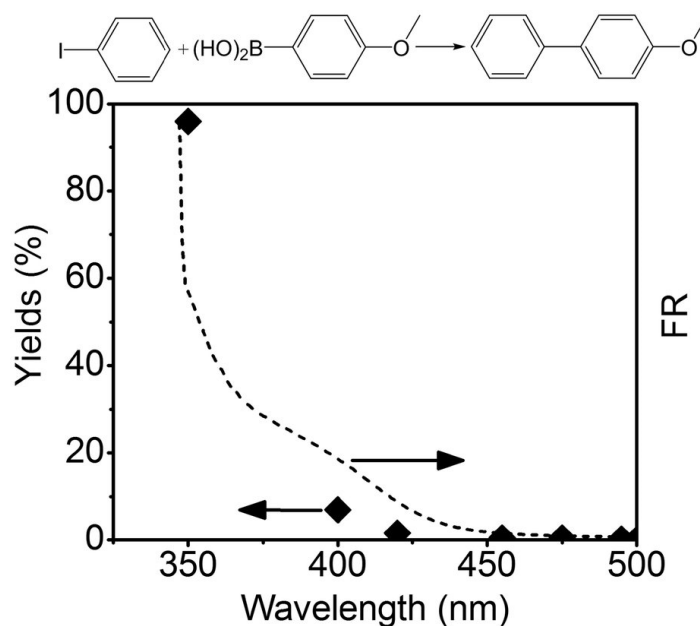


Figure 27. Wavelength dependent activity of Mott-Schottky photocatalyst and corresponding UV-vis absorbance spectra (FR) of mesoporous $g\text{-C}_3\text{N}_4$ nanorods. The coupling reaction of iodobenzene and 4-methoxybenzeneboronic acid was conducted under the following conditions: water (2.5 mL), EtOH (2.5 mL), 138 g of K_2CO_3 (1 mmol), 73 mg of 4-methoxybenzeneboronic acid (0.6 mmol), 0.017 mL of iodobenzene (0.15 mmol) and 10 mg of m-CNR-Pd (3 wt %) as the catalyst, 150 W Xe lamp, room temperature (25 ± 5 °C), 1 h. The nominal spectral output of the Xe lamp is located between 350 and 800 nm. The wavelength of the incident light was controlled using an appropriate cut-off filter. Reprinted from [181]. Copyright (2013), with permission from Macmillan Publishers Ltd.

Decreased product yield (49% after 12 h) was observed by filtering off the UV part of the Xe lamp (≤ 420 nm), however no product yield was observed when wavelengths of ≤ 460 nm were filtered off. Interestingly, the catalyst gave high conversion and selectivity in the coupling of iodobenzene and 4-methoxybenzeneboronic acid at elevated temperatures, even in the dark, but no conversion was observed at temperatures lower than 50 °C. In the same reaction system, light irradiation enabled the coupling reaction to occur, even at room temperature, which gave excellent conversion and selectivity. Both reactions could not occur without the presence of K_2CO_3 , as it is essential to activate boronic acid. No inert atmosphere was required.

Inspired by recent research efforts into the design of electron-rich catalytic sites which could carry out the oxidative addition of Pd^0 with aryl halide and facilitate the coupling reactions, Zhang et al. have successfully performed the activation of aryl chlorides, using heterogeneous multifunctional Pd/Au/porous nanorods of CeO_2 (PN- CeO_2) which are catalysts with a well-defined spatial configuration, under the irradiation of visible light (>400 nm) at room temperature [183]. In this heterogeneous catalyst, Au nanoparticles were deposited on ceria using the classical deposition-precipitation method. Pd was then selectively photo-deposited onto the surface of Au nanoparticles. It is worth noting that PN- CeO_2 have a band gap of 2.63 eV, which is lower than the value of an ideal CeO_2 crystal (3.2 eV), and can absorb part of visible light, generating electron/hole pairs. These photogenerated electrons can be injected into Au nanoparticles [184]. Gold not only absorbs visible light via LSPR excitation, but also serves as a charge mediator for the transfer of electrons to Pd nanocatalysts. When Pd/Au/PNCeO₂ catalysts is under the illumination of visible light, the hot electrons generated by Au, which display an excited hot state for up to 0.5–1 ps, will flow across the Au and Pd interface immediately, which enriches the electron density of Pd and allows the SMC to occur. This possible electron transfer has also been proven both in previous experiments

and in theoretical calculation results [174,176]. Along with the consumption of electrons on Pd during reaction, more and more hot electrons should be provided. Au^+ therefore needs to be supplemented with electrons for its recovery to the Au^0 state by the photogenerated electrons from PN-CeO₂ to mediate the electron transfer. The spatially selective deposition of Pd nanocatalysts onto the surface of Au nanoparticles favors the possibility of electron transfer from PN-CeO₂ to Au nanoparticles. Under such synergistic action, the multifunctional Pd/Au/PN-CeO₂ catalyst is able to activate different aryl chlorides at room temperature, as seen in Figure 28. The electron-rich Pd nanoparticles can activate aryl chlorides and facilitate the first step of the oxidative addition reaction of SMC by accelerating the formation of active radical ligand $\text{ArPd}^{\text{II}}\text{Cl}$. At the same time, electron/hole pairs created in PN-CeO₂, upon the absorption of the incident visible light, activate various arylboronic acids by cleaving the C–B bonds. The oxidized arylboronic acids close to Pd can react with the activated aryl chlorides, giving the final products.

Reaction conditions were as follows; water (1 mL), DMF (1 mL), K_2CO_3 (0.6 mmol), chlorobenzene (0.2 mmol), phenylboronic acid (0.24 mmol) and catalyst (15 mg). 91.6% conversion and 89.6% yield were achieved in the presence of the strong electron-withdrawing $-\text{NO}_2$ group (*p*-substituted with respect to Cl) after 6 h. When electron-donating substituents, *p*-substituted with respect to the halogen position were introduced to phenyl chloride, the yields of the cross-coupling products were reduced to 80.6% ($-\text{OCH}_3$), 56.8% ($-\text{CH}_2\text{OH}$) and 15.3% (conjugated alkynyl) for the cross-coupling product after 6 h of visible light irradiation. Furthermore, high catalytic activities were observed for arylboronic acids with electron-donating groups, again in the *p*-position with respect to Cl, such as $-\text{CH}_3$, aryl and tertiary butyl. On the other hand, the insertion in the same position of the electron-withdrawing group, $-\text{CHO}$, into arylboronic acid caused a drop in the yield of the cross-coupling product.

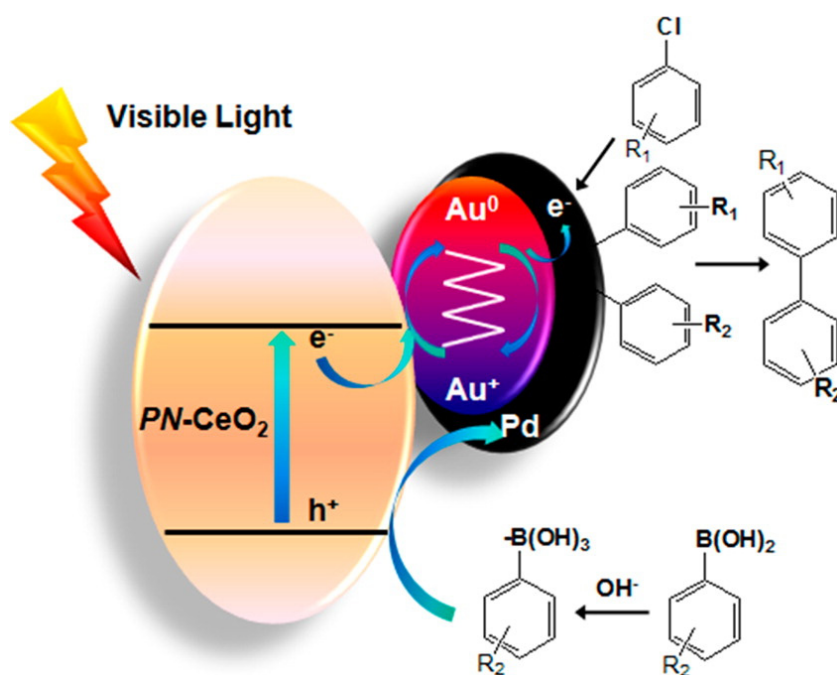


Figure 28. Schematic view of the proposed photocatalytic reaction mechanism over Pd/Au/PN-CeO₂ catalysts under visible light irradiation. Reprinted with permission from [183]. Copyright (2015), with permission from American Chemical Society.

A new $\text{Cu}_7\text{S}_4@Pd$ heteronanostructured photocatalyst, in which Pd nanoparticles and Cu_7S_4 domains are in intimate interfacial contact, were found to be excellent catalysts for solar-driven organic synthesis reactions [185]. Both simulation studies and experimental investigations demonstrated that a combination of the NIR LSPR light-harvesting property of Cu_7S_4 and the catalytic features of Pd

resulted in the enhanced photocatalytic activity that these systems show towards the SMC reaction. In particular, Pd displays no LSPR absorption above 1000 nm, whereas Cu_7S_4 or a physical mixture of Pd and Cu_7S_4 gave an absorption peak at about 1500 nm (this absorption was also observed by simulation, compare Figure 29a,b). Interestingly, $\text{Cu}_7\text{S}_4@\text{Pd}$ showed a red shift of the LSPR peak of about 500 nm compared to bare Cu_7S_4 . An explanation for such a spectroscopic feature is that the Pd on the Cu_7S_4 surface is possibly bound to S atoms, hence lowering its exposure to oxygen. This might, in turn, annihilate vacancies in Cu_7S_4 , and result in a red shift of the LSPR peak. The red shift also correlated to a refractive index change which was caused by the incorporation of palladium into the Cu_7S_4 surface.

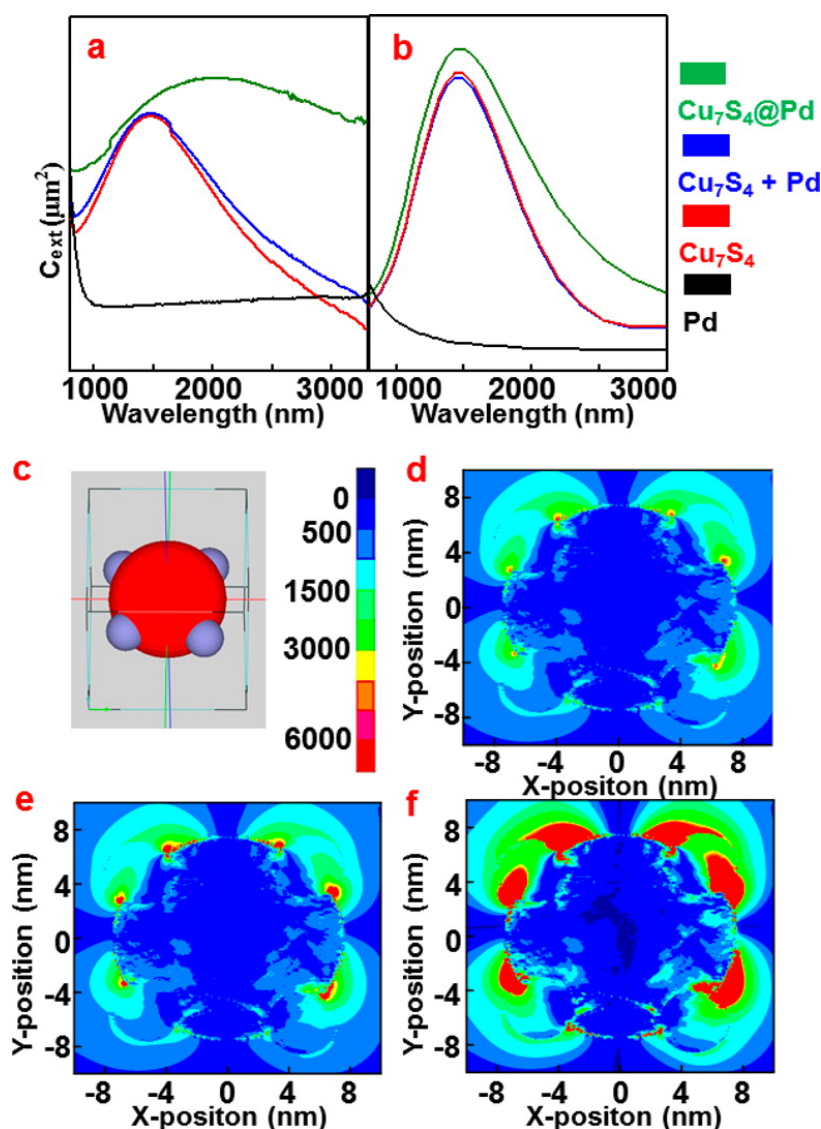


Figure 29. Localized surface plasmon resonance (LSPR) absorption spectra of different nanostructures obtained from experiment (a); and finite difference time domain (FDTD) simulation (b); Green curves: $\text{Cu}_7\text{S}_4@\text{Pd}$ heteronanostructures. Blue curves: physical mixture of Cu_7S_4 and Pd nanoparticles. Red curves: Cu_7S_4 nanoparticles. Black curves: Pd nanoparticles; (c) FDTD simulation setup for $\text{Cu}_7\text{S}_4@\text{Pd}$ and electrical field intensity scale; (d–f) The 2D contour of the electric field intensities around the $\text{Cu}_7\text{S}_4@\text{Pd}$ heteronanostructures under illumination of 808 nm (d); 980 nm (e); and 1500 nm (f); respectively. Reprinted from [185]. Copyright (2015), with permission from American Chemical Society.

The authors demonstrated the presence of a local electrical field enhancement, due to the LSPR effect, and studied how this enhancement is correlated with various wavelengths using a FDTD simulation (the Cu_7S_4 @Pd nanocrystal was located in the center of a simulated box, as shown in Figure 29c) of the 2D contour of the electron field intensity (XOY-plane, $z = 0$ nm) under different illumination sources (808, 980 and 1500 nm, Figure 29d–f). An electrical field enhancement was observed under irradiation at all examined wavelengths. In particular, the electrical field intensity for 1500 nm irradiation appears to be far stronger than that for 808 and 980 nm, and the same trend was obtained when evaluating the catalytic activity of Cu_7S_4 @Pd in the SMC reaction between iodobenzene and phenylboronic acid at different reaction time intervals (10, 20, and 30 min). As an example, 97% conversion was reached under 1500 nm irradiation in 30 min, whereas 45% and 50% conversions were obtained using the 808 and 980 nm irradiation wavelengths, respectively. Similar results were collected when phenylboronic acid was replaced by *p*-tolylboronic acid.

In this case, the use of cetyltrimethylammonium bromide (CTAB) was necessary to help the hydrophobic Cu_7S_4 @Pd nanoparticles disperse into water. It was proposed that the LSPR absorption of Cu_7S_4 gives rise to “hot holes” under 1500 nm illumination. These hot holes have enough energy to overcome the small Schottky barrier and inject themselves into the Pd domain, possibly rendering the Pd surface electron-deficient. In terms of the SMC reaction, theoretical studies indicated that the rate-limiting step is the oxidative addition of aryl halides onto Pd(0) [186]. Photoactivation favors the positively charged Pd surface, analogously to the action of electron-withdrawing ligands, and can promote the activation of aryl halides. Finally, differently to the majority of the traditional semiconductor–metal photocatalysts in which the LSPR effect of the noble metal nanoparticles serves the visible range absorption of the semiconductor, here Cu_7S_4 nanoparticles take advantage of NIR range photons via LSPR and grants the benefits to the metal.

6. Conclusions and Future Perspectives

Within the exploitation of SMC reactions, the use of unconventional technologies is allowing the advancement of a new chemistry with enormous potential, because it can promote processes and products that are more sustainable from both environmental and economic points of view. In particular, it has been shown that SMC is strongly facilitated by physical activation with MW, US, ball milling and light in a greener approach to process intensification. Despite the large fraction of papers here cited is dealing with the MW activation, the development of environmentally benign and often cost-effective procedures for SMC reactions is attracting a lot of interest. It was found that mainly either isolated Pd(II) species or supported Pd nanoparticles display a key role in the field of SMC catalyzed reaction in which the effects due to the combined use of the new methodologies can be investigated. Indeed, a great number of novel palladium-based catalysts has been reported in recent years for SMC. A careful examination of the catalysts reveals that it is important not only to regulate the Pd dispersion in terms of Pd(II) immobilization and of particle size, but also to consider the nature of the support as well as to optimise the synthetic procedure to control the morphology and the electronic properties of the obtained catalyst. It is worth noting that the optimised catalyst is required to be stable, recyclable and robust under the experimental conditions achieved by non conventional activation.

All these advances are well documented in recent literature, however, there are still a lot of problems that urgently require a solution: among these, to avoid the use of ligands, which can have environmental impact, is one of the main goals. Moreover, the requirement of ever-smaller amounts of metal catalyst to abate costs, as well as the need to produce recyclable catalysts are also main issues. The possibility to employ less reactive, but more attractive chloroarenes remains a challenge. In many cases, the selectivity is unsatisfactory when the reaction is driven by light, due to the involvement of free radical intermediates in UV-induced chemical reactions, giving for example, undesired autooxidation products, therefore leading to low selectivity of the desired product.

The current efforts in catalyst design can allow a more efficient exploitation of unconventional techniques. Recent discoveries here reported have demonstrated that highly selective reactions are feasible in the presence of an opportunely optimised catalyst and the right reaction conditions.

The results here described represent a helpful starting point to new green processes for SMC in the presence of innovative activation methodologies and open the door for significant improvement connected with the use of heterogeneous catalysts that permit product isolation by simple separation. In the near future, the green methodologies here examined combined with the catalyst design will be strategic to improve atom and energy efficiency, especially for industrial applications. In this frame, more intense efforts are required in the area of scaling up. In a future scenario, the most challenging problems that have to be overcome are: (i) to develop new active catalysts able to work in combination with unconventional activation methods; (ii) to provide cost analysis and (iii) to achieve progress in reactor engineering with new reliable flow systems that are well suited for industrial applications.

Acknowledgments: This work was supported by the University of Turin (Progetti Ricerca Locale 2015).

Conflicts of Interest: The authors declare no conflict of interest.

References

1. Phan, N.T.S.; Van Der Sluys, M.; Jones, C.W. On the nature of the active species in palladium catalyzed Mizoroki–Heck and Suzuki–Miyaura couplings—Homogeneous or heterogeneous catalysis, A critical review. *Adv. Synth. Catal.* **2006**, *348*, 609–679. [[CrossRef](#)]
2. Kappe, O.K.; Pieber, B.; Dallinger, D. Microwave effects in organic synthesis: Myth or reality? *Angew. Chem. Int. Ed.* **2013**, *52*, 1088–1094. [[CrossRef](#)] [[PubMed](#)]
3. Cravotto, G.; Cintas, P. Power ultrasound in organic synthesis: Moving cavitation chemistry from academia to innovative and large-scale applications. *Chem. Soc. Rev.* **2006**, *35*, 180–196. [[CrossRef](#)] [[PubMed](#)]
4. Lang, X.; Chen, X.; Zhao, J. Heterogeneous visible light photocatalysis for selective organic transformations. *Chem. Soc. Rev.* **2014**, *43*, 473–486. [[CrossRef](#)] [[PubMed](#)]
5. Suzuki, A. Kreuzkupplungen von Organoboranen: Ein einfacher Weg zum Aufbau von C-C-Bindungen (Nobel-Aufsatz). *Angew. Chem.* **2011**, *123*, 6854–6869. [[CrossRef](#)]
6. Miyaura, N.; Yamada, K.; Suzuki, A. A new stereospecific cross-coupling by the palladium-catalyzed reaction of 1-alkenylboranes with 1-alkenyl or 1-alkynyl halides. *Tetrahedron Lett.* **1979**, *20*, 3437–3440. [[CrossRef](#)]
7. Lennox, A.J.J.; Lloyd-Jones, G.C. Selection of boron reagents for Suzuki–Miyaura coupling. *Chem. Soc. Rev.* **2014**, *43*, 412–443. [[CrossRef](#)] [[PubMed](#)]
8. Suzuki, A. Cross-coupling reactions of organoboranes: An easy way to construct C–C bonds. *Angew. Chem. Int. Ed.* **2011**, *50*, 6722–6737. [[CrossRef](#)] [[PubMed](#)]
9. Hassan, J.; Sévignon, M.; Gozzi, C.; Schulz, E.; Lemaire, M. Aryl–Aryl bond formation one century after the discovery of the Ullmann reaction. *Chem. Rev.* **2002**, *102*, 1359–1470. [[CrossRef](#)] [[PubMed](#)]
10. Han, F.S. Transition-metal-catalyzed Suzuki–Miyaura cross-coupling reactions: A remarkable advance from palladium to nickel catalysts. *Chem. Soc. Rev.* **2013**, *42*, 5270–5298. [[CrossRef](#)] [[PubMed](#)]
11. Suzuki, A. Cross-coupling reactions via organoboranes. *J. Organomet. Chem.* **2002**, *653*, 83–90. [[CrossRef](#)]
12. Lipshutz, B.H.; Abela, A.R.; Boskovic, Z.V.; Nishikata, T.; Duplais, C.; Krasovskiy, A. “Greening up” cross-coupling chemistry. *Top. Catal.* **2010**, *53*, 985–990. [[CrossRef](#)]
13. Paul, S.; Islam, M.M.; Islam, S.M. Suzuki–Miyaura reaction by heterogeneously supported Pd in water: Recent studies. *RSC Adv.* **2015**, *5*, 42193–42221. [[CrossRef](#)]
14. Polshettiwar, V.; Decottignies, A.; Len, C.; Fihri, A. Suzuki–Miyaura cross-coupling reactions with low catalyst loading: A green and sustainable protocol in pure water. *ChemSusChem* **2010**, *3*, 502–522. [[CrossRef](#)] [[PubMed](#)]
15. Chatterjee, A.; Ward, T.R. Recent advances in the palladium catalyzed Suzuki–Miyaura cross-coupling reaction in water. *Catal. Lett.* **2016**, *146*, 820–840. [[CrossRef](#)]
16. Cravotto, G.; Garella, D.; Tagliapietra, S.; Stolle, A.; Schuessler, S.; Leonhardt, S.E.S.; Ondruschka, B. Suzuki cross-couplings of (hetero)aryl chlorides in the solid-state. *New J. Chem.* **2012**, *36*, 1304–1307. [[CrossRef](#)]
17. Larhed, M.; Moberg, C.; Hallberg, A. Microwave-accelerated homogeneous catalysis in organic chemistry. *Acc. Chem. Res.* **2002**, *35*, 717–727. [[CrossRef](#)] [[PubMed](#)]

18. Mehta, V.P.; Van der Eycken, E.V. Microwave-assisted C–C bond forming cross-coupling reactions: An overview. *Chem. Soc. Rev.* **2011**, *40*, 4925–4936. [[CrossRef](#)] [[PubMed](#)]
19. Bai, L.; Wang, J.X. Environmentally friendly Suzuki aryl–aryl cross-coupling reaction. *Curr. Org. Chem.* **2005**, *9*, 535–553. [[CrossRef](#)]
20. Hoogenboom, R.; Meier, M.A.R.; Schubert, U.S. The introduction of high-throughput experimentation methods for Suzuki–Miyaura coupling reactions in university education. *J. Chem. Educ.* **2005**, *82*, 1693–1696. [[CrossRef](#)]
21. Costa, N.E.; Pelotte, A.L.; Simard, J.M.; Syvinski, C.A.; Deveau, A.M. Discovering green, aqueous Suzuki coupling reactions: Synthesis of ethyl (4-phenylphenyl)acetate, a biaryl with anti-arthritis potential. *J. Chem. Educ.* **2012**, *89*, 1064–1067. [[CrossRef](#)]
22. Hill, N.J.; Bowman, M.D.; Esselman, B.J.; Byron, S.D.; Kreitinger, J.; Leadbeater, N.E. Ligand-free Suzuki–Miyaura coupling reactions using an inexpensive aqueous palladium source: A synthetic and computational exercise for the undergraduate organic chemistry laboratory. *J. Chem. Educ.* **2014**, *91*, 1054–1057. [[CrossRef](#)]
23. Soares, P.; Fernandes, C.; Chavarria, D.; Borges, F. Microwave-assisted synthesis of 5-phenyl-2-hydroxyacetophenone derivatives by a green Suzuki coupling reaction. *J. Chem. Educ.* **2015**, *92*, 575–578. [[CrossRef](#)]
24. Elumalai, V.; Sandtorv, A.H.; Bjorsvik, H.-R. A highly efficient Pd(PPh₃)₄-catalyzed Suzuki cross-coupling method for the preparation of 2-nitrobiphenyls from 1-chloro-2-nitrobenzenes and phenylboronic acids. *Eur. J. Org. Chem.* **2016**, *2016*, 1344–1354. [[CrossRef](#)]
25. Liu, J.; Robins, M.J. Fluoro, alkylsulfanyl, and alkylsulfonyl leaving groups in Suzuki cross-coupling reactions of purine 2'-deoxynucleosides and nucleosides. *Org. Lett.* **2005**, *7*, 1149–1151. [[CrossRef](#)] [[PubMed](#)]
26. Korn, T.J.; Schade, M.A.; Wirth, S.; Knochel, P. Cobalt(II)-catalyzed cross-coupling between polyfunctional arylcopper reagents and aryl fluorides or tosylates. *Org. Lett.* **2006**, *8*, 725–728. [[CrossRef](#)] [[PubMed](#)]
27. Wang, T.; Alfonso, B.J.; Love, J.A. Platinum(II)-catalyzed cross-coupling of polyfluoroaryl imines. *Org. Lett.* **2007**, *9*, 5629–5631. [[CrossRef](#)] [[PubMed](#)]
28. Guo, H.; Kong, F.; Kanno, K.-I.; He, J.; Nakajima, K.; Takahashi, T. Early transition metal-catalyzed cross-coupling reaction of aryl fluorides with a phenethyl Grignard reagent accompanied by rearrangement of the phenethyl group. *Organometallics* **2006**, *25*, 2045–2048. [[CrossRef](#)]
29. Ruiz, J.R.; Jimenez-Sanchidrian, C.; Mora, M. Suzuki cross-coupling reaction of fluorobenzene with heterogeneous Palladium catalysts. *J. Fluorine Chem.* **2006**, *127*, 443–445. [[CrossRef](#)]
30. Cargill, M.R.; Sandford, G.; Tadeusiak, A.J.; Yufit, D.S.; Howard, J.A.K.; Kilickiran, P.; Nelles, G. Palladium-catalyzed C–F activation of polyfluoronitrobenzene derivatives in Suzuki–Miyaura coupling reactions. *J. Org. Chem.* **2010**, *75*, 5860–5866.
31. Louvis, A.D.; Silva, N.A.; Semaan, F.S.; Da Silva, F.D.; Saramago, G.; de Souza, L.C.; Ferreira, B.L.; Castro, H.C.; Salles, J.P.; Souza, A.L.; et al. Synthesis, characterization and biological activities of 3-aryl-1,4-naphthoquinones—Green palladium-catalysed Suzuki cross coupling. *New J. Chem.* **2016**, *40*, 7643–7656. [[CrossRef](#)]
32. Fernandes, C.; Soares, P.; Gaspar, A.; Martins, D.; Gomes, L.R.; Low, J.N.; Borges, F. Synthesis of 6-aryl/heteroaryl-4-oxo-4H-chromene-2-carboxylic ethyl ester derivatives. *Tetrahedron Lett.* **2016**, *57*, 3006–3010. [[CrossRef](#)]
33. Kumar, S.; Ahmed, N. A facile approach for the synthesis of novel 1-oxa- and 1-aza-flavonyl-4-methyl-1H-benzo[d][1,3]oxazin-2(4H)-ones by microwave enhanced Suzuki–Miyaura coupling using bidentate chromen-4-one-based Pd(II)–diimine complex as catalyst. *RSC Adv.* **2015**, *5*, 77075–77087. [[CrossRef](#)]
34. Qu, R.Y.; Liu, Y.C.; Wu, Q.Y.; Chen, Q.; Yang, G.F. An efficient method for the syntheses of functionalized 6-bulkysubstituted salicylates under microwave irradiation. *Tetrahedron* **2015**, *71*, 8123–8130. [[CrossRef](#)]
35. Kadam, A.; Buckley, S.B.; Dinh, T.; Fitzgerald, R.; Zhang, W. Convertible fluororous linker assisted synthesis of tetrasubstituted furans. *Synlett* **2011**, *11*, 1608–1612.
36. Joy, M.N.; Bodke, Y.D.; Khader, K.K.A.; Sajith, A.M.; Venkatesh, T.; Kumar, A.K.A. Simultaneous exploration of TBAF·3H₂O as a base as well as a solvating agent for the palladium catalyzed Suzuki cross-coupling of 4-methyl-7-nonafluorobutylsulfonyloxy coumarins under microwave irradiation. *J. Fluorine Chem.* **2016**, *182*, 109–120. [[CrossRef](#)]
37. Vichier-Guerre, S.; Dugue, L.; Pochet, S. A convenient synthesis of 4(5)-(hetero)aryl-1H-imidazoles via microwave-assisted Suzuki–Miyaura cross-coupling reaction. *Tetrahedron Lett.* **2014**, *55*, 6347–6350. [[CrossRef](#)]

38. Fuse, S.; Ohuchi, T.; Asawa, Y.; Sato, S.; Nakamura, H. Development of 1-aryl-3-furanyl/thienyl-imidazopyridine templates for inhibitors against hypoxia inducible factor (HIF)-1 transcriptional activity. *Bioorg. Med. Chem. Lett.* **2016**, *26*, 5887–5890. [[CrossRef](#)] [[PubMed](#)]
39. Sandtorv, A.H.; Bjørsvika, H.-R. A three-way switchable process for Suzuki cross-coupling, hydrodehalogenation, or an assisted tandem hydrodehalogenation and Suzuki cross-coupling sequence. *Adv. Synth. Catal.* **2013**, *355*, 3231–3243. [[CrossRef](#)]
40. Wang, S.; Guo, R.; Li, J.; Zou, D.; Wu, Y.; Wu, Y. Efficient synthesis of 3-aryl-1*H*-indazol-5-amine by Pd-catalyzed Suzuki–Miyaura cross-coupling reaction under microwave-assisted conditions. *Tetrahedron Lett.* **2015**, *56*, 3750–3753. [[CrossRef](#)]
41. Liu, Y.-C.; Ye, C.-J.; Chen, Q.; Yang, G.-F. Efficient synthesis of bulky 4-substituted-isatins via microwave-promoted Suzuki cross-coupling reaction. *Tetrahedron Lett.* **2013**, *54*, 949–955. [[CrossRef](#)]
42. El Akkaoui, A.; Berteina-Raboin, S.; Mouaddib, A.; Guillaumet, G. Direct arylation of imidazo[1,2-*b*]pyridazines: Microwave-assisted one-pot Suzuki coupling/Pd-catalysed arylation. *Eur. J. Org. Chem.* **2010**, 862–871. [[CrossRef](#)]
43. Copin, C.; Henry, N.; Buron, F.; Routier, S. Synthesis of 2,6-disubstituted imidazo[2,1-*b*][1,3,4]thiadiazoles through cyclization and Suzuki–Miyaura cross-coupling reactions. *Eur. J. Org. Chem.* **2012**, *2012*, 3079–3083. [[CrossRef](#)]
44. Koini, E.N.; Avlonitis, N.; Martins-Duarte, E.S.; de Souza, W.; Vommaro, R.C.; Calogeropoulou, T. Divergent synthesis of 2,6-diaryl-substituted 5,7,8-trimethyl-1,4-benzoxazines via microwave-promoted palladium-catalyzed Suzuki–Miyaura cross coupling and biological evaluation. *Tetrahedron* **2012**, *68*, 10302–10309. [[CrossRef](#)]
45. Zukauskaitė, Z.; Buinauskaitė, V.; Solovjova, J.; Malinauskaitė, L.; Kveselyte, A.; Bieliauskas, A.; Ragaite, G.; Sackus, A. Microwave-assisted synthesis of new fluorescent indoline-based building blocks by ligand free Suzuki–Miyaura cross-coupling reaction in aqueous media. *Tetrahedron* **2016**, *72*, 2955–2963. [[CrossRef](#)]
46. Prieur, V.; Pujol, M.D.; Guillaumet, G. A strategy for the triarylation of pyrrolopyrimidines by using microwave-promoted cross-coupling reactions. *Eur. J. Org. Chem.* **2015**, *2015*, 6547–6556. [[CrossRef](#)]
47. El Bouakher, A.; Allouchi, H.; Abrunhosa-Thomas, I.; Troin, Y.; Guillaumet, G. Suzuki–Miyaura reactions of halospirooxindole derivatives. *Eur. J. Org. Chem.* **2015**, 3450–3461. [[CrossRef](#)]
48. Qu, G.-R.; Xin, P.-Y.; Niu, H.-Y.; Jin, X.; Guo, X.-T.; Yang, X.-N.; Guo, H.-M. Microwave promoted palladium-catalyzed Suzuki–Miyaura cross-coupling reactions of 6-chloropurines with sodium tetraarylborate in water. *Tetrahedron* **2011**, *67*, 9099–9103. [[CrossRef](#)]
49. Kabri, Y.; Crozet, M.D.; Szabo, R.; Vanelle, P. Efficient and original microwave-assisted Suzuki–Miyaura cross-coupling reaction in the 4*H*-pyrido[1,2-*a*]pyrimidin-4-one series. *Synthesis* **2011**, *19*, 3115–3122. [[CrossRef](#)]
50. Kabri, Y.; Crozet, M.D.; Primas, N.; Vanelle, P. One-pot chemoselective bis(Suzuki–Miyaura cross-coupling): Efficient access to 3,9-bis[(hetero)aryl]-4*H*-pyrido[1,2-*a*]pyrimidin-4-one derivatives under microwave irradiation. *Eur. J. Org. Chem.* **2012**, *28*, 5595–5604. [[CrossRef](#)]
51. Kabri, Y.; Crozet, M.D.; Terme, T.; Vanelle, P. Efficient access to 2,6,8-trisubstituted 4-aminoquinazolines through microwave-assisted one-pot chemoselective tris-Suzuki–Miyaura or S_NAr/bis-Suzuki–Miyaura reactions in water. *Eur. J. Org. Chem.* **2015**. [[CrossRef](#)]
52. Gallagher-Duval, S.; Hervé, G.; Sartori, G.; Enderlin, G.; Len, C. Improved microwave-assisted ligand-free Suzuki–Miyaura cross-coupling of 5-iodo-2'-deoxyuridine in pure water. *New J. Chem.* **2013**, *37*, 1989–1995. [[CrossRef](#)]
53. Darses, S.; Genet, J.-P. Potassium organotrifluoroborates: New perspectives in organic synthesis. *Chem. Rev.* **2008**, *108*, 288–325. [[CrossRef](#)] [[PubMed](#)]
54. Gary, A. Molander organotrifluoroborates: Another branch of the mighty oak. *J. Org. Chem.* **2015**, *80*, 7837–7848.
55. Kim, T.; Song, J.H.; Jeong, K.H.; Lee, S.; Ham, J. Potassium (1-organo-1*H*-1,2,3-triazol-4-yl)trifluoroborates from ethynyltrifluoroborate through a regioselective one-pot Cu-catalyzed azide–alkyne cycloaddition reaction. *Eur. J. Org. Chem.* **2013**. [[CrossRef](#)]
56. Jain, P.; Yi, S.; Flaherty, P.T. Suzuki–Miyaura cross-coupling of potassium organoborates with 6-sulfonate benzimidazoles using microwave irradiation. *J. Heterocycl. Chem.* **2013**, *50*, E166–E173. [[CrossRef](#)]

57. Henderson, L.; Knight, D.W.; Rutkowski, P.; Williams, A.C. Optimised conditions for styrene syntheses using Suzuki–Miyaura couplings and catalyst–ligand–base pre-mixes. *Tetrahedron Lett.* **2012**, *53*, 4654–4656. [[CrossRef](#)]
58. Brooker, M.D.; Cooper, S.M., Jr.; Hodges, D.R.; Carter, R.R.; Wyatt, J.K. Studies of microwave-enhanced Suzuki–Miyaura vinylation of electron-rich sterically hindered substrates utilizing potassium vinyltrifluoroborate. *Tetrahedron Lett.* **2010**, *51*, 6748–6752. [[CrossRef](#)] [[PubMed](#)]
59. Huang, Z.-Y.; Yang, J.-F.; Song, K.; Chen, Q.; Zhou, S.-L.; Hao, G.-F.; Yang, G.-F. One-pot approach to *N*-quinolyl 3'/4'-biaryl carboxamides by microwave-assisted Suzuki–Miyaura coupling and *N*-boc deprotection. *J. Org. Chem.* **2016**, *81*, 9647–9657. [[CrossRef](#)] [[PubMed](#)]
60. Huang, Z.-Y.; Yang, J.-F.; Chen, Q.; Cao, R.-J.; Huang, W.; Hao, G.-F.; Yang, G.-F. An efficient one-pot access to *N*-(pyridin-2-ylmethyl) substituent biphenyl-4-sulfonamides through water-promoted, palladium-catalyzed, microwave-assisted reactions. *RSC Adv.* **2015**, *5*, 75182–75186. [[CrossRef](#)]
61. Grob, J.E.; Nunez, J.; Dechantsreiter, M.A.; Hamann, L.G. One-pot reductive amination and Suzuki–Miyaura cross-coupling of formyl aryl and heteroaryl imidazoles in array format. *J. Org. Chem.* **2011**, *76*, 4930–4940. [[CrossRef](#)] [[PubMed](#)]
62. Park, K.-Y.; Kim, B.T.; Heo, J.-N. Direct one-pot synthesis of naphthoxindoles from 4-bromooxindoles by Suzuki–Miyaura coupling and aldol condensation reactions. *Eur. J. Org. Chem.* **2014**, *1*, 164–170. [[CrossRef](#)]
63. Hooper, A.; Zambon, A.; Springer, C.J. A novel protocol for the one-pot borylation/Suzuki reaction provides easy access to hinge-binding groups for kinase inhibitors. *Org. Biomol. Chem.* **2016**, *14*, 963–969. [[CrossRef](#)] [[PubMed](#)]
64. Cívicos, J.F.; Alonso, D.A.; Nájera, C. Oxime palladacycle-catalyzed Suzuki–Miyaura alkenylation of aryl, heteroaryl, benzyl, and allyl chlorides under microwave irradiation conditions. *Adv. Synth. Catal.* **2011**, *353*, 1683–1687. [[CrossRef](#)]
65. Cívicos, J.F.; Alonso, D.A.; Nájera, C. Oxime-palladacycle-catalyzed Suzuki–Miyaura arylation and alkenylation of aryl imidazolesulfonates under aqueous and phosphane-free conditions. *Eur. J. Org. Chem.* **2012**, *2012*, 3670–3676. [[CrossRef](#)]
66. Susanto, W.; Chu, C.-Y.; Ang, W.J.; Chou, T.-C.; Lo, L.-C.; Lam, Y. Development of a fluororous, oxime-based palladacycle for microwave-promoted carbon–carbon coupling reactions in aqueous media. *Green Chem.* **2012**, *14*, 77–80. [[CrossRef](#)]
67. Dawood, K.M.; Elamin, M.B.; Farag, A.M. Microwave-assisted synthesis of 2-acetyl-5-arylthiophenes and 4-(5-arylthiophen-2-yl)thiazoles via Suzuki coupling in water. *ARKIVOC* **2015**, *7*, 50–62.
68. Hanhan, M.E.; Martínez-Mañez, R.; Ros-Lis, J.V. Highly effective activation of aryl chlorides for Suzuki coupling in aqueous media using a ferrocene-based Pd(II)–diimine catalyst. *Tetrahedron Lett.* **2012**, *53*, 2388–2391. [[CrossRef](#)]
69. Balam-Villarreal, J.A.; Sandoval-Chavez, C.I.; Ortega-Jimenez, F.; Toscano, R.A.; Carreon-Castro, M.P.; Lopez-Cortes, J.G.; Ortega-Alfaro, M.C. Infrared irradiation or microwave assisted cross-coupling reactions using sulfur-containing ferrocenyl-palladacycles. *J. Organomet. Chem.* **2016**, *818*, 7–14. [[CrossRef](#)]
70. Yılmaz, Ü.; Şireci, N.; Deniz, S.; Küçükbay, H. Synthesis and microwave-assisted catalytic activity of novel bis-benzimidazole salts bearing furfuryl and thenylmoieties in Heck and Suzuki cross-coupling reactions. *Appl. Organomet. Chem.* **2010**, *24*, 414–420.
71. Yılmaz, Ü.; Küçükbay, H.; Şireci, N.; Akkurt, M.; Günald, S.; Durmaz, R.; Tahir, M.N. Synthesis, microwave-promoted catalytic activity in Suzuki–Miyaura cross-coupling reactions and antimicrobial properties of novel benzimidazole salts bearing trimethylsilyl group. *Appl. Organomet. Chem.* **2011**, *25*, 366–373. [[CrossRef](#)]
72. Silarska, E.; Trzeciak, A.M.; Pernak, J.; Skrzypczak, A. [IL]₂[PdCl₄] complexes (IL = imidazolium cation) as efficient catalysts for Suzuki–Miyaura cross-coupling of aryl bromides and aryl chlorides. *Appl. Catal. A* **2013**, *466*, 216–223. [[CrossRef](#)]
73. Hanhan, M.E.; Senemoglu, Y. Microwave-assisted aqueous Suzuki coupling reactions catalyzed by ionic palladium(II) complexes. *Transit. Met. Chem.* **2012**, *37*, 109–116. [[CrossRef](#)]
74. Shen, L.; Huang, S.; Nie, Y.; Lei, F. An efficient microwave-assisted Suzuki reaction using a new pyridine-pyrazole/Pd(II) species as catalyst in aqueous media. *Molecules* **2013**, *18*, 1602–1612. [[CrossRef](#)] [[PubMed](#)]

75. Naik, S.; Kumaravel, M.; Mague, J.T.; Balakrishna, M.S. Bisamino(diphosphonite) with dangling olefin functionalities: Synthesis, metal chemistry and catalytic utility of Rh^I and Pd^{II} complexes in hydroformylation and Suzuki–Miyaura reactions. *Dalton Trans.* **2014**, *43*, 1082–1095. [[CrossRef](#)] [[PubMed](#)]
76. Basauri-Molina, M.; Hernández-Ortega, S.; Morales-Morales, D. Microwave-assisted C–C and C–S couplings catalysed by organometallic Pd-SCS or coordination Ni-SNS pincer complexes. *Eur. J. Inorg. Chem.* **2014**, *27*, 4619–4625. [[CrossRef](#)]
77. Gayakhe, V.; Ardhpure, A.; Kapdi, A.R.; Sanghvi, Y.S.; Serrano, J.L.; Garcia, L.; Perez, J.; Garcia, J.; Sanchez, G.; Fischer, C.; et al. Water-soluble Pd-imidate complexes: Broadly applicable catalysts for the synthesis of chemically modified nucleosides via Pd-catalyzed cross-coupling. *J. Org. Chem.* **2016**, *81*, 2713–2729. [[CrossRef](#)] [[PubMed](#)]
78. Glorius, F. Asymmetric cross-coupling of non-activated secondary alkyl halides. *Angew. Chem. Int. Ed.* **2008**, *47*, 8347–8349. [[CrossRef](#)] [[PubMed](#)]
79. Glasson, C.R.K.; Meehan, G.V.; Motti, C.A.; Clegg, J.K.; Turner, P.; Jensen, P.; Lindoy, L.F. New nickel(II) and iron(II) helicates and tetrahedra derived from expanded quaterpyridines. *Dalton Trans.* **2011**, *40*, 10481–10490. [[CrossRef](#)] [[PubMed](#)]
80. Lee, G.M.; Loechtefeld, R.; Menssen, R.; Bierer, D.E.; Riedl, B.; Baker, R.T. Synthesis of bromodifluoromethyl (arylsulfonyl) compounds and microwave-assisted nickel catalyzed cross coupling with arylboronic acids. *Tetrahedron Lett.* **2016**, *57*, 5464–5468. [[CrossRef](#)]
81. Baghbanzadeh, M.; Pilger, C.; Kappe, C.O. Rapid nickel-catalyzed Suzuki–Miyaura cross-couplings of aryl carbamates and sulfamates utilizing microwave heating. *J. Org. Chem.* **2011**, *76*, 1507–1510. [[CrossRef](#)] [[PubMed](#)]
82. De Luna Martins, D.; Aguiar, L.C.S.; Antunes, O.A.C. Microwave promoted Suzuki reactions between aroyl chlorides and boronic acids catalyzed by heterogeneous and homogeneous phosphine-free palladium catalysts. *J. Organomet. Chem.* **2011**, *696*, 2845–2849. [[CrossRef](#)]
83. Feng, G.; Liu, F.; Lin, C.; Li, W.; Wang, S.; Qi, C. Crystalline mesoporous γ -Al₂O₃ supported palladium: Novel and efficient catalyst for Suzuki–Miyaura reaction under controlled microwave heating. *Catal. Commun.* **2013**, *37*, 27–31. [[CrossRef](#)]
84. Smith, S.E.; Siamaki, A.R.; Gupton, B.F.; Carpenter, E.E. CuPd nanoparticles as a catalyst in carbon–carbon cross-coupling reactions by a facile oleylamine synthesis. *RSC Adv.* **2016**, *6*, 91541–91545. [[CrossRef](#)]
85. Molnár, Á. Efficient, selective, and recyclable palladium catalysts in carbon–carbon coupling reactions. *Chem. Rev.* **2011**, *111*, 2251–2320. [[CrossRef](#)] [[PubMed](#)]
86. Kim, S.W.; Kim, M.; Lee, W.Y.; Hyeon, T. Fabrication of hollow palladium spheres and their successful application to the recyclable heterogeneous catalyst for Suzuki coupling reactions. *J. Am. Chem. Soc.* **2002**, *124*, 7642–7643. [[CrossRef](#)] [[PubMed](#)]
87. Fihri, A.; Bouhrara, M.; Nekoueshahraki, B.; Basset, J.-M.; Polshettiwar, V. Nanocatalysts for Suzuki cross-coupling reactions. *Chem. Soc. Rev.* **2011**, *40*, 5181–5203. [[CrossRef](#)] [[PubMed](#)]
88. Scheuermann, G.M.; Rumi, L.; Steurer, P.; Bannwarth, W.; Mulhaupt, R. Palladium nanoparticles on graphite oxide and its functionalized graphene derivatives as highly active catalysts for the Suzuki–Miyaura coupling reaction. *J. Am. Chem. Soc.* **2009**, *131*, 8262–8270. [[CrossRef](#)] [[PubMed](#)]
89. Kotadia, D.A.; Patel, U.H.; Gandhi, S.; Soni, S.S. Pd doped SiO₂ nanoparticles: An efficient recyclable catalyst for Suzuki, Heck and Sonogashira reactions. *RSC Adv.* **2014**, *4*, 32826–32833. [[CrossRef](#)]
90. Ciriminna, R.; Pandarus, V.; Gingras, G.; Beland, F.; Demma Cara, P.; Pagliaro, M. Heterogeneously catalyzed Suzuki–Miyaura conversion of broad scope. *RSC Adv.* **2012**, *2*, 10798–10804. [[CrossRef](#)]
91. Verho, O.; Nagendiran, A.; Johnston, E.V.; Tai, C.; Baekvall, J.-E. Nanopalladium on amino-functionalized mesocellular foam. An efficient catalyst for Suzuki reactions and transfer hydrogenations. *ChemCatChem* **2013**, *5*, 612–618. [[CrossRef](#)]
92. Parvulescu, A.N.; Van der Eycken, E.; Jacobs, P.A.; De Vos, D.E. Microwave-promoted racemization and dynamic kinetic resolution of chiral amines over Pd on alkaline earth supports and lipases. *J. Catal.* **2008**, *255*, 206–212. [[CrossRef](#)]
93. Chang, W.; Chae, G.H.; Jang, S.R.; Shin, J.; Ahn, B.J. An efficient microwave-assisted Suzuki reaction using Pd/MCM-41 and Pd/SBA-15 as catalysts in solvent-free condition. *J. Ind. Eng. Chem.* **2012**, *18*, 581–585. [[CrossRef](#)]

94. Zheng, Z.; Li, H.; Liu, T.; Cao, R. Monodisperse noble metal nanoparticles stabilized in SBA-15: Synthesis, characterization and application in microwave-assisted Suzuki–Miyaura coupling reaction. *J. Catal.* **2010**, *270*, 268–274. [[CrossRef](#)]
95. Luo, M.; Dai, C.; Han, Q.; Fan, G.; Song, G. Preparation and characterization of palladium immobilized on silica-coated Fe₃O₄ and its catalytic performance for Suzuki reaction under microwave irradiation. *Surf. Interface Anal.* **2016**, *48*, 1066–1071. [[CrossRef](#)]
96. Nehlig, E.; Waggeh, B.; Millot, N.; Lalatonne, Y.; Motte, L.; Guenin, E. Immobilized Pd on magnetic nanoparticles bearing proline as a highly efficient and retrievable Suzuki–Miyaura catalyst in aqueous media. *Dalton Trans.* **2015**, *44*, 501–505. [[CrossRef](#)] [[PubMed](#)]
97. Cravotto, G.; Orio, L.; Calcio Gaudino, E.; Martina, K.; Tavor, D.; Wolfson, A. Efficient synthetic protocols in glycerol under heterogeneous catalysis. *ChemSusChem* **2011**, *4*, 1130–1134. [[CrossRef](#)]
98. Martina, K.; Leonhardt, S.E.; Ondruschka, B.; Curini, M.; Binello, A.; Cravotto, G. In situ cross-linked chitosan Cu(I) or Pd(II) complexes as a versatile, eco-friendly recyclable solid catalyst. *J. Mol. Catal. A* **2011**, *334*, 60–64. [[CrossRef](#)]
99. Leonhardt, S.E.S.; Stolle, A.; Ondruschka, B.; Cravotto, G.; De Leo, C.; Jandt, K.D.; Keller, T.F. Chitosan as a support for heterogeneous Pd catalysts in liquid phase catalysis. *Appl. Catal. A* **2010**, *379*, 30–37. [[CrossRef](#)]
100. Baran, T.; Sargin, I.; Kaya, M.; Mentés, A. Green heterogeneous Pd(II) catalyst produced from chitosan-cellulose micro beads for green synthesis of biaryls. *Carbohydr. Polym.* **2016**, *152*, 181–188. [[CrossRef](#)] [[PubMed](#)]
101. Cravotto, G.; Calcio Gaudino, E.; Tagliapietra, S.; Carnaroglio, D.; Procopio, A. A green approach to heterogeneous catalysis using ligand-free, metal-loaded cross-linked cyclodextrins. *Green Proc. Synth.* **2012**, *1*, 269–273. [[CrossRef](#)]
102. Martina, K.; Baricco, F.; Caporaso, M.; Berlier, G.; Cravotto, G. Cyclodextrin-grafted silica-supported Pd nanoparticles: An efficient and versatile catalyst for ligand-free C–C coupling and hydrogenation. *ChemCatChem* **2016**, *8*, 1176–1184. [[CrossRef](#)]
103. Isfahani, A.L.; Mohammadpoor-Baltork, I.; Mirkhani, V.; Khosropour, A.R.; Moghadam, M.; Tangestaninejad, S.; Kia, R. Palladium nanoparticles immobilized on nano-silica triazine dendritic polymer (Pdnp-nSTDP): An efficient and reusable catalyst for Suzuki–Miyaura cross-coupling and Heck reactions. *Adv. Synth. Catal.* **2013**, *355*, 957–972. [[CrossRef](#)]
104. Borkowski, T.; Zawartka, W.; Pospiech, P.; Mizerska, U.; Trzeciak, A.M.; Cypryk, M.; Tylus, W. Reusable functionalized polysiloxane-supported palladium catalyst for Suzuki–Miyaura cross-coupling. *J. Catal.* **2011**, *282*, 270–277. [[CrossRef](#)]
105. Massaro, M.; Schembri, V.; Campisciano, V.; Cavallaro, G.; Lazzara, G.; Milioto, S.; Noto, R.; Parisi, F.; Riela, S. Design of PNIPAAm covalently grafted on halloysite nanotubes as a support for metal-based catalysts. *RSC Adv.* **2016**, *6*, 55312–55318. [[CrossRef](#)]
106. Massaro, M.; Riela, S.; Cavallaro, G.; Colletti, C.G.; Milioto, S.; Noto, R.; Parisi, F.; Lazzara, G. Palladium supported on Halloysite-triazolium salts as catalyst for ligand free Suzuki cross-coupling in water under microwave irradiation. *J. Mol. Catal. A* **2015**, *408*, 12–19. [[CrossRef](#)]
107. Massaro, M.; Riela, S.; Lazzara, G.; Gruttadauria, M.; Milioto, S.; Noto, R. Green conditions for the Suzuki reaction using microwave irradiation and a new HNT-supported ionic liquid-like phase (HNT-SILLP) catalyst. *Appl. Organomet. Chem.* **2014**, *28*, 234–238. [[CrossRef](#)]
108. Baruah, D.; Das, R.N.; Hazarika, S.; Konwar, D. Biogenic synthesis of cellulose supported Pd(0) nanoparticles using hearth wood extract of *Artocarpus lakoocha* Roxb—A green, efficient and versatile catalyst for Suzuki and Heck coupling in water under microwave heating. *Catal. Commun.* **2015**, *72*, 73–80. [[CrossRef](#)]
109. Baran, T.; Sargin, I.; Kaya, M.; Mentés, A.; Ceter, T. Design and application of sporopollenin microcapsule supported palladium catalyst: Remarkably high turnover frequency and reusability in catalysis of biaryls. *J. Coll. Interface Sci.* **2017**, *486*, 194–203. [[CrossRef](#)] [[PubMed](#)]
110. Baran, T.; Sargin, I.; Mentés, A.; Kaya, M. Exceptionally high turnover frequencies recorded for a new chitosan-based palladium(II) catalyst. *Appl. Catal. A* **2016**, *523*, 12–20. [[CrossRef](#)]
111. Baran, T.; Sargin, I.; Kaya, M.; Mentés, A. An environmental catalyst derived from biological waste materials for green synthesis of biaryls via Suzuki coupling reactions. *J. Mol. Catal. A* **2016**, *420*, 216–221. [[CrossRef](#)]
112. Shah, D.; Kaur, H. Supported palladium nanoparticles: A general sustainable catalyst for microwave enhanced carbon-carbon coupling reactions. *J. Mol. Catal. A* **2016**, *424*, 171–180. [[CrossRef](#)]

113. Kaur, H.; Shah, D.; Pal, U. Resin encapsulated palladium nanoparticles: An efficient and robust catalyst for microwave enhanced Suzuki–Miyaura coupling. *Catal. Commun.* **2011**, *12*, 1384–1388. [[CrossRef](#)]
114. Djakovitch, L.; Dufaud, V.; Zaidi, R. Heterogeneous palladium catalysts applied to the synthesis of 2- and 2,3-functionalised indoles. *Adv. Synth. Catal.* **2006**, *348*, 715–724. [[CrossRef](#)]
115. Djakovitch, L.; Koehler, K. Heck reaction catalyzed by Pd-modified zeolites. *J. Am. Chem. Soc.* **2001**, *123*, 5990–5999. [[CrossRef](#)] [[PubMed](#)]
116. Giacalone, F.; Campisciano, V.; Calabrese, C.; La Parola, V.; Liotta, L.F.; Aprile, C.; Gruttadauria, M. Supported C₆₀-IL-PdNPs as extremely active nanocatalysts for C–C cross-coupling reactions. *J. Mat. Chem. A* **2016**, *4*, 17193–17206. [[CrossRef](#)]
117. Guerra, R.R.G.; Martins, F.C.P.; Lima, C.G.S.; Gonçalves, R.H.; Leite, E.R.; Pereira-Filho, E.R.; Schwab, R.S. Factorial design evaluation of the Suzuki cross-coupling reaction using a magnetically recoverable palladium catalyst. *Tetrahedron Lett.* **2017**, *58*, 903–908. [[CrossRef](#)]
118. Moussa, S.; Siamaki, A.R.; Gupton, B.F.; El-Shall, M.S. Pd-partially reduced graphene oxide catalysts (Pd/PRGO): Laser synthesis of Pd nanoparticles supported on PRGO nanosheets for carbon-carbon cross coupling reactions. *ACS Catal.* **2012**, *2*, 145–154. [[CrossRef](#)]
119. Tsukahara, Y.; Higashi, A.; Yamauchi, T.; Nakamura, T.; Yasuda, M.; Baba, A.; Wada, Y. In situ observation of nonequilibrium local heating as an origin of special effect of microwave on chemistry. *J. Phys. Chem. C* **2010**, *114*, 8965–8970. [[CrossRef](#)]
120. Horikoshi, S.; Osawa, A.; Abe, M.; Serpone, N. On the generation of hot-spots by microwave electric and magnetic fields and their impact on a microwave-assisted reaction in the presence of metallic Pd nanoparticles on an activated carbon support. *J. Phys. Chem. C* **2011**, *115*, 23030–23035. [[CrossRef](#)]
121. Gomez-Martinez, M.; Buxaderas, E.; Pastor, I.M.; Alonso, D.A. Palladium nanoparticles supported on graphene and reduced graphene oxide as efficient recyclable catalyst for the Suzuki–Miyaura reaction of potassium aryltrifluoroborates. *J. Mol. Catal. A* **2015**. [[CrossRef](#)]
122. Garcia-Suarez, E.J.; Lara, P.; Garcia, A.B.; Ojeda, M.; Luque, R.; Philippot, K. Efficient and recyclable carbon-supported Pd nanocatalysts for the Suzuki–Miyaura reaction in aqueous-based media: Microwave vs. conventional heating. *Appl. Catal. A* **2013**, *468*, 59–67. [[CrossRef](#)]
123. Sanhes, D.; Raluy, E.; Rétory, S.; Saffon, N.; Teuma, E.; Gomez, M. Unexpected activation of carbon–bromide bond promoted by palladium nanoparticles in Suzuki C–C couplings. *Dalton Trans.* **2010**, *39*, 9719–9726. [[CrossRef](#)] [[PubMed](#)]
124. Schmidt, B.; Riemer, M.; Karras, M. 2,2'-biphenols via protecting group-free thermal or microwave-accelerated Suzuki–Miyaura coupling in water. *J. Org. Chem.* **2013**, *78*, 8680–8688. [[CrossRef](#)] [[PubMed](#)]
125. Al-Amin, M.; Akimoto, M.; Tameno, T.; Ohki, Y.; Takahashi, N.; Hoshiya, N.; Shuto, S.; Arisawa, M. Suzuki–Miyaura cross-coupling reactions using a low-leaching and highly recyclable gold-supported palladium material and two types of microwave equipments. *Green Chem.* **2013**, *15*, 1142–1145. [[CrossRef](#)]
126. Heinrich, F.; Kessler, M.T.; Dohmen, S.; Singh, M.; Pechtl, M.H.G.; Mathur, S. Molecular palladium precursors for Pd⁰ nanoparticle preparation by microwave irradiation: Synthesis, structural characterization and catalytic activity. *Eur. J. Inorg. Chem.* **2012**, *2012*, 6027–6033. [[CrossRef](#)]
127. Siamaki, A.R.; Abd El Rahman, S.K.; Abdelsayed, V.; El-Shall, M.S.; Gupton, B.F. Microwave-assisted synthesis of palladium nanoparticles supported on graphene: A highly active and recyclable catalyst for carbon-carbon cross-coupling reactions. *J. Catal.* **2011**. [[CrossRef](#)]
128. Elazab, H.A.; Siamaki, A.R.; Moussa, S.; Gupton, B.F.; El-Shall, M.S. Highly efficient and magnetically recyclable graphene-supported Pd/Fe₃O₄ nanoparticle catalysts for Suzuki and Heck cross-coupling reactions. *Appl. Catal. A* **2015**, *491*, 58–69. [[CrossRef](#)]
129. Ni, Z.; Masel, R.I. Rapid production of metal-organic frameworks via microwave-assisted solvothermal synthesis. *J. Am. Chem. Soc.* **2006**, *128*, 12394–12395. [[CrossRef](#)]
130. Li, Y.; Liu, Y.; Gao, W.; Zhang, L.; Liu, W.; Lu, J.; Wang, Z.; Deng, Y.J. Microwave-assisted synthesis of UIO-66 and its adsorption performance towards dyes. *Cryst. Eng. Commun.* **2014**, *16*, 7037–7042. [[CrossRef](#)]
131. Dong, W.; Feng, C.; Zhang, L.; Shang, N.; Gao, S.; Wang, C.; Wang, Z. Pd@UiO-66: An efficient catalyst for Suzuki–Miyaura coupling reaction at mild condition. *Catal. Lett.* **2016**, *146*, 117–125. [[CrossRef](#)]
132. Huang, J.; Wang, W.; Li, H. Water-medium organic reactions catalyzed by active and reusable Pd/Y heterobimetal-organic framework. *ACS Catal.* **2013**, *3*, 1526–1536. [[CrossRef](#)]

133. Prasad, K.S.; Noh, H.-B.; Reddy, S.S.; Reddy, A.E.; Shim, Y.-B. Catalytic properties of Au and Pd nanoparticles decorated on Cu₂O microcubes for aerobic benzyl alcohol oxidation and Suzuki–Miyaura coupling reactions in water. *Appl. Catal. A* **2014**, *476*, 72–77. [[CrossRef](#)]
134. Veerakumar, P.; Madhu, R.; Chen, S.-M.; Veeramani, V.; Hung, C.-T.; Tang, P.-H.; Wang, C.-B.; Liu, S.-B. Highly stable and active palladium nanoparticles supported on porous carbon for practical catalytic applications. *J. Mater. Chem. A* **2014**, *2*, 16015–16022. [[CrossRef](#)]
135. Misch, L.M.; Birkel, A.; Figg, C.A.; Fors, B.P.; Hawker, C.J.; Stucky, G.D.; Seshadri, R. Rapid microwave-assisted sol-gel preparation of Pd-substituted LnFeO₃ (Ln = Y, La): Phase formation and catalytic activity. *Dalton Trans.* **2014**, *43*, 2079–2087. [[CrossRef](#)] [[PubMed](#)]
136. Lennox, A.J.J.; Lloyd-Jones, G.C. Organotrifluoroborate hydrolysis: Boronic acid release mechanism and an acid–base paradox in cross-coupling. *J. Am. Chem. Soc.* **2012**, *134*, 7431–7441. [[CrossRef](#)] [[PubMed](#)]
137. Shil, A.K.; Guha, N.R.; Sharma, D.; Das, P. A solid supported palladium(0) nano/microparticle catalyzed ultrasound induced continuous flow technique for large scale Suzuki reactions. *RSC Adv.* **2013**, *3*, 13671–13676. [[CrossRef](#)]
138. Das, P.; Sharma, D.; Shil, A.K.; Kumari, A. Solid-supported Pd nano and microparticles: An efficient heterogeneous catalyst for ligand-free Suzuki–Miyaura cross coupling reaction. *Tetrahedron Lett.* **2011**, *52*, 1176–1178. [[CrossRef](#)]
139. Azua, A.; Mata, J.A.; Heymes, P.; Peris, E.; Lamaty, F.; Martinez, J.; Colacino, E. Palladium *N*-heterocyclic carbene catalysts for the ultrasound-promoted Suzuki–Miyaura reaction in glycerol. *Adv. Synth. Catal.* **2013**, *355*, 1107–1116. [[CrossRef](#)]
140. Chaudhary, A.R.; Bedekar, A.V. 1-(α -Aminobenzyl)-2-naphthol as phosphinefree ligand for Pd-catalyzed Suzuki and one-pot Wittig–Suzuki reaction. *Appl. Organomet. Chem.* **2012**, *26*, 430–437. [[CrossRef](#)]
141. Chaudhary, A.R.; Bedekar, A.V. Application of 1-(α -aminobenzyl)-2-naphthols as air-stable ligands for Pd-catalyzed Mizoroki–Heck coupling reaction. *Synth. Commun.* **2012**, *42*, 1778–1785.
142. Ghotbinejad, M.; Khosropour, A.R.; Mohammadpoor-Baltork, I.; Moghadam, M.; Tangestaninejad, S.; Mirkhani, V. Ultrasound-assisted C–C coupling reactions catalyzed by unique SPION-A-Pd(EDTA) as a robust nanocatalyst. *RSC Adv.* **2014**, *4*, 8590–8596. [[CrossRef](#)]
143. Wang, Z.; Chen, W.; Han, Z.; Zhu, J.; Lu, N.; Yang, Y.; Ma, D.; Chen, Y.; Huang, S. Pd embedded in porous carbon (Pd@CMK-3) as an active catalyst for Suzuki reactions: Accelerating mass transfer to enhance the reaction rate. *Nano Res.* **2014**, *7*, 1254–1262. [[CrossRef](#)]
144. Suresh, N.; Prasanna, G.L.; Rao, M.V.B.; Pal, M. Ultrasound assisted synthesis of 6-flavonyl substituted 1,4-dihydro-benzo[*d*][1,3]oxazin-2-ones via Suzuki–Miyaura coupling under Pd/C catalysis. *Arab. J. Chem.* **2016**. [[CrossRef](#)]
145. Kulkarni, K.; Friend, J.; Yeo, L.; Perlmutter, P. An emerging reactor technology for chemical synthesis: Surface acoustic wave-assisted closed-vessel Suzuki coupling reactions. *Ultrason. Sonochem.* **2014**, *21*, 1305–1309. [[CrossRef](#)] [[PubMed](#)]
146. Senapati, K.K.; Roy, S.; Borgohain, C.; Phukan, P. Palladium nanoparticle supported on cobalt ferrite: An efficient magnetically separable catalyst for ligand free Suzuki coupling. *J. Mol. Catal. A* **2012**, *352*, 128–134. [[CrossRef](#)]
147. Singh, A.S.; Patil, U.B.; Nagarkar, J.M. Palladium supported on zinc ferrite: A highly active, magnetically separable catalyst for ligand free Suzuki and Heck coupling. *Catal. Commun.* **2013**, *35*, 11–16. [[CrossRef](#)]
148. Su, X.; Vinu, A.; Aldeyab, S.S.; Zhong, L. Highly uniform Pd nanoparticles supported on g-C₃N₄ for efficiently catalytic Suzuki–Miyaura reactions. *Catal. Lett.* **2015**, *145*, 1388–1395. [[CrossRef](#)]
149. Li, J.; Bai, X. Ultrasonic synthesis of supported palladium nanoparticles for room-temperature Suzuki–Miyaura coupling. *J. Mater. Sci.* **2016**, *51*, 9108–9122. [[CrossRef](#)]
150. Berry, D.E.; Carrie, P.; Fawkes, K.L.; Rebner, B.; Xing, Y. The mechanochemical reaction of palladium(II) chloride with a bidentate phosphine. *J. Chem. Educ.* **2010**, *87*, 533–534. [[CrossRef](#)]
151. Ojeda, M.; Balu, A.M.; Barron, V.; Pineda, A.; Coletto, A.G.; Romero, A.A.; Luque, R. Solventless mechanochemical synthesis of magnetic functionalized catalytically active mesoporous SBA-15 nanocomposites. *J. Mater. Chem. A* **2014**, *2*, 387–393. [[CrossRef](#)]
152. Siamaki, A.R.; Lin, Y.; Woodberry, K.; Connell, J.W.; Gupton, B.F. Palladium nanoparticles supported on carbon nanotubes from solventless preparations: Versatile catalysts for ligand-free Suzuki cross coupling reactions. *J. Mater. Chem. A* **2013**, *1*, 12909–12918. [[CrossRef](#)]

153. Zhang, A.; Liu, M.; Liu, M.; Xiao, Y.; Li, Z.; Chen, J.; Sun, Y.; Zhao, J.; Fang, S.; Jia, D.; et al. Homogeneous Pd nanoparticles produced in direct reactions: Green synthesis, formation mechanism and catalysis properties. *J. Mater. Chem. A* **2014**, *2*, 1369–1374. [[CrossRef](#)]
154. Schneider, F.; Ondruschka, B. Mechanochemical solid-state Suzuki reactions using an in situ generated base. *ChemSusChem* **2008**, *1*, 622–625. [[CrossRef](#)] [[PubMed](#)]
155. Schneider, F.; Stolle, A.; Ondruschka, B.; Hopf, H. The Suzuki–Miyaura reaction under mechanochemical conditions. *Org. Process Res. Dev.* **2009**, *13*, 44–48. [[CrossRef](#)]
156. Braga, D.; D’Addario, D.; Polito, M.; Grepioni, F. Mechanically induced expeditious and selective preparation of disubstituted pyridine/pyrimidine ferrocenyl complexes. *Organometallics* **2004**, *23*, 2810–2812. [[CrossRef](#)]
157. Saha, P.; Naskar, S.; Paira, P.; Hazra, A.; Sahu, K.B.; Paira, R.; Banerjee, S.; Mondal, N.B. Basic alumina-supported highly effective Suzuki–Miyaura cross-coupling reaction under microwave irradiation: Application to fused tricyclic oxa-aza-quinolones. *Green Chem.* **2009**, *11*, 931–934. [[CrossRef](#)]
158. Bernhardt, F.; Trotzki, R.; Szuppa, T.; Stolle, A.; Ondruschka, B. Solvent-free and time-efficient Suzuki–Miyaura reaction in a ball mill: The solid reagent system KF–Al₂O₃ under inspection. *Beilstein J. Org. Chem.* **2010**. [[CrossRef](#)]
159. Jiang, Z.-J.; Li, Z.-H.; Yu, J.-B.; Su, W.-K. Liquid-assisted grinding accelerating: Suzuki–Miyaura reaction of aryl chlorides under high-speed ball-milling conditions. *J. Org. Chem.* **2016**, *81*, 10049–10055. [[CrossRef](#)] [[PubMed](#)]
160. Linic, S.; Christopher, P.; Ingram, D.B. Plasmonic-metal nanostructures for efficient conversion of solar to chemical energy. *Nat. Mater.* **2011**, *10*, 911–921. [[CrossRef](#)] [[PubMed](#)]
161. Christopher, P.; Xin, H.; Marimuthu, A.; Linic, S. Singular characteristics and unique chemical bond activation mechanisms of photocatalytic reactions on plasmonic nanostructures. *Nat. Mater.* **2012**, *11*, 1044–1050. [[CrossRef](#)] [[PubMed](#)]
162. Sarina, S.; Bai, S.; Huang, Y.; Chen, C.; Jia, J.; Jaatinen, E.; Ayoko, G.A.; Bao, Z.; Zhu, H. Visible light enhanced oxidant free dehydrogenation of aromatic alcohols using Au–Pd alloy nanoparticle catalysts. *Green Chem.* **2014**, *16*, 331–341. [[CrossRef](#)]
163. Li, G.; Wang, Y.; Mao, L. Recent progress in highly efficient Ag-based visible-light photocatalysts. *RSC Adv.* **2014**, *4*, 53649–53661. [[CrossRef](#)]
164. Verma, P.; Kuwahara, Y.; Moriab, K.; Yamashita, H. Synthesis and characterization of a Pd/Ag bimetallic nanocatalyst on SBA-15 mesoporous silica as a plasmonic catalyst. *J. Mater. Chem. A* **2015**, *3*, 18889–18897. [[CrossRef](#)]
165. Tanaka, A.; Fuku, K.; Nishi, T.; Hashimoto, K.; Kominami, H. Functionalization of Au/TiO₂ plasmonic photocatalysts with Pd by formation of a core–shell structure for effective dechlorination of chlorobenzene under irradiation of visible light. *J. Phys. Chem. C* **2013**, *117*, 16983–16989. [[CrossRef](#)]
166. Tanaka, A.; Nakanishi, K.; Hamada, R.; Hashimoto, K.; Kominami, H. Simultaneous and stoichiometric water oxidation and Cr(VI) reduction in aqueous suspensions of functionalized plasmonic photocatalyst Au/TiO₂–Pt under irradiation of green light. *ACS Catal.* **2013**, *3*, 1886–1891. [[CrossRef](#)]
167. Verma, P.; Kuwahara, Y.; Moriab, K.; Yamashita, H. Pd/Ag and Pd/Au bimetallic nanocatalysts on mesoporous silica for plasmon-mediated enhanced catalytic activity under visible light irradiation. *J. Mater. Chem. A* **2016**, *4*, 10142–10150. [[CrossRef](#)]
168. Smith, J.G.; Faucheaux, J.A.; Jain, P.K. Plasmon resonances for solar energy harvesting: A mechanistic outlook. *Nano Today* **2015**, *10*, 67–80. [[CrossRef](#)]
169. Del Fatti, N.; Voisin, C.; Achermann, M.; Tzortzakos, S.; Christofilos, D.; Vallée, F. Nonequilibrium electron dynamics in noble metals. *Phys. Rev. B* **2000**, *61*, 16956–16966. [[CrossRef](#)]
170. Link, S.; Link, S.; El-Sayed, M.A.; El-Sayed, M. Spectral properties and relaxation dynamics of surface plasmon electronic oscillations in gold and silver nanodots and nanorods. *J. Phys. Chem. B* **1999**, *103*, 8410–8426. [[CrossRef](#)]
171. Burda, C.; Chen, X.; Narayanan, R.; El-Sayed, M.A. Chemistry and properties of nanocrystals of different shapes. *Chem. Rev.* **2005**, *105*, 1025–1102. [[CrossRef](#)] [[PubMed](#)]
172. Evanoff, D.D.; Chumanov, G. Synthesis and optical properties of silver nanoparticles and arrays. *ChemPhysChem* **2005**, *6*, 1221–1231. [[CrossRef](#)] [[PubMed](#)]

173. Tanaka, A.; Fuku, K.; Nishi, T.; Hashimoto, K.; Kominami, H. Gold–titanium(IV) oxide plasmonic photocatalysts prepared by a colloid-photodeposition method: Correlation between physical properties and photocatalytic activities. *J. Phys. Chem. C* **2013**, *117*, 16983–16989. [[CrossRef](#)]
174. Sarina, S.; Zhu, H.; Jaatinen, E.; Xiao, Q.; Liu, H.; Jia, J.; Chen, C.; Zhao, J. Enhancing catalytic performance of palladium in gold and palladium alloy nanoparticles for organic synthesis reactions through visible light irradiation at ambient temperatures. *J. Am. Chem. Soc.* **2013**, *135*, 5793–5801. [[CrossRef](#)] [[PubMed](#)]
175. Xiao, Q.; Sarina, S.; Jaatinen, E.; Jia, J.; Arnold, D.P.; Liu, H.; Zhu, H. Efficient photocatalytic Suzuki cross-coupling reactions on Au–Pd alloy nanoparticles under visible light irradiation. *Green Chem.* **2014**, *16*, 4272–4285. [[CrossRef](#)]
176. Wang, F.; Li, C.; Chen, H.; Jiang, R.; Sun, L.-D.; Li, Q.; Wang, J.; Yu, J.C.; Yan, C.-H. Plasmonic harvesting of light energy for Suzuki coupling reactions. *J. Am. Chem. Soc.* **2013**, *135*, 5588–5601. [[CrossRef](#)]
177. Wang, F.; Sun, L.-D.; Feng, W.; Chen, H.J.; Yeung, M.H.; Wang, J.F.; Yan, C.-H. Heteroepitaxial growth of core–shell and core–multishell nanocrystals composed of palladium and gold. *Small* **2010**, *6*, 2566–2575. [[CrossRef](#)]
178. Wang, F.; Li, C.H.; Sun, L.-D.; Wu, H.S.; Ming, T.; Wang, J.F.; Yu, J.C.; Yan, C.-H. Heteroepitaxial growth of high-index-faceted palladium nanoshells and their catalytic performance. *J. Am. Chem. Soc.* **2011**, *133*, 1106–1111. [[CrossRef](#)]
179. Hu, J.-W.; Li, J.-F.; Ren, B.; Wu, D.-Y.; Sun, S.-G.; Tian, Z.-Q. Palladium-coated gold nanoparticles with a controlled shell thickness used as surface-enhanced Raman scattering substrate. *J. Phys. Chem. C* **2007**, *111*, 1105–1112. [[CrossRef](#)]
180. Trinh, T.T.; Sato, R.; Sakamoto, M.; Fujiyoshi, Y.; Haruta, M.; Kurata, H.; Teranishi, T. Visible to near-infrared plasmon-enhanced catalytic activity of Pd hexagonal nanoplates for the Suzuki coupling reaction. *Nanoscale* **2015**, *7*, 12435–12444. [[CrossRef](#)] [[PubMed](#)]
181. Li, X.-H.; Baar, M.; Blechert, S.; Antonietti, M. Facilitating room-temperature Suzuki coupling reaction with light: Mott-Schottky photocatalyst for C–C-coupling. *Sci. Rep.* **2013**, *3*, 1743. [[CrossRef](#)]
182. Möhlmann, L.; Baar, M.; Rieß, J.; Antonietti, M.; Wang, W.; Blecher, S. Carbon nitride-catalyzed photoredox C–C bond formation with *N*-aryltetrahydroisoquinolines. *Adv. Synth. Catal.* **2012**, *354*, 1909–1913. [[CrossRef](#)]
183. Zhang, S.; Chang, C.; Huang, Z.; Ma, Y.; Gao, W.; Li, J.; Qu, Y. Visible-light-activated Suzuki–Miyaura coupling reactions of aryl chlorides over the multifunctional Pd/Au/porous nanorods of CeO₂. *ACS Catal.* **2015**, *5*, 6481–6488. [[CrossRef](#)]
184. Zhang, S.; Li, J.; Gao, W.; Qu, Y. Insights into the effects of surface properties of oxides on the catalytic activity of Pd for C–C coupling reactions. *Nanoscale* **2015**, *7*, 3016–3021. [[CrossRef](#)] [[PubMed](#)]
185. Cui, J.; Li, Y.; Liu, L.; Chen, L.; Xu, J.; Ma, J.; Fang, G.; Zhu, E.; Wu, H.; Zhao, L.; Wang, L.; Huang, Y. Near-infrared plasmonic-enhanced solar energy harvest for highly efficient photocatalytic reactions. *Nano Lett.* **2015**, *15*, 6295–6301. [[CrossRef](#)] [[PubMed](#)]
186. Miyaura, N.; Suzuki, A. Palladium-catalyzed cross-coupling reactions of organoboron compounds. *Chem. Rev.* **1995**, *95*, 2457–2483. [[CrossRef](#)]

